

Photogrammetry in Mediterranean Archaeology

by

Colin Wallace

A thesis
presented to the University of Waterloo
in fulfilment of the
thesis requirement for the degree of
Master of Environmental Studies
in
Geography

Waterloo, Ontario, Canada, 2016

© Colin Wallace 2016

Author's Declaration

I hereby declare that I am the sole author of this thesis. This is a true copy of the thesis, including any required final revisions, as accepted by my examiners.

I understand that my thesis may be made electronically available to the public.

Abstract

Digital photogrammetry has progressed to a level at which it no longer requires expensive equipment or significant training in order to produce professional results. In the field of Mediterranean archaeology requirements for documentation and in particular digital documentation are increasing demanding new and innovative means to enable more sites to accomplish these results. During several field seasons working with people of the American School of Classical Studies in Athens, primarily in Ancient Corinth as well as several other Greek sites, modern methods in photogrammetric recording and processing have been explored in an attempt to produce highly accurate, quantifiable three dimensional documentation of archaeological site and artifacts within an extremely limited budget. This thesis explores the craft's history, methodology and demonstrates using several real world examples how, with little or no money current goals can be achieved and offers a tutorial that can be used by other individuals hoping to produce similar results.

Acknowledgements

My humble thanks to all of those people who have waited for this. In particular I would like to express my deep appreciation and gratitude to my advisor, Peter Deadman for his encouragement, his thoughtful guidance and his limitless patience and good nature. This thesis is the culmination of several years of field work, not to mention a complete change in topic partway and Pete has believed in me the entire time; giving me sound advice while giving me the freedom to run with new ideas.

I would like to thank my committee members, Rob Feick, Maria Liston and Dorina Moullou for their time, guidance, thought-provoking suggestions. Thank you Rob for your enthusiasm for this project and insightful suggestions for its continuation which are greatly appreciated. Thank you Maria for teaching me so much over the years, for showing me the grandeur of Greece and for so many thoughtful edits of this thesis. Thank you Dorina for being a trail blazer in the use of digital photogrammetry in archaeology, for being an inspiration in your love of this field and for your selfless generosity with your time.

I would also like to thank all of my colleagues in Ancient Corinth, Greece for giving me so many opportunities to learn and to work on the projects that have fueled this thesis. Guy Sanders, James Herbst, Ioulia Tzonou-Herbst and Nicol Anastassatou in particular believed in me before I believed in myself and their friendship and faith in me has been a great gift. James set this in motion when, years ago, he asked if I had heard of a thing called photogrammetry.

The encouragement of my friends has been invaluable and so very much appreciated when things seemed dark and undoable.

Lastly thank you to my mum and dad for their encouragement and interest in their son's mad idea that he might, halfway through his life, become an archaeologist.

Dedication

I dedicate this work to my children, Oliver, Riley and Hailey who inspire all that I do in life. This journey began in the year 2000 when I started an undergrad in Anthropology, not dreaming of where it would lead but simply wanting to set an example for you three. May you all follow your own dreams and have them come true as I have.

Table of Contents

Author’s Declaration	ii
Acknowledgements	iv
Dedication.....	v
Table of Figures	viii
Table of Tables.....	x
Chapter 1 - Introduction	1
Chapter 2 - History and Development.....	7
2.1 - Early Attempts at Portraying Three Dimensions	7
2.2 - Photogrammetry Emerges.....	8
2.3 - Further Developments.....	9
Chapter 3 - General Methodology	17
3.1 - Introduction.....	17
3.2 - Photography	18
3.3 - Lighting.....	21
3.4 - Software	23
3.5 - Georeferencing.....	25
3.6 – Modelling	27
Chapter 4 – In Situ Documentation	33
4.1 - Sites.....	36
4.1.1 - Thebes Temple and Graves.....	36
4.1.2 - Frankish Structures in Ancient Corinth	48
4.1.3 – Asklepieion	61
4.4 – Fountain of the Lamps	67
4.2 – Features	74
4.2.1 - The Eutychia Mosaic	74
4.2.1.A - In Situ Mosaic Recording Methodology (2014)	81
4.2.1.B - Mosaic Reinstallation Methodology (2015)	88
IV.2.2 – Inscriptions.....	99
4.2.2.A - Inscription Methodology.....	101
4.2.3 – Osteology	105
Chapter 5 – Museum Objects	107
5.1 – Sculpture	107
5.1.1 - Julius Caesar Bust Methodology	109
5.1.2 - Julius Caesar Torso and Arm Methodology.....	111
5.2 - Small objects.....	119
5.3.1 - Pottery Methodology	121
5.3.2 – Bone Methodology.....	122
Chapter 6 - Summary of Techniques and Results.....	125
Chapter 7 - Conclusion	129
Sources Cited.....	132

Sources consulted but not Cited	137
Image Credits.....	138
Appendix 1 – Tutorial.....	139
Appendix 2 – Camera Calibrations	144

Table of Figures

Figure 1 - Aerial Photogrammetry	3
Figure 2 - Close Range Photogrammetry.....	3
Figure 3 - Woodcut from Albrecht Dürer's Underweysung der Messung.....	8
Figure 4 - Comparison of photogrammetric methods.....	10
Figure 5 - The first photogrammetric recording of the Acropolis.....	11
Figure 6 - Acropolis. Photomosaic of the plan view.....	12
Figure 7 - Comparison of photogrammetric recording and line drawing.....	13
Figure 8 - Acropolis laser scanning and photogrammetry orthographic results	15
Figure 9 - Orthographic model view of the Ancient Corinthian Asklepieion.....	20
Figure 10 - Unique targets as produced by Agisoft Photoscan.....	27
Figure 11 - Sparse point cloud: Peirene Fountain, Ancient Corinth	28
Figure 12 - Camera angles represented with blue rectangles representing the focal plane ..	30
Figure 13 - Mesh with textures added: Peirene Fountain, Ancient Corinth.....	32
Figure 14 - Hand drawing orthographic site details.....	34
Figure 15 - Temple of Ismenios Apollo and Graves - Thebes	36
Figure 16 - Thebes model detail using initial technique.....	38
Figure 17 - Thebes model detail using later technique	38
Figure 18 - Camera locations and image overlap: Thebes.....	40
Figure 19 - GCP Locations: Thebes.....	41
Figure 20 - Reconstructed digital elevation model: Thebes	43
Figure 21 - Camera locations and image overlap: Thebes Revised.....	44
Figure 22 - Ground Control Points - Thebes Revised.....	45
Figure 23 - Reconstructed Digital Elevation Model - Thebes Revised	47
Figure 24 - Frankish section of Ancient Corinth excavations.....	48
Figure 25 - low level view produced from only high altitude photos: Frankish area.....	49
Figure 26 - James Herbst launching a kite over the Frankish area	50
Figure 27 - Helium balloon and camera apparatus	51
Figure 28 - Phantom III drone	52
Figure 29 - Frankish area model from drone photos.....	53
Figure 30 - Camera locations and image overlap: Frankish area.....	54
Figure 31 - GCP locations: Frankish area.....	55
Figure 32 - Reconstructed digital elevation model: Frankish area balloon model	57
Figure 33 - Camera locations and image overlap Frankish area drone modelling	58
Figure 34 - Camera locations and error estimates: Frankish area drone modelling	59
Figure 35 - Reconstructed digital elevation model: Frankish area drone modelling.....	60
Figure 36 - Ancient Corinthian Asklepieion	61
Figure 37 - Asklepieion model looking Southeast.....	63
Figure 38 - Camera locations and image overlap: Asklepieion	64
Figure 39 - Camera locations and error estimates: Asklepieion	65
Figure 40 - Reconstructed digital elevation model.....	66
Figure 41 - Fountain of the Lamps before cleaning.....	68
Figure 42 - Fountain of the Lamps immediately after cleaning.....	69
Figure 43 - Fountain of the Lamps overgrown again months after clearing	69
Figure 44 - Fountain of the lamps after excavation in 1972	73
Figure 45 - Fountain of the lamps one year after clean up in 2012	73
Figure 46 - Central panel of the Eutychia Mosaic	77
Figure 47 - North East corner of central surround depicting a Rooster.....	78

Figure 48 - Floral pattern on south edge of central panel	79
Figure 49 - Eutychia Mosaic in situ before removal.....	81
Figure 50 - Camera locations and image overlap: Eutychia mosaic.....	83
Figure 51 - Eutychia Mosaic GCP locations.....	85
Figure 52 - Eutychia mosaic reconstructed digital elevation model.....	87
Figure 53 - finished model showing Agisoft targets.....	90
Figure 54 - Moving of section T21; the central panel of the mosaic to be photographed. ...	92
Figure 55 - Example of how the images were trimmed along each tessera's edge.....	94
Figure 56 - Camera locations and image overlap for T21	96
Figure 57 - Ground control points for Eutychia mosaic T21	97
Figure 58 - Reconstructed digital elevation model of T21	98
Figure 66 - Inscription in the Athenian Agora	99
Figure 67- Camera locations and image overlap for Agora inscription.....	103
Figure 68 - Reconstructed digital elevation model of Agora inscription.....	104
Figure 69 - Model of Skeleton, Gietz, Poland produced from two 2008 photographs.....	105
Figure 59 - 3D model of bust of Julius Caesar - Ancient Corinth Museum: S 2771	109
Figure 60 - Roman Torso (Ancient Corinth Museum: S 1081A)	111
Figure 61 - Roman Torso Model (Ancient Corinth Museum: S 1081A).....	112
Figure 62 - Roman Arm	113
Figure 63 - 3D model of Roman torso with arm relocated	115
Figure 64 - Camera locations and image overlap for torso joined with arm	116
Figure 65 - Reconstructed digital elevation model of combined arm and torso	118
Figure 72 - Photograph of earring from Stymphalos and illustration of same.....	120
Figure 73 - Photogrammetric model of an oinochoe	121
Figure 70 - Photogrammetric mesh of a skull.....	122
Figure 71 - Cow scapula illustrating the perils of complex backgrounds.....	124
Figure 74 - Sparse point cloud of a mosaic panel showing georeferenced targets	140
Figure 75 - Dense point cloud of mosaic panel	141
Figure 76 - Mesh applied to mosaic panel.....	142
Figure 77 - Closeup of mesh showing points joined by triangles.....	142

Table of Tables

Table 1 – Comparison of available photogrammetric and computer vision software	25
Table 2 - Thebes cameras	40
Table 3 - Thebes control points	41
Table 4 - Thebes revisited cameras	44
Table 5 - Ground Control Points - Thebes Revised Model	46
Table 6 - Frankish area balloon cameras	54
Table 7 - Control points: Frankish area balloon modelling	55
Table 8 - Cameras: Frankish area drone modelling	58
Table 9 - Average camera location error: Frankish drone modelling	59
Table 10 - Asklepieion Cameras	64
Table 11 - Average camera location error: Asklepieion	65
Table 12 - Eutychia mosaic cameras	83
Table 13 - Eutychia mosaic control points	85
Table 14 - Mosaic section T21 cameras	96
Table 15 - Ground control points: T21	97
Table 16 - Agora inscription cameras	103
Table 17 - Joined torso cameras	116
Table 18 - Model statistical summary	126

Chapter 1 - Introduction

Two of the greatest hurdles in the study of archaeological sites have always been the destructiveness of time and the destructive nature of archaeological practice. Archaeological sites deteriorate over time prior to their discovery but that deterioration accelerates once a site is excavated. In fact, excavation per se is a destructive process. Erosion, vegetation and vandalism all conspire to reduce the information that could have been extracted in the site's optimum condition. In multi-stratigraphic sites continued excavation removes higher, younger stratigraphic levels and consequently the ability to retrospectively measure or examine them. The more complex stratigraphy of the Mediterranean region with its long history and dense archaeological record exemplifies this challenge. As A. Snodgrass comments in reference to Greece, "any excavation, even that of a ten-meter square undertaken to prepare the way for the building of a modest office block in a provincial town, is likely to produce a significant crop of material from a variety of periods, spanning millennia rather than centuries" (Snodgrass 1987, 97).

Outline of the Problem

Archaeological practice requires monuments, structures, sites, artefacts and organic remains to be carefully examined, recorded, studied, conserved and, when needed, restored. Artefacts and any organic remains, while having been recorded in situ, are necessarily removed from their context. Their documentation imposes the recording of location, form and dimensions. This constitutes a necessary part of all field work and museum work, using, in each case, the optimal methodology and equipment, depending on the type of

measurements, the scale of the final product, the size, the complexity of the object and the budget available (Moysiadis and Perakis, 2011, 1292). New theories and practices of documentation developed over time can benefit revisiting both the original site and its findings. Current archaeological practice recognizes the destructiveness of leaving a site excavated and a trend in preservation towards backfilling further justifies the need to use 3D documentation (Moullou and Mavromati 2007, 518). Future practices in archaeology are yet to be known but preservation of the maximum information available prepares archaeologists for these eventualities. In advocating the use of photogrammetry in preparation for future needs and technologies back in 1975, Ch. Bouras wrote that “[i]t is obvious ... that we are in need of precise measurements which will enable us to retain even those traits which have not been explored so far, and whose actual significance may become apparent in the future” (Bouras 1975, 101). Photography and mapping of a site, no matter how thorough, do not allow either exact measuring, lines of sight or simply the feeling of being at the site and understanding how it was arranged. On the other hand, aerial or close range photogrammetry and aerial or terrestrial laser scanning can be applied, separately or in combination, in order to produce accurate 3D models. Their use differs according to the aforementioned criteria (measurements, scale, size, complexity and budget).

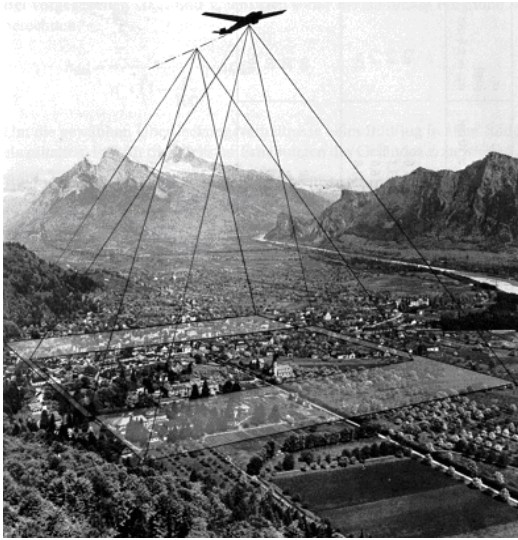


Figure 1 - Aerial Photogrammetry (Marinov 2003, 2)



Figure 2 - Close Range Photogrammetry (Marinov 2003, 3)

For most archaeological documentation projects, especially where large scales and high accuracy are needed, photogrammetry in combination with 3D laser scanning is preferable. This method is usually expensive requiring specialized equipment, laborious processing and large amounts of data storage space. Quotes obtained in July 2013 for an airborne LIDAR survey of Ancient Corinth were priced in the \$35,000 U.S. range. In 2007, the total budget for the 3D documentation (through laser scanning and photogrammetry) of the Acropolis of Athens and the implementation of a GIS came to 885, 390.00 €, while the time required for carrying out the work was 18 months (Moullou 2010, 12). As an example of the amounts of data storage required, in the modelling of “the Erechtheion, more than 5 billion points have been collected by laser scanning. This amount of data is impossible to handle as a whole. A reduced, but still large, 10 million polygon model has been produced” (Moullou et al. 2008, 1075).

Goal and Objectives

In this thesis, through the use of close range photogrammetry, several aspects of archaeological documentation and their inherent problems will be examined. How they can be solved efficiently and cost effectively is detailed in order to show the advantages that photogrammetry provides in augmenting or replacing traditional methods. These advantages are enhanced by current and upcoming photogrammetric software which allows for the use of a hand held camera, making it portable and flexible as well as time and cost efficient; the latter being an important aspect considering budget restraints on many archaeological sites.

Moreover, this thesis will show how photogrammetry can be used in broad range of archaeological applications to create a more thorough, robust record with greater flexibility of uses. Using necessary variations in methodology, the examples used in this thesis will demonstrate that current and emerging methods in photogrammetry can excel regardless of the size, complexity or diversity of the subject matter.

Since cost is a significant factor in any archaeological documentation this thesis will demonstrate through case studies how the use of photogrammetry can significantly reduce costs. Since examples presented in this thesis were achieved with relatively small budgets and in some cases no funding at all, the methods used prove themselves to solve the cost problem that is becoming a more important consideration in archaeological work. Even some very large scale projects used as examples involved no costs, cost of a large helium balloon (approximately 200€) or the one time cost of a drone at \$1,700 to be amortized over a number of seasons and projects in Ancient Corinth and the Athenian Agora.

Another problematic aspect of documentation is that of efficiency both in time and labour. While many previous methods involved extensive setup, interruption of excavations and labour intensive operations, the case studies presented here show how much more streamlined data collection can be using photogrammetry.

Methods and Results

This thesis is based on experience gained from various projects during four field seasons in the summers of 2012, 2013, 2014 and 2015 spent working for The American School of Classical Studies in Athens on the archaeological site of Ancient Corinth. This work has involved taking over several thousand photos and producing three dimensional geo-referenced models from them. When this work commenced there was very little documentation on the application of photogrammetry in archaeology using minimalist methods in the field and using readily available commercial image based modelling software for processing models. The methods used were developed and refined by James Herbst (site architect at Ancient Corinth) and the author on a project by project basis.

All examples used in this thesis were produced using a digital single reflex camera (DSLR) and affordable software. Methods of deployment, while primarily on foot, included ladders, balloon, kites and drone.

The results are encouraging and specialists in site architecture, lithics, ceramics, sculpture, osteology and inscriptions have all shown a great deal of interest in having their work examined utilizing these methods.

Outline of thesis

Using real world examples there will be an endeavour to demonstrate the practical application of these techniques to several areas of archaeology and the mapping of excavations. In addition to the ability of this technology to be used in current excavations, well photographed and documented historic excavations will be revisited and modelled. The case studies are the temple of Ismenios Apollo on the Acropolis of Thebes, Frankish structures, the Asklepieion, the Fountain of the Lamps, the Eutychia (Good Luck) Mosaic in Ancient Corinth, a marble bust of Julius Caesar and torso of a Roman soldier in the archaeological museum of Ancient Corinth, an arm thought to belong to the torso stored in a warehouse in Ancient Corinth, an inscription from the Athenian Agora, human bone from the Roman period excavated in Ancient Corinth (as well as medieval human bone from Gietz, Poland used as a comparative example) and an oenochoe (wine jug) from Ancient Corinth. In each example where previous methods of documenting are unique to that type of object there will be a description of how these examples would have been documented prior to the use of photogrammetry.

These real world examples demonstrate the broad range of subject matter that photogrammetry can be applied to including but not limited to excavations, architecture, artwork, sculpture, skeletal remains and a variety of small objects. In order to characterize varieties of photo documentation methods these examples will be divided into In Situ Documentation and Museum Objects.

Chapter 2 - History and Development

Photogrammetry is the science of using multiple photographs to produce three dimensional models in order to acquire accurate measurements from a landscape or three dimensional objects. Once used primarily for cartography, current methods are finding countless new applications including many within the archaeological world. Although modern photogrammetry employs digital photographs, computers and complex software, its roots lie in the development and understanding of linear perspective.

2.1 - Early Attempts at Portraying Three Dimensions

It only takes a visit to a local theatre, seeing people sit in the dark wearing special spectacles, dodging imaginary objects to confirm that human kind's long fascination with capturing and experiencing our three dimensional world is very much alive.

Early attempts at representing artificial depth or three dimensionality are referred to by Vitruvius when he attributes the technique of skenographia (from the Greek meaning "scene painting") to "one Agatharcos, set designer for Aeschylus just before the mid 5th c BC" (Smith & Plantzos 2012).

While there are ample examples of the Roman use of an, albeit flawed, form of one point perspective, the technique disappears entirely during the Middle Ages and it is not until the Renaissance that it re-emerges.

Although artists as early as the 14th century had begun to see and use perspective, it wasn't

until 1525 that Albrecht Dürer developed a device that could, using the laws of perspective, produce an accurate perspective drawing.

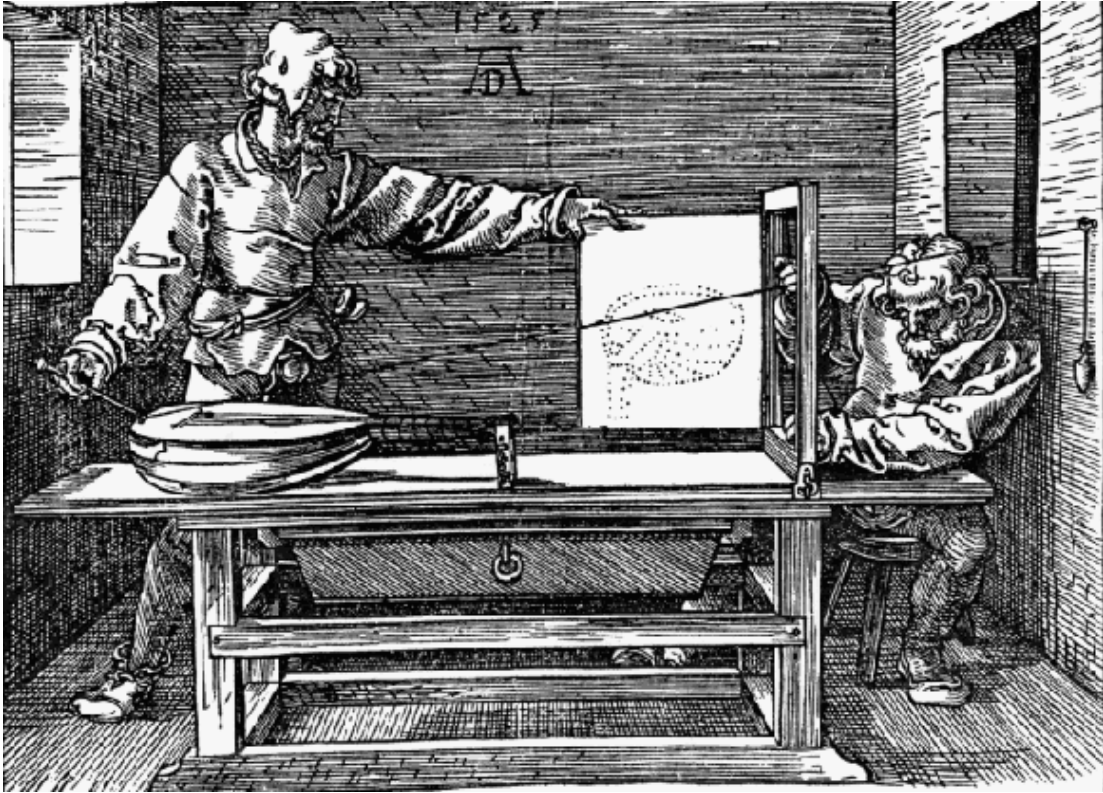


Figure 3 Woodcut from Albrecht Dürer's Underweysung der Messung, 2nd edition (Nuremberg, 1538) illustrating his perspective device. (<http://www.uh.edu/engines/durer1.gif>)

In 1864 the first topographic map produced solely using land based photographs was made by French cartographer, Colonel Aimé Laussedat, who is known as the father of photogrammetry (von Brevem, 2011, 57). By doing so he proved that accurate measurements could be derived from photographs on a plane table.

2.2 - Photogrammetry Emerges

The term photogrammetry was first coined by Albrecht Meydenbauer in 1893 (<http://spatial.curtin.edu.au/local/docs/HistoryOfPhotogrammetry.pdf>). He was a German

architect who, in 1858 had the idea of using photogrammetric method to document buildings. He later founded the Royal Prussian Photogrammetric Institute. Meydenbauer's advances in the development of cameras made specifically for photogrammetry led to devices that were both a camera and a measuring instrument (Albertz 2001). Hence, in 1874 photogrammetry was used by Franz Stolze in Persia to record the archaeological remains of Persepolis and the temple of Djamaht; constituting the first known use of photogrammetric technique in archaeology (Albertz 2001, 21). Using the second generation of stereoscopic camera-theodolite developed by Meydenbauer, Stolze applied the principle of plane table photogrammetry which involves a technique used in architecture to take architectural drawing views and combine them to produce a three dimensional rendering by running lines from one drawing to another between common points. Photogrammetry simply replaces those drawings with photographs sharing common points and, in the case of plane table photogrammetry, produces a line drawing in three dimensions of the object or a plan view depending on what technique is used.

In 1886 Edouard Deville, Surveyor General of Canada, developed a method using stereoscopic images to produce his maps with a trace point within the model. With this method Deville successfully mapped the Rocky Mountains. (Birrell 1981, 54)

2.3 - Further Developments

Since the 19th century there have been many developments in photogrammetry: from the plane table technique to the analogue (1900-1960), the analytical (1960-to the end of the 20th century) and the digital photogrammetry of the present (Konecny 1985, Doyle 1964, Collier 2002) In any given period, photogrammetry has been used to record archaeological sites around the world (Fussel 1982) but as we shall see, not always with success.

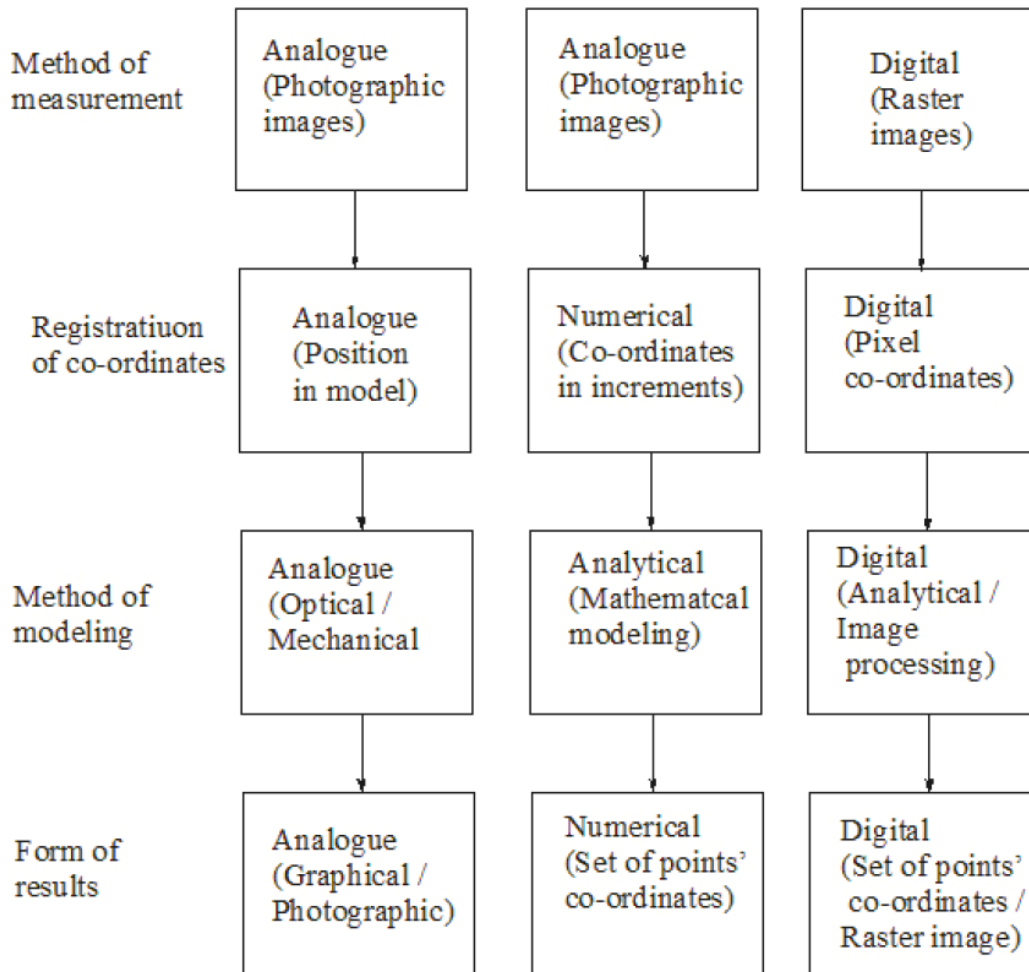


Figure 4 - Comparison of photogrammetric methods (Marinov 2003, 10)

Analogue photogrammetric techniques involved using mechanical apparatus to render the orthographic image. Edouard Deville developed such a device in 1896 called the stereoscopic planograph but it proved too complex and was seldom used. During the first half of the twentieth century analogue photogrammetry was used primarily as a surveying technique; used to produce topographic maps and site plans.

(<http://spatial.curtin.edu.au/local/docs/HistoryOfPhotogrammetry.pdf>) (Schenk 2005, 8).

Analytical photogrammetry employs “rigorous mathematical calculation of coordinates of points in object space based upon camera parameters, measured photo coordinates, and

ground control” (Wolf et al. 2014, 233). Although the mathematical elements of the process were understood for a long time it was only with the technological progress of computing that they were able to be utilized (Wolf et al. 2014, 233) (Schenk 2005, 8).

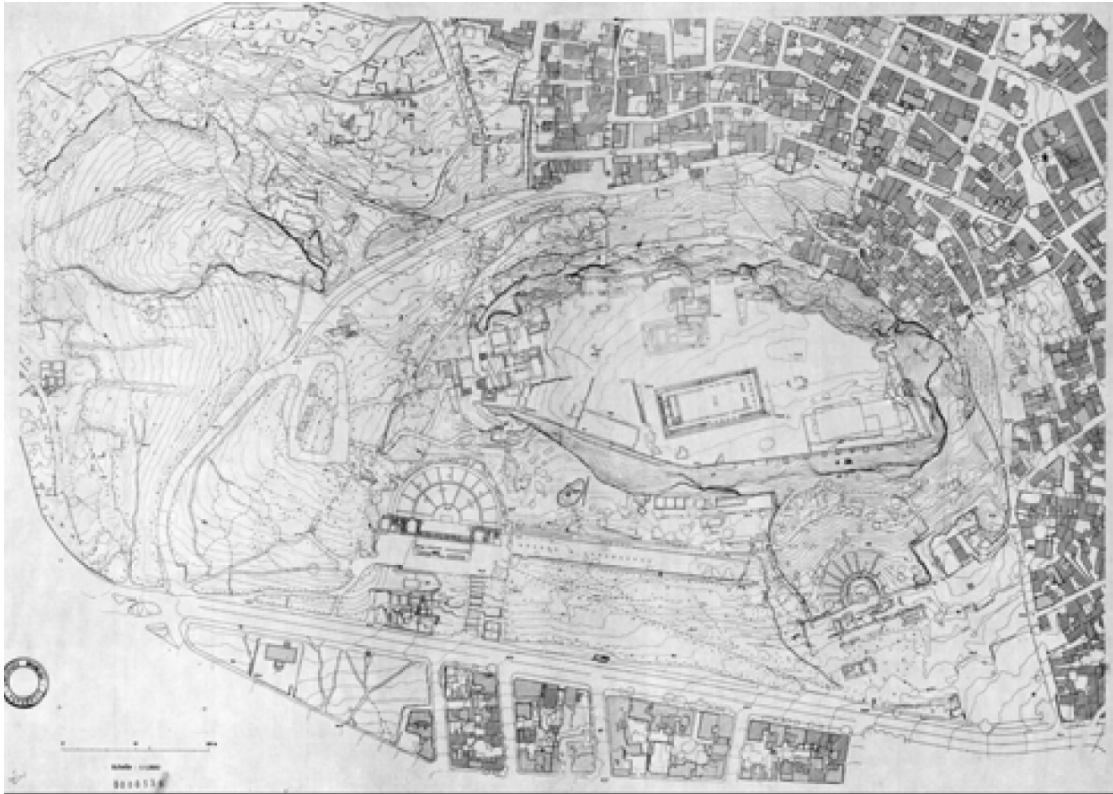


Figure 5 - The first photogrammetric recording of the Acropolis by the Insitut Géographique National in Paris-UNESCO (Moullou and Mavromati 2007, 515)

While used primarily for mapping and surveying, analytical photogrammetry also began to emerge as tool for archaeological documentation, albeit strictly for orthographic viewpoints. “The first [analytical] photogrammetric recording of the Acropolis by the Institut Géographique National in Paris” was done in 1971 and 1974 (Moullou and Mavromati 2007, 515) (see Figure 5). A photomosaic of the plan view of the Acropolis (see Figure 6 - Acropolis. Photomosaic of the plan view. By the Photogrammetry Laboratory of the NTUA (Moullou and Mavromati 2007, 515)) was conducted in 1976 by the National Technical

University of Athens (NTUA). Photogrammetric recording of the Acropolis monuments began with the Erechtheion in 1977.



Figure 6 - Acropolis. Photomosaic of the plan view. By the Photogrammetry Laboratory of the NTUA (Moullou and Mavromati 2007, 515)

Ultimately photogrammetric documentation from the monuments was not used because of problems with the accuracy and detail of the process. As can be seen in Figure 7 the photogrammetric results fail to define specific stones, features and their pathologies and required significant manual correction to be useful. The extra labour involved negated any advantage that had been hoped for in using photogrammetry. The upshot of this was that the “Acropolis Committee and the staff of the Technical office were reluctant to use photogrammetric drawings thereafter”. (Moullou and Mavromati 2007, 515)

The fourth major development in photogrammetry was that of digital photogrammetry. With the advent of the digital photograph, software processing now enabled direct access to the data that constituted the digital photograph enabling analysis of the parallax between digital elements and allowing the calculation of spacial relationships without enormous

amounts of data input.

While digital photogrammetry showed promise, the amount of manual labour still required to produce models was significantly high. Since the early 2000's due to the labour intensity and lack of automation in photogrammetric computer vision “many photogrammetric scientists shifted their research interests to laser scanning, slowing advances and new developments in automated procedures using photogrammetric technology”. (Remondino et al. 2014, 146)

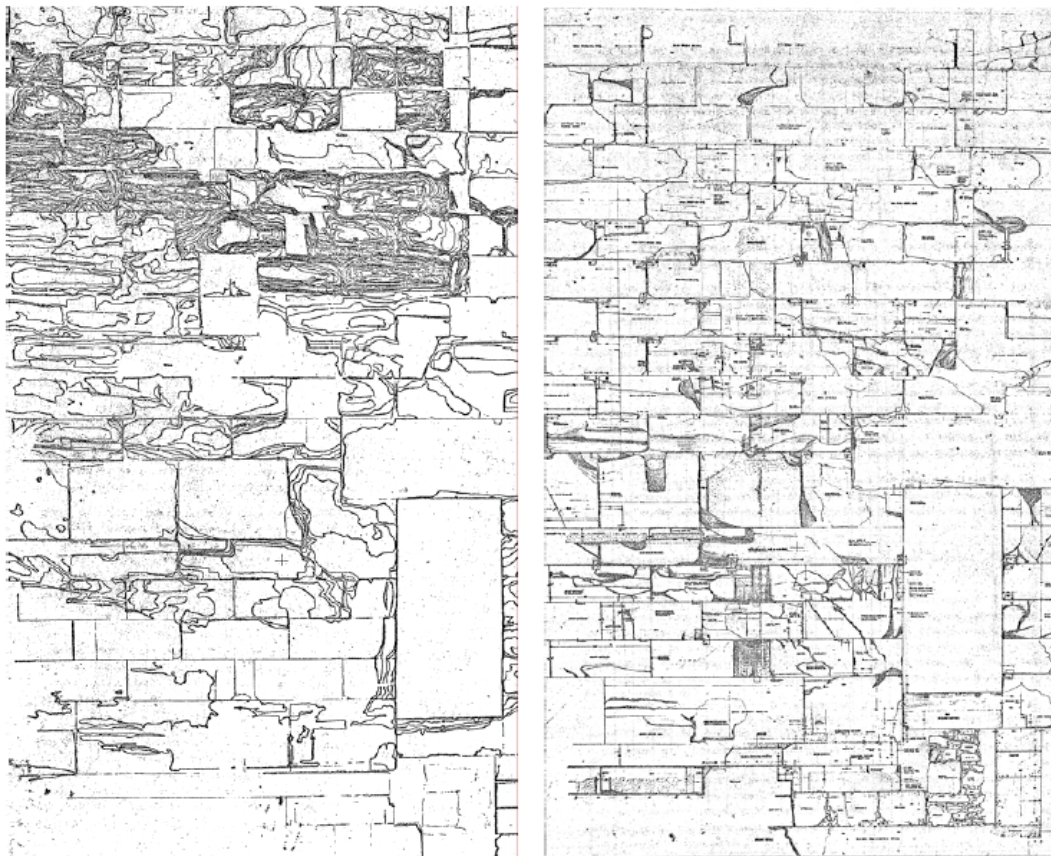


Figure 7 - Comparison of photogrammetric recording of the Erechtheion South Wall (left) and line drawing of the same section taken from photogrammetric results and corrected by architect E. Moutopoulos.

With the introduction of laser scanning, highly accurate recordings were able to be achieved. Compared to previous methods, terrestrial laser scanning offered many advantages due to relatively rapid data acquisition and simple use of the equipment. Costs however, were significantly higher than that of photogrammetry and data processing (of the point cloud) was a time consuming task. When lasers were used to record objects with complex geometry or that were not easily accessible, occlusions (gaps in the coverage) could appear. In their documentation of the 3D modelling of the poros remains of Arrephorion at the Acropolis of Athens (necessary due to backfilling of the site for preservation), Moullou and Mavromati (2007, 518) note that “[d]ue to the object’s morphology it was impossible to avoid surface occlusions In some cases it was impossible even to place the scanner conveniently. For the future, the filling of the voids of the scanning process and the production of orthomosaics [(using photogrammetry)] for the plan view and each façade of the monument are scheduled”. El-Hakim et al., (2008, 1078) in their modelling of the Erectheion on the Athenian Acropolis observed that “The size, setting, and the monument surface created several problems. The height made coverage from ground level difficult on top parts. Some problems due to obstructions and terrain ... caused delays and resulted in missed areas. Some parts shape complexity caused self-occlusions, and impediments from plants/trees created holes in the coverage”. Therefore laser scanning often needed to be supplemented by photogrammetry through which greater mobility and variability in vantage points was able to negate or reduce the number of occlusions.



Figure 8 - Acropolis laser scanning and photogrammetry orthographic results - General Plan © YSMA Archive

Close range photogrammetry, despite sometimes presenting difficulties in data acquisition, was a valuable method due to correct image geometry and the high spatial resolution of photographic imaging (Moysiadis and Perakis 2011, 1294-1295). More recent development of algorithms and automation have fuelled a resurgence in photogrammetry with its relative simplicity, mobility and low cost, giving it a significant advantage over laser scanning. Photogrammetry has progressed to a stage where it is able to three dimensionally recreate an archaeological site, feature or artefact quickly and inexpensively. It now "constitutes a powerful textured representation ... where the vectorised interpretation ... is left to the corresponding specialists" (archaeologists, architects, conservators, engineers etc.) (Moullou and Mavromati 2007, 515-516).

Given that there is now greater access to inexpensive or open source software and high resolution digital cameras, photogrammetry has reached a point at which it can be utilized to produce high quality 3D phototextured models for archaeological documentation with measurable accuracy, efficiency of time and labour and low costs giving it accessibility to a more widespread user group within the field.

Chapter 3 - General Methodology

3.1 – Introduction

The terrestrial image based 3D modelling methods described in the following section involve using a Digital Single Lens Reflex camera (DSLR) for close range photogrammetry during several seasons on archaeological sites in Greece. Photographs are stored and shared on Dropbox and, using automated processing software, are used to produce three dimensional digital models of the subject matter.

The circumstances and the methods employed by the user within those circumstances are unique in every case. Comparison of the author's results with those produced by James Herbst have been mutually beneficial in determining which techniques are best used in a given situation. While there is a quantifiable methodology involved there is also an instinct based on experience that the user gains and applies to each subsequent project. Such is the case in the methods used as examples in this thesis.

In approaching each new project, experience from previous ones reinforced the need to carefully question the person requesting the work as to what the ultimate purpose of the model would be. Such purposes differ greatly and having a clear picture of what is desired shapes how one approaches the photography of the subject. Moullou and Mavromati (2007, 520) find that “the end product must be clearly specified a priori, according to strictly defined needs. It is only then that the pursued results will be accomplished”. This approach guided the techniques applied in each of the examples given hereafter by determining lighting, time of day, number of photographs, amount of detail, prioritised elements and scope of coverage.

3.2 - Photography

In order to create a photogrammetric model, a series of (dense) photographs must be taken around an object, preferentially at different levels, forming a sphere of photographic perspectives. If measurements and scale are to be obtained, a reference coordinate system is also required upon which the photogrammetric measurements are based. The following is a summary of the preferences for optimum results as found in our field testing. The photogrammetric model should have between 20 and 100 exposures in order to obtain a measureable, georeferenceable model. I have produced models with as little as three photos, giving a single wall a relief appearance for simple presentation. At the other end of the scale was the Hellenic temple on the Acropolis of Thebes which required close to four hundred photos in order to capture its complexity and make all elements of the site accessible and measureable. 3.500 photos were used for the needs of the Acropolis of Athens photogrammetric model (Tsingas et al. 2008, 1102).

Each photograph must have overlap with those adjacent to it in order for the photogrammetry software to calculate using common points. The more overlap, the more able the software will be to calculate the photograph's relations to each other. This technique of moving around the subject taking photos is referred to as Structure from Motion (SfM) (Verhoeven et al. 2013, 165). Where possible a common centre of interest or a few select centres of interest should be chosen in order to make the array of photos more cohesive.

A camera as simple as that in a modern cell phone can be used for rudimentary models but for optimum results a digital single reflex lens camera with higher resolution is preferable.

We found that using an 18 mm wide angle lens created a greater coverage area and more overlap between photographs with a resulting acceptance by the software of a higher number of photos in the series. Photogrammetric SfM is dependent on objects in the foreground and background in order to calculate the parallax between photos. In order to achieve this, photos should be taken using the greatest amount of depth of field that the equipment is able to produce in a given lighting condition. In order to do this the aperture of the lens should be at its smallest. Aperture is measured in F stops and, counterintuitively, the smaller the number, eg. F/2.8 will have a much larger aperture than that of F/22. The smaller the aperture, the less light enters the camera, requiring a much longer exposure time. In our tests, best results were achieved with the smallest possible aperture that would still allow crisp shots in a location's environment. The logical solution is to use a tripod or monopod and carefully shoot each photograph with the smallest aperture, longest exposure and thus greatest depth of field. It is the site conditions themselves that limit us in this.

Another method that became useful when dealing with larger sites was to do a less detailed model of the entire site; then to take detailed photos of individual features, model them and stitch them into the larger, vaguer model. This can help reduce the overall size in megabytes of the model.



Figure 9 - Orthographic model view of the Ancient Corinthian Asklepieion

Photographing skeletal remains; while benefiting from their size and portability, results in its own set of challenges. If a human skull is placed on a table, the photogrammetric model will attempt to build the table top as part of the skull. Then, if we are to achieve a full three dimensional model of the skull, it must be flipped. Unfortunately, once again this results in not only the table being added to the top of the skull in the model but also confusion by the software because common elements in the background of the photos are mixed up in the two views resulting in a confused conjoining of the two views of the skull.

Our solution to this was to hang the bone from fishing line between two tripods. An outdoor attempt was a failure as there was too much background detail with trees, mountains and buildings all competing to be modelled rather than the lowly bovine scapula that we were

attempting to record. The outdoor lighting was also too intense to give the model an evenly lit look.

Pottery, sculpture, architectural members and less complex finds that can be easily circled capturing all aspects but their underside, require much less effort. Engravings, however, do require that the photographer be more conscious of what end result they wish to achieve. The entire face should be photographed from a ninety degree perspective; head on to capture the depths of all characters, then photographed at both subtle and extreme angles to capture the nuances of the edges of each character. It is important to include areas that seem to have no engraving as what is indiscernible to the eye, may be able to be retrieved using photogrammetric technique.

3.3 – Lighting

Lighting quality plays a significant role in the results of photogrammetric modelling and preferences can vary greatly depending on what the desired result is. If an aesthetic for presentation or public viewing is desired over a highly accurate, measureable model then broad daylight is to be favoured over indirect dusk or dawn lighting.

In outdoor sites, when modelling for accuracy, James Herbst and the author were able to acquire the most visually contiguous information when shooting before there is direct sunlight on the site or after the sun has begun to set. This allowed the lighting to remain relatively consistent so that visual points that the photogrammetric software used to create three dimensions didn't change because of the sun moving. We also found that elements of a site could get lost in the shadows of full sunlight. The logical solution would be to wait for an overcast day. In four summers of work in Greece I have yet to see such a day.

A constraint to shooting in the early morning or evening is that many sites are guarded and fenced, requiring special permissions from the Ephorate of Antiquities (the authority of the Hellenic Ministry of Culture and Sports responsible for overseeing archaeological sites locally) to have access outside of regular hours. In such cases, these photos not only benefit from better lighting but also a lack of sightseers. In order for photogrammetric modelling to work, there must be as much consistency between photos as possible. The appearance of tourist groups, stray dogs, wandering goats, windblown objects, the movement of the sun throughout a shoot or even the photographer's own shadow can contribute significantly in causing photos to be rejected by the photogrammetric software.

While the technique of photographing a site in indirect sunlight achieves best results for archaeological documentation, mapping, modelling and measurement, the author also found that taking photos at high noon resulted in models that were more conducive to presentation and explaining a site or aspect of it to non-archaeologists. The lighting is more like what they see upon visiting in person and so is more conducive to a 3D walkthrough. There are also features that cannot be modelled in dim lighting. In an excavated area in Ancient Corinth, a number of wells and robbing pits had been unearthed. All of them were too deep and narrow to allow photos in dim lighting, with myself blotting out what little light there is with my own body and camera.

On June 21, 2012: the summer solstice, the author photographed the wells of the most recently excavated site at Ancient Corinth, gaining lighting that lit their entire depth, and with light reflected within, was able to achieve detail from even the un-illuminated walls. Details such as these can later, once modelled, be stitched into low light models that were

not able to capture them, resulting in a comprehensive measurable model of every detail of the site.

With regard to bone, in some cases, an even lighting may be less preferable if pathology or trauma is intended to be captured in great detail for viewing rather than modelling. In such cases a consistent oblique lighting will accentuate the lesion making it more readable by the viewer once geometry is built and texture is applied.

Where possible, when not shooting for visually accentuated trauma details, it is best to shoot bone suspended, indoors with even, indirect lighting. The background in the room should lack complexity. This is not to say that the outdoor models or those done without suspending are unusable but that they require significant effort to clean them up and align their components to make them come close to the results that can be achieved, should a little extra effort be taken during the initial shooting.

Even in museum/indoor lighting it is important to remember that light coming from outside can affect results. The same expediency used to shoot outdoors should be applied indoors if there are windows allowing natural light into the room as the hot spot and shadows will shift with time.

3.4 - Software

In recent years a number of new or improved software have come onto the market. Prices cover a broad range, as do approaches. Some software is run on a local machine while others are run on the developer's server. Software available includes Agisoft Photoscan, Photomodeler Scanner (quite expensive), Smart3DCaptured at an unknown price,

123DCapture (an online 3D modeller which is free in its basic form), MenciEvo, Simactive (meant primarily for satellite and aerial photography), and My3DScanner (another free online 3d modeller).

123DCapture has a limit of 70 photographs in its free basic form. It runs online, with the user uploading photographs and Autodesk's computers processing them. Processing time is very fast. Models can only be exported in Autodesk's file formats however although the software is capable of producing some very impressive "flyovers". Like 123D Capture, PhotoSynth and Arc3D are also run online. With variable internet reliability in the field this was not a viable option.

Photomodeler Scanner, while offering more versatility, also requires a lot more manipulation and photogrammetric knowledge.

After researching and experimenting with the above mentioned modelling software suites, we chose to use Agisoft Photoscan based on its price relative to its power and accuracy. It is able to export in a number of the most common file types; obj, dxf, 3ds, wrl, dae, ply, u3d and pdf, bringing us closer to the secure long term access required of archaeological records. Orthophotos can also be exported in the popular formats of tif, jpg and png. The software's local installation meant that a reliable internet connection was not necessary. Also the software's ability to export DEMs was considered to be an asset.

Table 1 – Comparison of available photogrammetric and computer vision software after Verhoeven, G., Doneus, N., Doneus, M., & Štuhec, S., 30/2015., 168-169

Company	Software	Free	S M	F	MVS	Web	Ortho photo
Agisoft LLC	PhotoScan Standard		X		X		
Agisoft LLC	PhotoScan Professional		X		X		X
Matis Laboratory (I.G. N.)	Apero	X	X				
Matis Laboratory (I.G. N.)	MicMac	X			X		X
Univ. of Washington & Microsoft Corp.	Bundler	X	X				
Microsoft Corporation	PhotoSynth	X	X			X	
University of Washington	VisualSFM	X	X		X		
AutoDesk	123D Catch	X	X		X	X	
KU Leuven	Arc3D	X	X		X	X	
Eos Systems Inc.	PhotoModeler Scanner			X	X		X
Univ. of Illinois & Univ. of Washington	PMVS2	X			X		
3Dflow SRL	3DF Samantha	X	X				
Henri Astre & Microsoft Corp.	PhotoSynth Toolkit	X	X		X		
CTU Prague	CMPMVS	X	X		X	X	X
Acute3D	Smart3DCapture		X		X		

SFM = Structure from Motion, MVS = Multi-View Stereo

3.5 – Georeferencing

In order to obtain proper scale and measurements from a model, the surroundings of the actual site or object need to be georeferenced. Georeferencing is the process of determining where, within a physical space, specific points with real coordinates are in the 3-dimensions of that space, their relationship to each other and the distances between them. In photogrammetry it involves assigning those points to their corresponding locations on each photograph. This allows us to position the photogrammetric model within its context in the world, in a site or relative to other models. If we know the distances between the

georeferenced points then within our photogrammetric model we are able to obtain measurements between any two points. Initially, in the field we used the nail heads of pre-existing control points and used a total station to record them. In addition we used official geodetic reference points as recorded by the Greek military using the Hellenic Geodetic Reference System 1987 or HGRS87 (presenting its own set of problems due to the Greek system not being able to associate with other world systems). The HGRS87 uses 30 triangulated points assigned by the military, each using a point at the national observatory in Athens as a meridian and so the country is broken up into thirty maps. Conversion formulas that work for one map are not effective on others. “HGRS87 suffer from local distortions and systematic errors which are not easily detectable” (Dimitriadis and Ampatzidis 2014, 45). Even available map specific conversion formulas failed to provide any usable accuracy but fortunately with the release of ESRI’s ArcMap v.10 a perfected algorithm was included.

During summer 2015 we began positioning unique targets printed from the Agisoft software (Figure 10 - Unique targets as produced by Agisoft Photoscan) at positions that are easily seen and surveyed from the most possible vantage points around the sites. These unique targets not only provide a point of survey but also their design allows the software to discern their orientation relative to each other and using a total station we have recorded the reference points and entered them into the models during the software phase. We also georeferenced using a GPS in order to be able to place our models within a broader context.

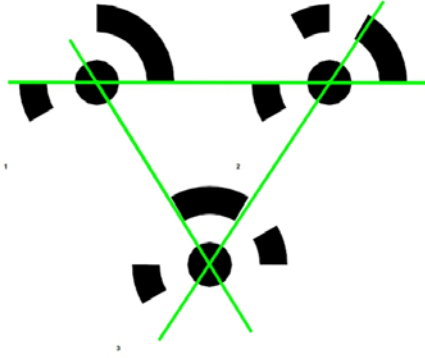


Figure 10 - Unique targets as produced by Agisoft Photoscan

3.6 – Modelling

Once a set of photographs has been taken and edited for consistency, lighting, contiguousness and lack of contamination by extraneous objects, the photos are added to the project. A sparse point cloud is then initiated under workflow with choice given to how accurate the processing is to be. The software examines the photographs, finding arrays of common points, associating them and then calculating from their parallax, their relative distance and position within a 3-dimensional space. This forms a point cloud; hundreds, thousands or even hundreds of thousands of points within an X Y and Z coordinate. 3D modelling of the Pirene fountain in Ancient Corinth involved using 293 photos (after the software rejected 8 for focus, lighting or irrelevance due to a lack of overlap) and produced a point cloud of 687,445 points.

On a large project, producing a model of the least possible accuracy can be of great assistance and time saving in assessing the viability of the model. In minutes we can determine if the software is misinterpreting the photos. More accurate models can require large amounts of time and processing power. Photoscan allows multiple models known as chunks to be constructed within a project. If the more accurate version of the model is going

to be too unwieldy, multiple chunks can be combined after all processing is completed.

Once the sparse point cloud is produced, steps are taken to georeference control points, allowing the software to better align the images. First the software automatically recognizes targets within the point cloud. Surveyed georeferenced points are then imported into the model and those points appear on each photograph. Most markers then appear on the photos as confirmed location flags while others form the “smoking points” that Photoscan uses to denote suggested locations for markers. Each of these smoking points, sometimes in the hundreds, then have to be individually adjusted into place over the centre of each target. Once every flag is in place in all of the photos, the cameras (photos) must be automatically optimized.

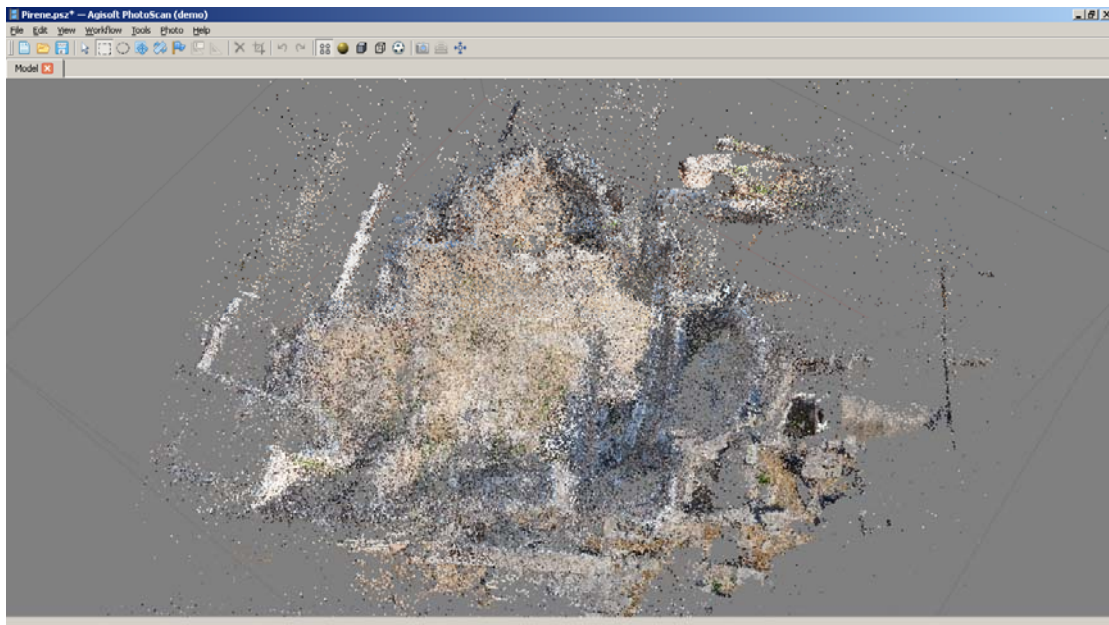


Figure 11 - Sparse point cloud: Peirene Fountain, Ancient Corinth

At this point, with a large number of points chosen, the basic shape of the structure can be perceived, giving the modeller an idea of whether it is worth continuing as well as the

opportunity to “cut off the chafe” before devoting a large amount of processing time to building the geometry of the model. Also for the first time we are able to see our camera angles as represented by blue rectangles around the point cloud. This can be very useful in learning what angles achieve the best results and honing one’s technique with each model.

The Dense Cloud is then able to be constructed. This is done using Multi-View Stereo (MVS) algorithms (Verhoven 2013, 169). It is a process similar to the production of the sparse cloud but with significantly more points and detail. This is due to the fact that the sparse point cloud is only made from noticeably unique points in the photographs while the dense cloud is made of all possible points on a pixel by pixel basis now that the orientation of the photographs is known. The dense cloud also has variable options for accuracy. Once produced the object is recognizable enough to perceive greater details, allowing further editing to remove unwanted elements. When the dense point cloud has been trimmed to represent exactly what we want in our model it is ready for geometry building (triangulation).

When geometry building commences the software creates vectors joining each point in the model to two adjacent points, forming a triangle. Each side of each triangle, apart from those on the periphery, is joined to the side of another triangle, the sum of which forms a mesh.

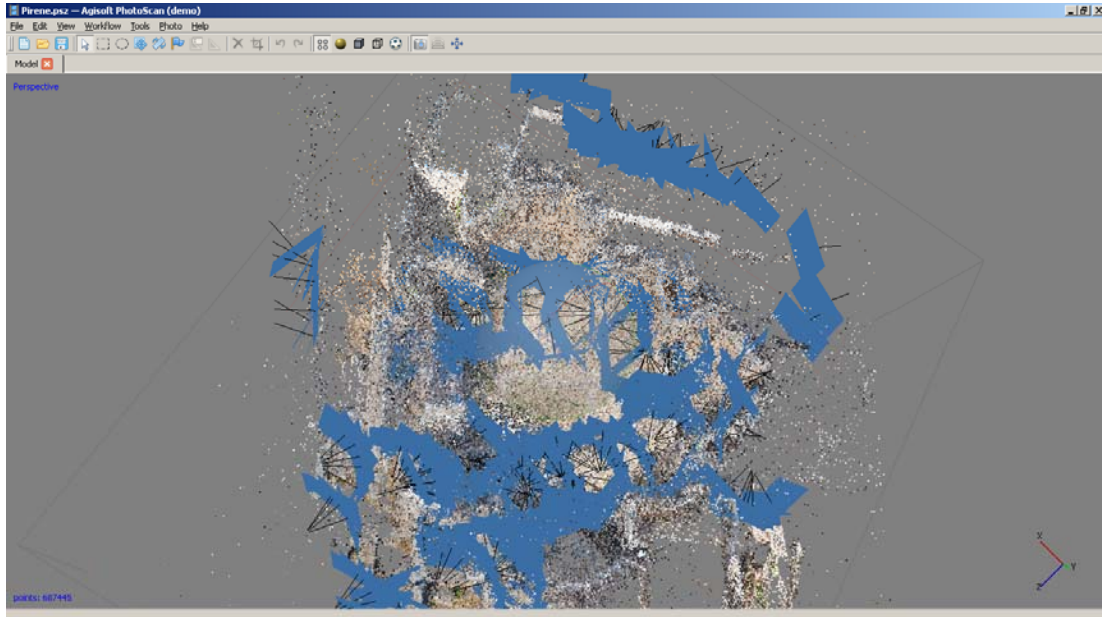


Figure 12 - Camera angles represented with blue rectangles representing the focal plane: Peirene Fountain, Ancient Corinth

Basic colours of the points are averaged into the mesh giving it a recognizable but slightly artificial look. In some cases, this is all that is necessary for having a useable, exportable model. The resulting mesh is the true 3D model and is now capable of being used in many 3D applications. For example, the mesh can now be used to produce a digital elevation model with accurate, measureable XYZ dimensions. For presentation purposes we may want to add texture. Photoscan takes a section of photograph that correlates to within each set of three points (the triangles) and applies it to the mesh. This stage allows several options as far as accuracy and effect. Experimentation eventually leads to better results. At this point the model is completed and can be exported in the file format best suited to its intended use. For example, if the model is to be used to produce orthographic drawings of an excavation it is exported as a dxf so that it can be imported into AutoCAD.

The methods described here, while continually evolving with experience leading to greater accuracy, have been found to satisfy some of the most important archaeological criteria as

mentioned in the introduction: measurements, scale, size, complexity and budget. While questions of accuracy and error have been continuously reduced with better targets, target placement and surveying, other problems such as occlusions, unwanted inclusions, variations in exposure, etc. have been addressed through trial and error and coming to understand what will and will not work in a given situation. Accuracy has been further enhanced by honing the operations, settings and order of model production at the software phase.

Using a new version of the Agisoft Photoscan software that separates sparse cloud building and dense cloud building allows for adjustments that enhance the accuracy of the model. In between the two steps, coordinates are imported and the markers for those coordinates are manually adjusted on each individual photo, dragging a flag for a possible location (shown as a puff of smoke) onto the exact location. The alignment of the photos is then optimized generating a camera calibration based on the ground control points – GCP (using the “optimize cameras” command). The dense point cloud is then produced.

Another step taken in the improved models is the ability to apply texture using a set texture size and then telling the software to use X number of images of that size. For example the texture size requested can be 4096 pixels repeated four times. The result has more accuracy and a greater visual detail and appeal.

A step by step tutorial of these improvements in technique is described in Appendix 1 – Tutorial and the effect on accuracy can be seen in 4.2.1.B - Mosaic Reinstallation Methodology (2015).

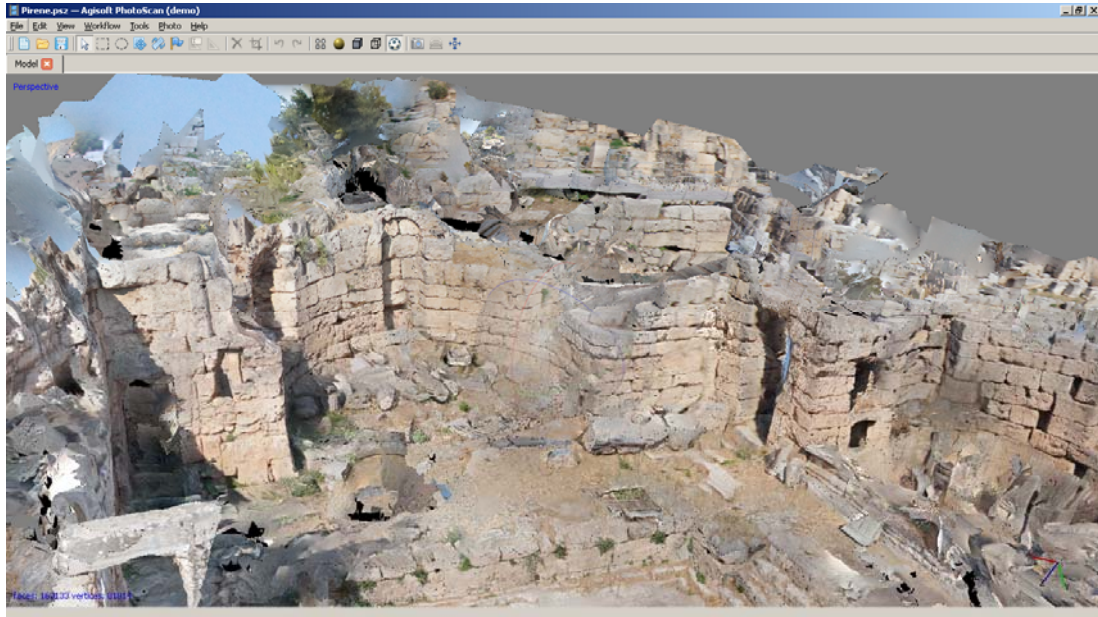


Figure 13 - Mesh with textures added: Peirene Fountain, Ancient Corinth

Chapter 4 – In Situ Documentation

Archaeological excavation, the basis of archaeological interpretation, can be defined as the process of controlled unearthing and recording of archaeological remains using appropriate methods and tools within a specified area (for the problems in archaeological interpretation see indicatively Hodder et al. 1995, Hodder and Hutson 2003). Since excavation is an unrepeatable, irreversible process, the ongoing goal of any excavator is to document the project in an objective manner (Hodder 1997, 691-700, Lucas 2001, Bradley 2015, 23- 41).

In order to address the issue of objectivity, - or rather subjectivity-, archaeologists have been using a variety of technological applications. As already mentioned (Chapter 2 - History and Development), photogrammetry and 3D technologies have been used for many years in a plethora of archaeological projects in order to document structures and landscapes. Recently, 3D technologies have been applied in the excavation workflow, aiming at making the process virtually reversible (Forte et al. 2012, Forte 2014). Previously photo documentation and drawings were used to document a site as it was excavated. Photo documentation often focussed on individual details and even when photos were taken from a more comprehensive viewpoint less consideration was given to overlap than is the case with photogrammetry and could result in gaps in the record. Any aspect of the site that was not measured at the time was less likely to be measureable after the fact. Orthographic drawings were done by the site architect in cases of a structural site as shown in Figure 14. These required setup, removal of people from the drawing area and a considerable amount of time to render. The resulting drawings, although relatively accurate, do rely on the illustrator's eye for detail whereas the shapes and dimensions captured using photogrammetry are completely objective.



Figure 14 - Site Architect for Ancient Corinth, James Herbst hand drawing orthographic site details (Photo - Rossana Valente).

With the use of photogrammetry it is now possible to document a site as it is being excavated at each level without undue intrusion on the process and for relatively little money and effort.

This chapter will present case studies of documentation of current archaeological

excavations, previous excavations that are still accessible, the use of archival excavation photos to recreate sites and specific smaller scale features from within an excavation. It will describe the sites or features, the goals and the methodology used in each case.

4.1 - Sites

4.1.1 - Thebes Temple and Graves



Figure 15 - Temple of Ismenios Apollo and Graves - Thebes

In summer 2013 James Herbst and the author travelled to Thebes, Greece to document the temple of Ismenios Apollo and numerous stone cut Byzantine graves at the homonymous sanctuary on a grassy hill within the city. The temple has “dimensions 21,60 X 9,30 m and

columns respectively 12X6, built perhaps after the battle of Leuktra (371 B.C.)” (Ministry of Culture and Sports | Thebes).

The 3d modelling was to be used as both a detailed record of the topography (thousands of points rather than just the few that could be surveyed) as well as being able to facilitate orthographic drawings. The temple was built in 371 BC and replaced a previous temple built circa 700 BC which had still been in use in the fifth century BC. (Symeonoglou 1985, 131-133). The site is interspersed with a large numbers of trees. The challenge with the trees was that they would create inconsistent lighting conditions.

The first step was for us to survey the site using the total station. We used 15 control points for the surveying/shooting; all of which were positioned to be visible from multiple vantage points in and around the site. Our solution to the lighting problem was to take photos as quickly as possible at dusk and dawn. This created two constraints for us. The first and most obvious is that the sun is relentlessly moving without consideration of how many photographs we need to take. In the case of the Thebes temple, hundreds of photographs needed to be taken in the 30 to 40 minutes of consistent lighting available to us. We took two approaches. Herbst used a ladder to capture more of the site but by necessity was able to take less photos. I circled around and through the site on foot and was able to take more photos but ones that were more dependent on their neighbours for continuity. The graves, which were cut into the bedrock during the Byzantine period, needed to be photographed first in the evening and last in the morning in order to capture enough light to preserve detail. As discussed in the lighting section of the general methodology, the goal is to keep the exposure time at its longest for the greatest depth of field but the elements of shooting in twilight and of shooting handheld require a compromise. As a result, my photos were taken

at 1/80 of a second with apertures ranging from f/5.6 to f/10 using an ISO-6400; a compromise that gave us our best result: a cohesive site with high detail.



Figure 16 - Thebes model detail using initial technique



Figure 17 - Thebes model detail using later technique

The resulting model used 158 of the 185 photos that were input. Maximum height variation while shooting was just over 3 metres. The model had an overall error of 0.024625 metres or 2.5 centimetres meaning that in a model with a length of over 26 metres (the temple itself is 21.60 X 9.3 metres) there was an error of 1.04 millimetres per metre. Error data is

provided by the software while producing a report. While the surveying of the site with total station was accurate, the low light in combination with using the nail heads of marker tags; which in many cases were not discernible in photos involving any distance, made calibration of the photos during the modelling process difficult and not as comprehensive as desired. With the newer unique markers which are far more visible both to the naked eye and the modelling software as well as techniques that have been honed on subsequent projects this error could be significantly reduced. Just using the new processing techniques outlined at the end of the General Methodology chapter has resulted in the overall error decreasing from 0.024625 metres to 0.011593 metres. This is reflected in the clarity of modelling as shown in Figure 16 - Thebes model detail using initial technique and Figure 17.

Thebes Original Modelling

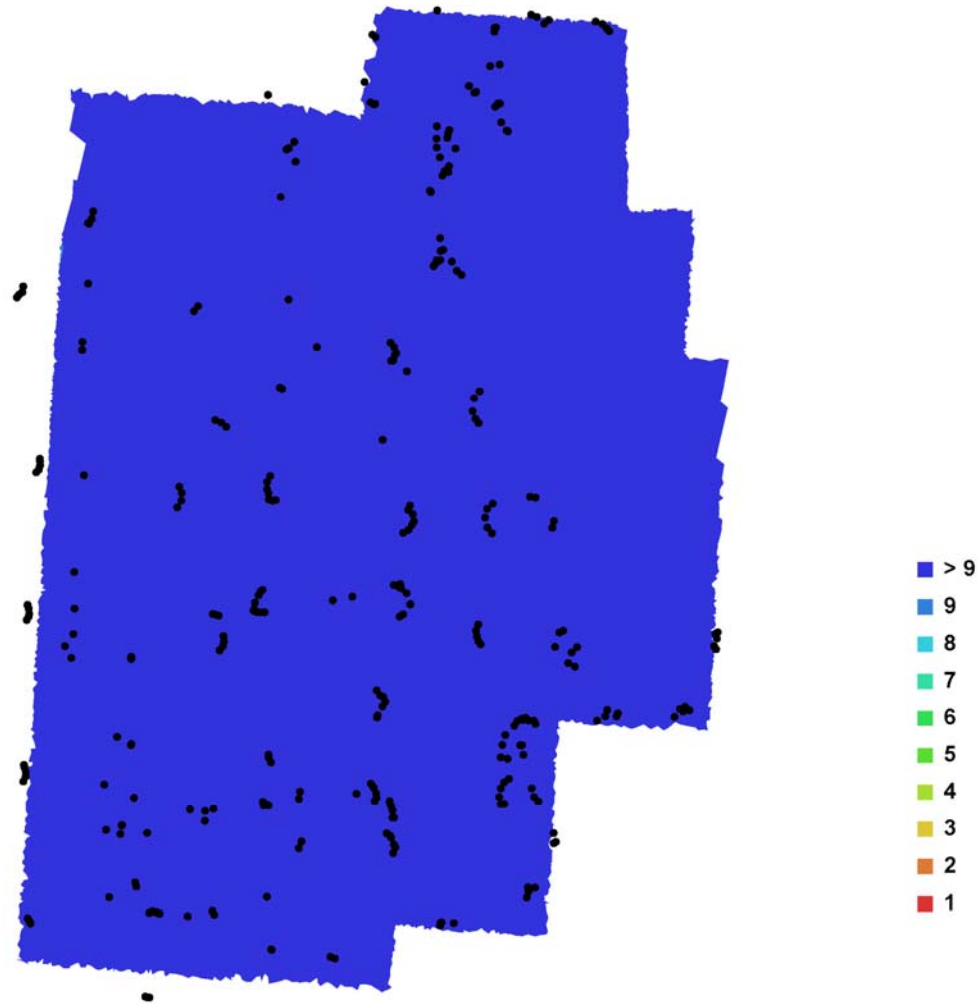


Figure 18- Camera locations and image overlap: Thebes

Number of images:	324	Camera stations:	308
Flying altitude:	3.00493 m	Tie-points:	884297
Ground resolution:	0.00104464 m/pix	Projections:	2044485
Coverage area:	0.000441923 sq km	Error:	0.691223 pixels

Table 2 - Thebes cameras

Camera Model	Resolution	Focal Length	Pixel Size	Precalibrated
SLT-A35 (18 mm)	4912 x 3264	18 mm	4.89089 x 4.89089 um	No
SLT-A35 (18 mm)	4912 x 3264	18 mm	4.89089 x 4.89089 um	No



Figure 19 - GCP Locations: Thebes

Table 3 - Thebes control points

Label	X error (m)	Y error (m)	Z error (m)	Error (m)	Projections	Error (pix)
01	-0.004448	0.001976	0.017447	0.018113	8	5.598013
02	-0.020235	0.008156	-0.002796	0.021995	6	6.075157
03	0.032296	0.009562	-0.008425	0.034719	4	12.468351
04	-0.018509	-0.014768	-0.012026	0.026557	9	11.986769
05	0.009288	0.038462	0.002608	0.039653	6	24.175851
06	-0.018068	0.013028	0.009935	0.024390	3	3.018125

07	0.033495	0.008131	-0.000274	0.034469	12	10.189140
08	0.008819	-0.024537	-0.008913	0.027555	12	16.601247
09	-0.000000	-0.000000	-0.000000	0.000000		
10	0.005296	0.002706	0.011242	0.012718	3	8.813260
12	0.015052	0.001233	-0.000316	0.015105	4	4.330530
14	0.000161	-0.000539	-0.007088	0.007110	8	7.754287
15	-0.020896	-0.009870	-0.008446	0.024605	11	7.337007
Total	0.017799	0.014686	0.008597	0.024625	86	11.741173

Thebes - Digital Elevation Model

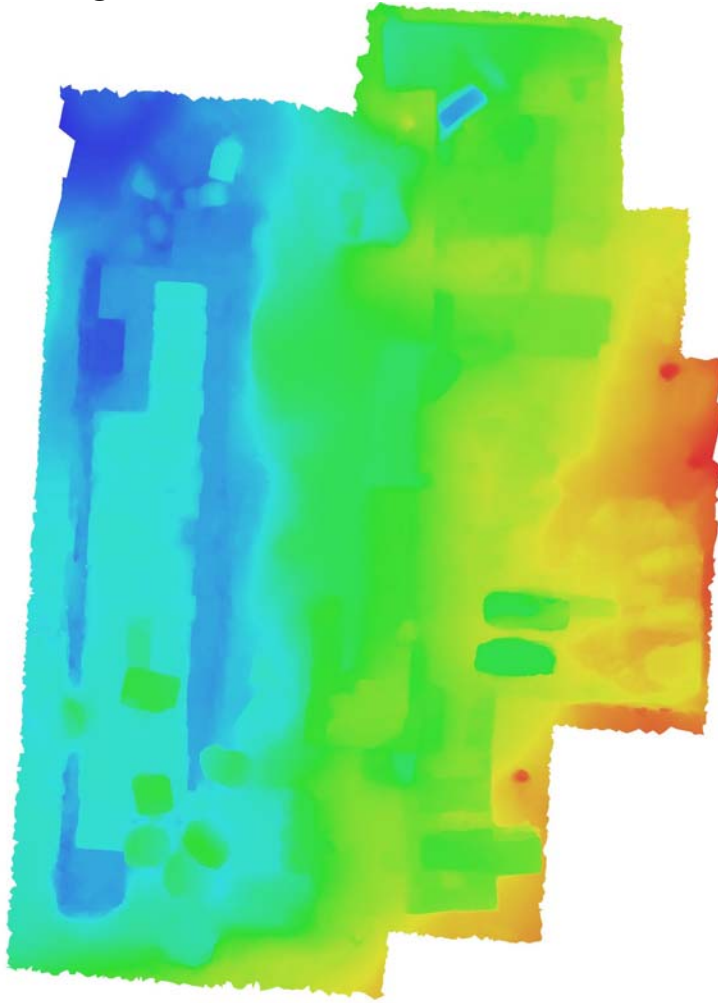


Figure 20 - Reconstructed digital elevation model: Thebes

Resolution: 0.00835709 m/pix
Point density: 14318.2 points per sq m

Thebes Revised Modelling

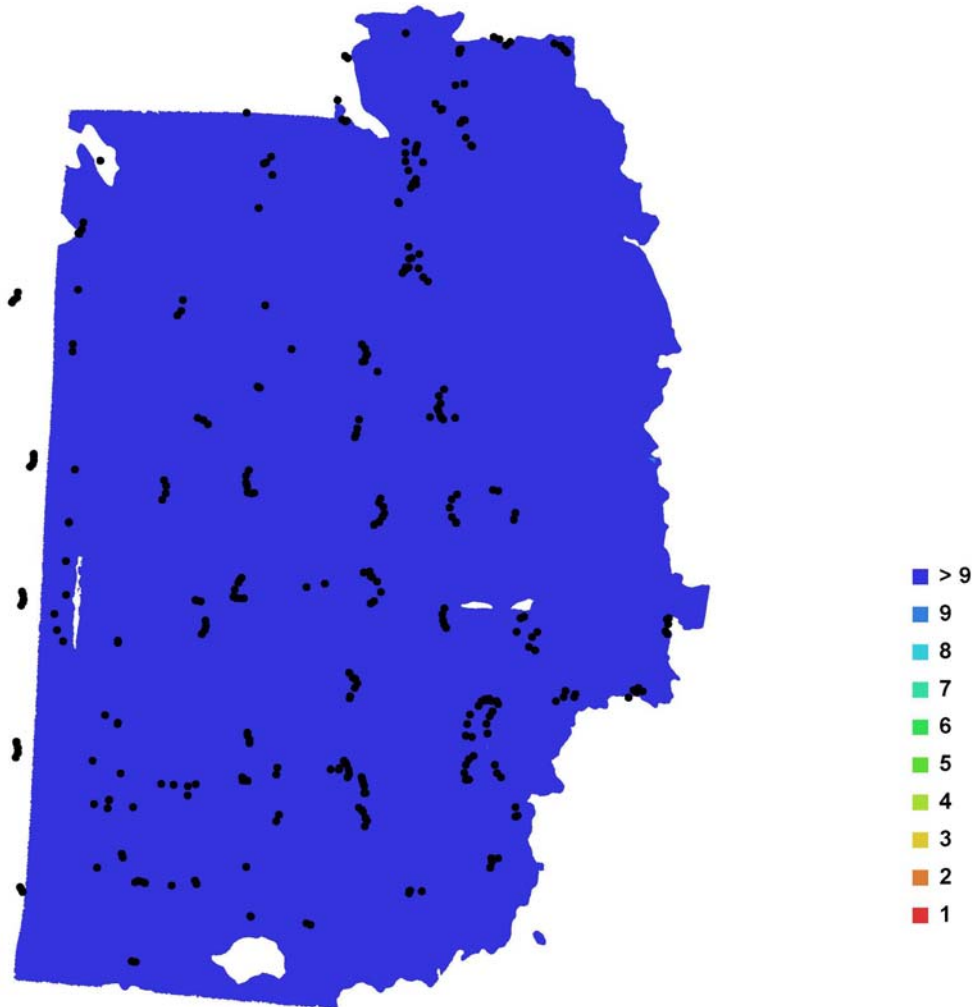


Figure 21 - Camera locations and image overlap: Thebes Revised

Number of images:	324	Camera stations:	324
Flying altitude:	3.13011 m	Tie-points:	71452
Ground resolution:	0.000857417 m/pix	Projections:	237909
Coverage area:	0.000473845 sq km	Error:	1.0489 pix

Table 4 - Thebes revisited cameras

Camera Model	Resolution	Focal Length	Pixel Size	Precalibrated
SLT-A35 (18 mm)	4912 x 3264	18 mm	4.89089 x 4.89089 um	No
SLT-A35 (18 mm)	4912 x 3264	18 mm	4.89089 x 4.89089 um	No

Thebes Improved Modelling



Figure 22 - Ground Control Points - Thebes Revised

Table 5 - Ground Control Points - Thebes Revised Model

Label	X error (m)	Y error (m)	Z error (m)	Error (m)	Projections	Error (pix)
01	0.003984	0.004494	0.020375	0.021242	9	2.549567
02	-0.003549	0.011071	-0.006687	0.013412	24	4.098864
03	-0.003484	0.003398	-0.008150	0.009493	12	2.120575
04	-0.002472	-0.010812	-0.003054	0.011504	9	13.833974
05	-0.001070	0.004702	0.010001	0.011103	6	1.888760
06	0.000853	0.000561	-0.002144	0.002374	3	3.100250
07	0.014314	-0.000654	-0.000306	0.014333	15	7.718813
08	0.000261	-0.001688	-0.006955	0.007162	14	4.534638
09	0.000192	-0.002388	-0.000268	0.002411	1	0.000000
10	-0.000187	0.000158	0.001164	0.001189	3	5.563926
12	0.011659	0.005099	-0.001405	0.012803	5	3.513489
14	0.003395	0.000449	-0.009261	0.009874	9	5.748219
15	-0.010867	-0.005050	-0.009790	0.015474	11	2.438379
Total	0.006320	0.005221	0.008198	0.011593	121	5.740452

Thebes Revisited - Digital Elevation Model

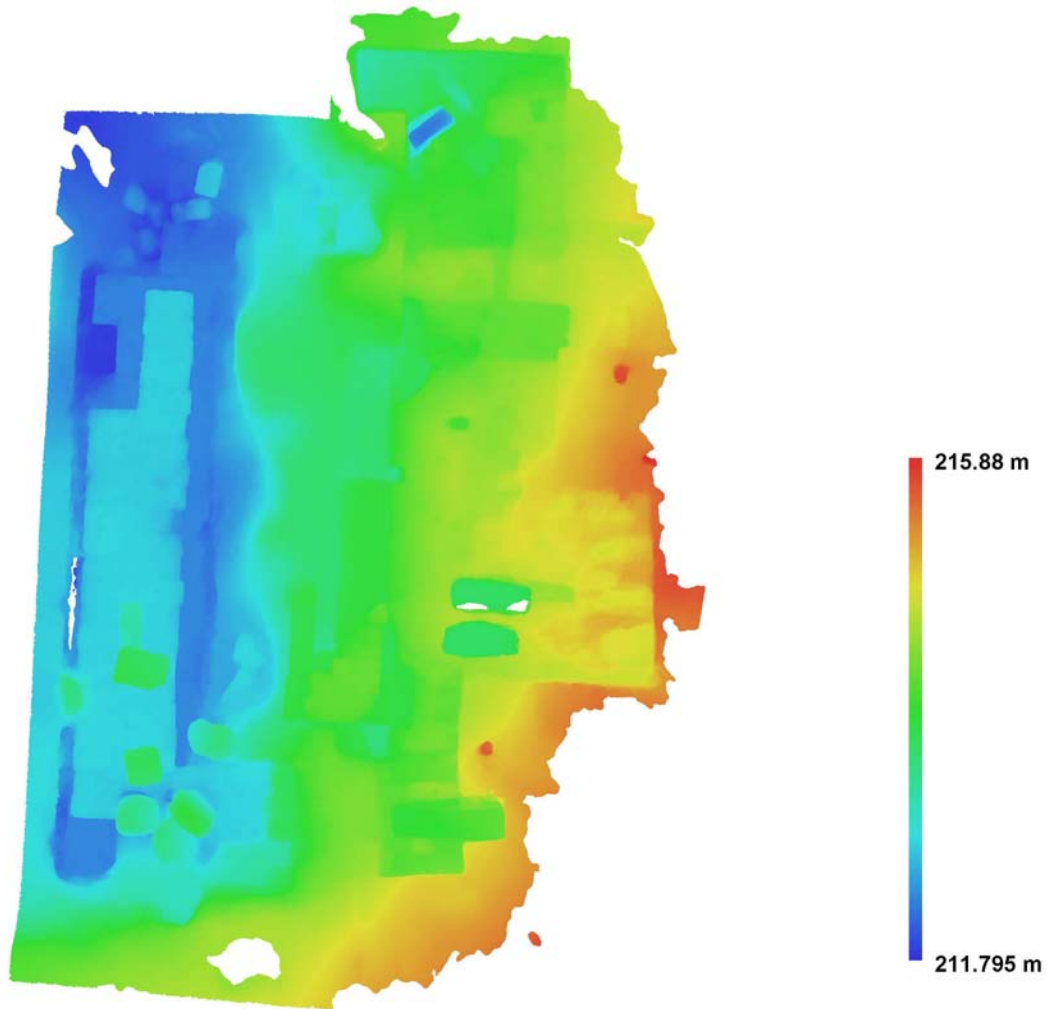


Figure 23 - Reconstructed Digital Elevation Model - Thebes Revised

Resolution: 0.00342967 m/pix
Point density: 85015.1 points per sq m

4.1.2 - Frankish Structures in Ancient Corinth



Figure 24 - Frankish section of Ancient Corinth excavations

In the summer of 2014 James Herbst and the author documented a large area of excavation while it underwent preservation measures. Known as the “Frankish section south of Temple E”, this area consisting of an urban domestic assemblage, shops, a church, monastic structures and graves was part of the city of Corinth during the Frankish period (13th and

14th century AD). (For further information on the Frankish area see Williams 2003, 4)

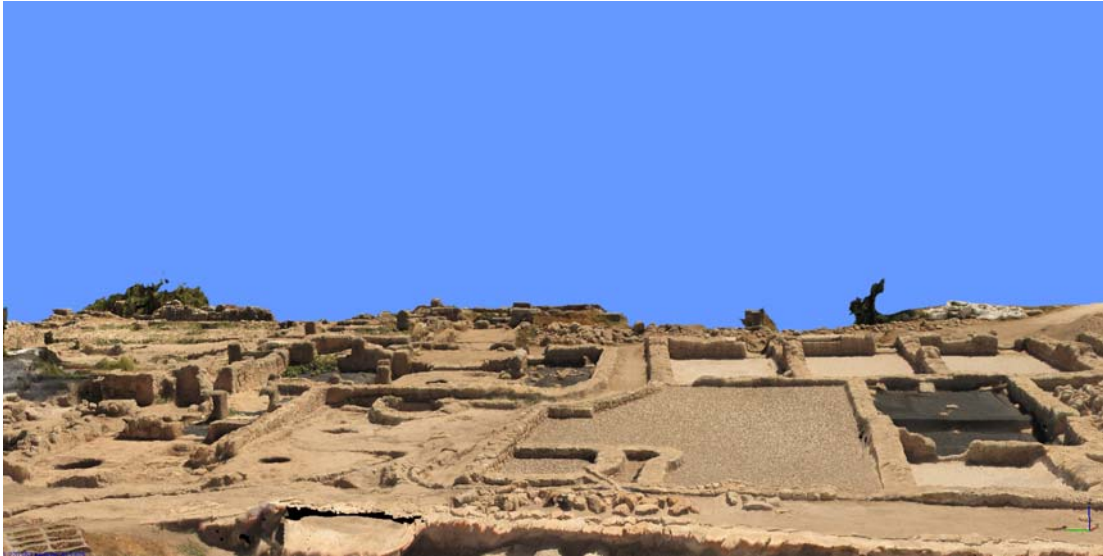


Figure 25 - low level view produced from only high altitude photos: Frankish area

The purpose of this model was both to experiment with new means of elevating our view as well as recording both the preservation efforts and the 2014 season excavations.

After a number of experiments with very large kites which proved to have variable reliability, weather dependency and even dangerous behaviour, we used a large helium balloon about two metres across combined with a camera that Herbst had modified in order to have it take a photo every five seconds. We each had a tether of over 100 metres and would position ourselves on opposite sides of the subject area. Then by moving one person or the other or both we were able to continuously move the balloon over new areas. Our movements were based on estimates of how much overlap we were achieving and what areas we wanted coverage of. The results were excellent and an illustration of the amount of overlap appears in Figure 30 - Camera locations and image overlap: Frankish area.



Figure 26 - James Herbst launching a kite over the Frankish area

There was, however, the problem of getting close to trees as the balloon was delicate. In addition there was the inability of getting under and between trees to capture features that would otherwise be hidden by them. Our solution at the time was to combine our aerial shots with ground level shots. Although this solution was effective it did involve using different cameras and exposures as well as not allowing us to access less accessible areas. In 2015 Herbst introduced a better, more versatile solution with the purchase of a Phantom III drone (Figure 28).



Figure 27 - Helium balloon and camera apparatus

The drone was not only versatile enough to move under and between trees but it was also less susceptible to high winds and had a greater range and altitude than the balloon. Furthermore, the drone is able to transmit its live image to a smartphone on the ground so that the user is able to see exactly what the drone is seeing; helping to ensure that there is sufficient overlap in the photographs. While taking aerial photographs at a site like Ancient Corinth one restriction is that we must not fly kites, balloons or drones over top of tourists. The altitude and controllability of the drone allows the user to be offset from the subject and still be able to produce accurate orthographic views from our models. A problem with the drone, however, is that it can be subject to drift in high winds or at higher altitudes. As long as enough photos are taken and care is given to watching for and preventing drift an accurate model can be produced using ground points.



Figure 28 - Phantom III drone

The resulting model of 2014 used 115 of the 121 photos input. Maximum height variation while shooting was just over 15.1182 metres. The resulting model had an overall error of 0.188689 metres. This technique allowed us to document a site on a much larger scale of 4233.260m².

The models produced using these methods allowed us to accurately document ongoing stages of preservation and excavation so that there is both a 3 dimensional snapshot of that stage of the site and so that Herbst was able to update orthographic drawings of the site.



Figure 29 - Frankish area model from drone photos

Frankish Area Balloon Modelling

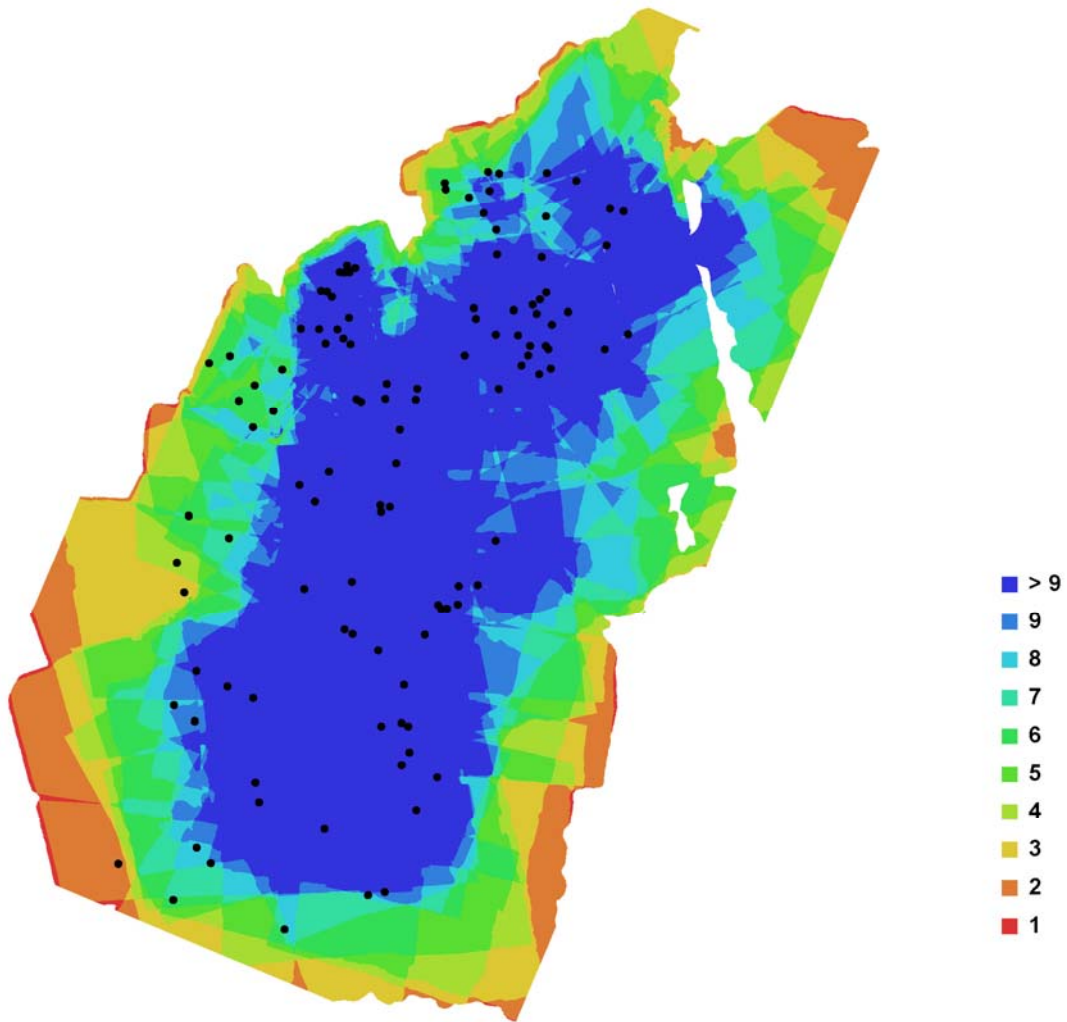


Figure 30 - Camera locations and image overlap: Frankish area

Number of images:	121	Camera stations:	115
Flying altitude:	15.1182 m	Tie-points:	202734
Ground resolution:	0.00389136	Projections:	563417
m/pix		Error:	0.779176
Coverage area: 4233.260m ²		pix	

Table 6 - Frankish area balloon cameras

Camera Model	Resolution	Focal Length	Pixel Size	Precalibrated
Canon PowerShot G10 (6.1 mm)	4416 x 3312	6.1 mm	1.67953 x 1.67953 um	No



Figure 31 - GCP locations: Frankish area

Table 7 - Control points: Frankish area balloon modelling

Label	X error (m)	Y error (m)	Z error (m)	Error (m)	Projections	Error (pix)
2	-0.028326	0.005092	0.003885	0.029041	4	0.592271
3	0.000000	0.000000	0.000000	0.000000		
4	0.122956	0.039178	-0.039563	0.134975	4	2.610579
5	-0.643622	-0.009409	-0.023709	0.644127	4	0.448597
6	0.137541	-0.025279	-0.012850	0.140434	3	1.115818
7	0.100139	-0.028462	0.009321	0.104522	4	2.037185
9	0.075597	-0.008334	0.032986	0.082900	6	1.173724

10	0.071065	0.016334	0.012586	0.073996	9	1.084887
11	0.010861	-0.008458	0.209195	0.209647	3	10.482194
12	0.059031	0.040737	-0.010633	0.072507	9	1.137574
13	0.017563	0.036835	-0.019664	0.045299	3	4.852060
14	0.009344	-0.030513	0.040406	0.051488	4	1.802656
15	0.019210	-0.016984	-0.013797	0.029118	2	0.167087
16	0.028372	-0.034605	-0.003208	0.044864	4	7.637500
17	0.005209	-0.039527	-0.024332	0.046707	5	2.986858
18	0.000000	0.000000	0.000000	0.000000		
19	0.043846	-0.134722	-0.052592	0.151124	2	2.534643
20	0.085737	-0.128288	0.024606	0.156251	3	5.709582
21	0.135795	-0.139654	-0.003158	0.194817	2	0.287384
22	0.229948	-0.079278	-0.099950	0.262966	3	1.033212
23	0.186715	-0.120844	-0.143777	0.264835	1	0.000000
24	0.000000	0.000000	0.000000	0.000000		
25	0.000000	0.000000	0.000000	0.000000		
26	0.251156	-0.143343	0.107443	0.308497	1	0.000000
27	0.000000	0.000000	0.000000	0.000000		
28	0.148737	-0.002281	0.230528	0.274355	1	0.000000
29	0.163513	-0.056035	-0.023962	0.174501	2	1.136286
Total	0.161299	0.063594	0.074444	0.188689	79	3.352968

Frankish Structures - Digital Elevation Model

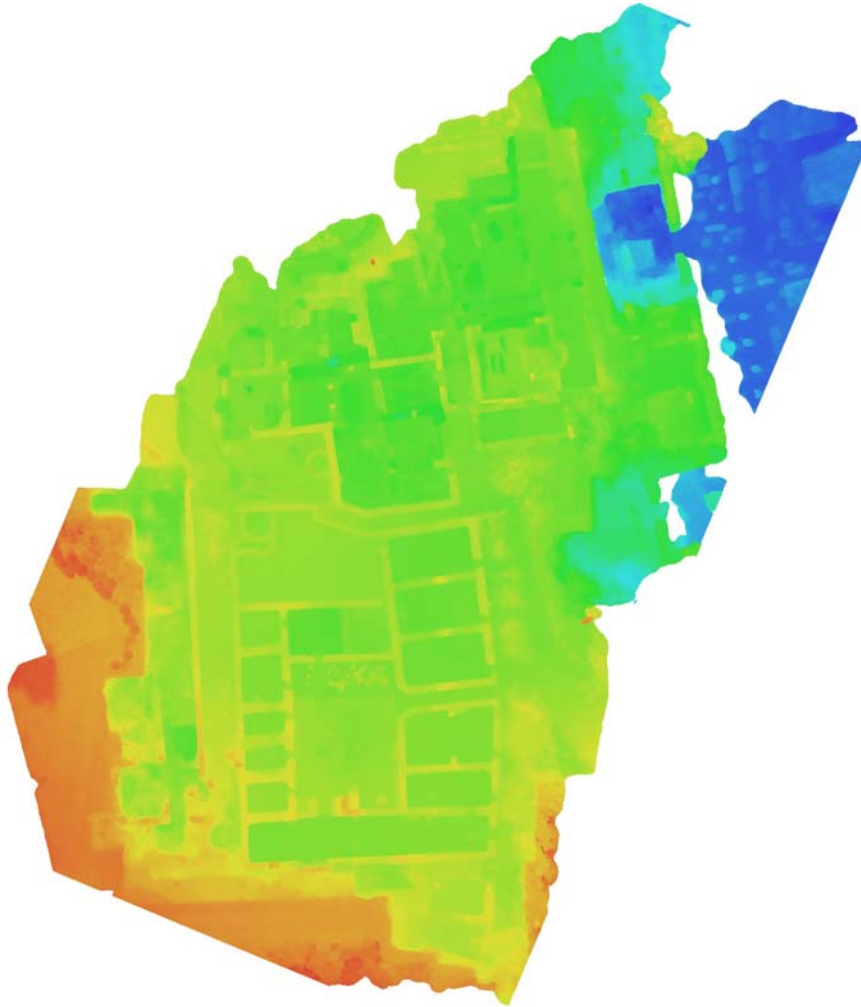


Figure 32 - Reconstructed digital elevation model: Frankish area balloon model

Resolution: 0.0155654 m/pix,
Point density: 4127.41 points per sq m)

Frankish Area Drone Modelling

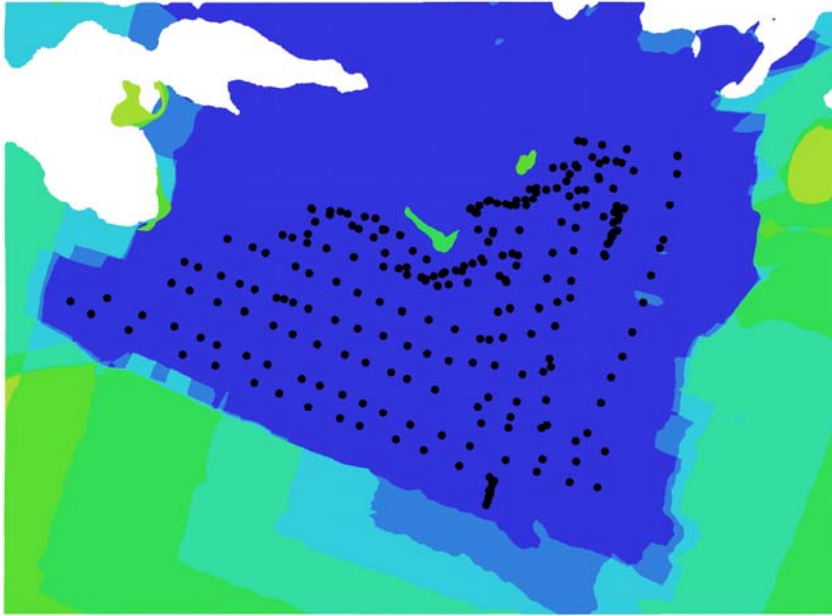


Figure 33 - Camera locations and image overlap Frankish area drone modelling

Number of images:	257	Camera stations:	257
Flying altitude:	8.46703 m	Tie-points:	31666
Ground resolution:	0.00273729 m/pix	Projections:	267690
Coverage area:	0.00352356 sq km	Error:	1.0414 pix

Table 8 - Cameras: Frankish area drone modelling

Camera Model	Resolution	Focal Length	Pixel Size	Precalibrate
FC300X	4000 x 3000	unknown	unknown	No

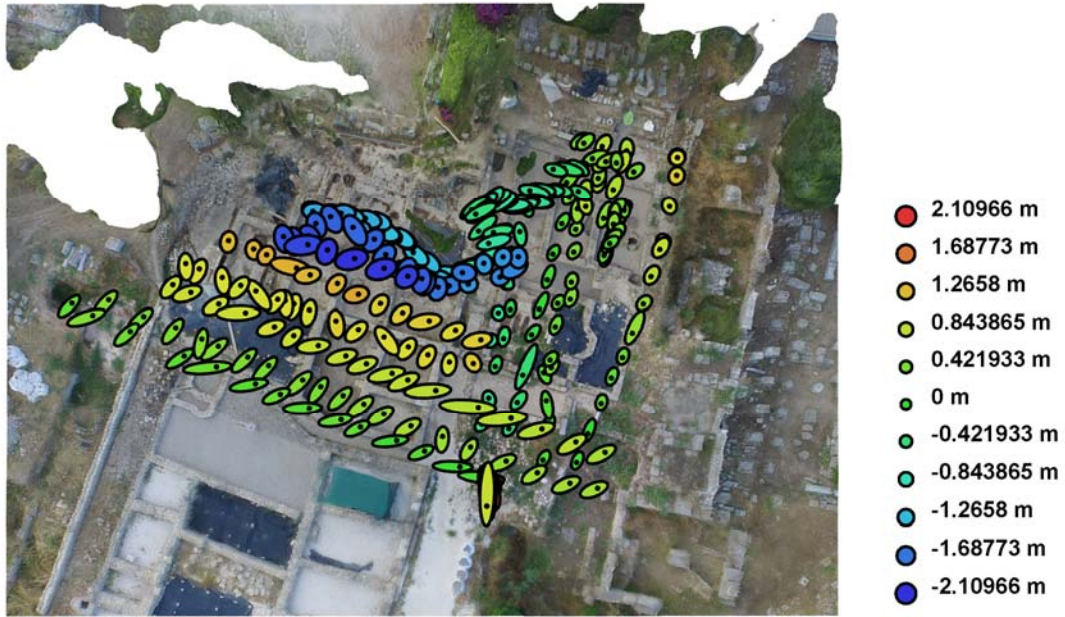


Figure 34 - Camera locations and error estimates: Frankish area drone modelling
Z error is represented by ellipse colour. X,Y errors are represented by ellipse shape.
Estimated camera locations are marked with a black dot.

Table 9 - Average camera location error: Frankish drone modelling

X error (m)	Y error (m)	Z error (m)	Total error (m)
0.466746	0.482195	0.927180	1.144564

Frankish Drone Modelling – Digital Elevation Model

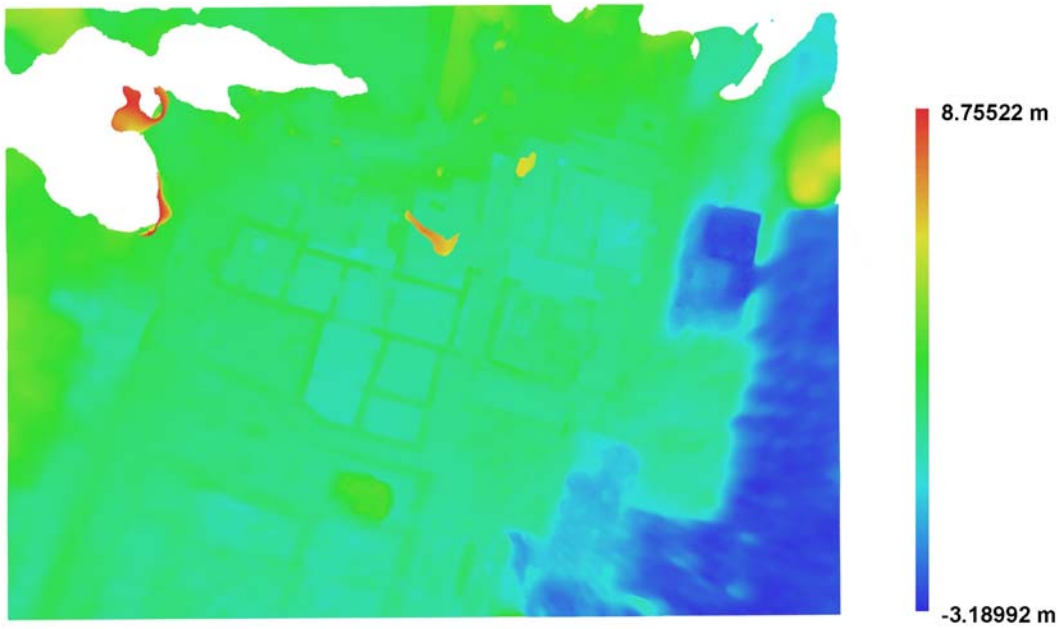


Figure 35 - Reconstructed digital elevation model: Frankish area drone modelling

Resolution: 0.0218984 m/pix
Point density: 2085.34 points per sq m

4.1.3 – Asklepieion



Figure 36 - Ancient Corinthian Asklepieion

The Ancient Corinthian Asklepieion is a vast multidimensional temple complex of which little of the surface structures remain. The main temple was built in the 4th century BC while other aspects of the site date back to the 5th century BC. The complex was built at the north end of the city on the edge of a plateau and over top of a fresh water supply and was used as a hospital; medicine and religion being intertwined at that time. “The rock formation here is favorable to a steady supply of water. The edge of the plateau consists of a thin cap of poros or shelly conglomerate lying on thick beds of yellow clay on which water seeps from the higher levels to the south to issue out at the base of the cliff.” (Roebuck 1951, 1). Large rooms of the abaton where patients were treated are cut into the bedrock at the west end of the site and a number of them remain intact. The temple is centrally located in the complex with a stoa along the north edge. The layout can be discerned by foundation cuttings in the the rock. “The court fell into disuse during the Roman period and it

gradually filled with earth. In the 6th and 7th centuries A.D. the court and reservoirs were used for Christian burials.” (Corinth Monument Asklepieion n.d. For more information see Roebuck 1951 and Pfaff 2003.)

Photography of the site was done in summer 2014 by James Herbst and the author. The purpose of this modelling was to add these features to a larger more comprehensive mapping of the entire city of Ancient Corinth. We did not survey the site but instead used the gps readings from inside the camera. Targets were laid out on the site initially but their inferior quality combined with higher altitudes rendered them unusable.

Due to the size of the site we used the large balloon, transporting it in a truck bed through the narrow and thorny streets of the village prior to dawn. Because the site is large we needed to begin as early as possible to get all of our photos before the sun rose. Parts of the site are unstable, there are pitfalls, sheer ledges and rough terrain. Despite this the two of us were able to develop a technique by which we were able to achieve coverage of the entire site. Once again we used two long tethers for manouvering.

The model presented in this example used 86 photos, all of which were included by the software and with a high enough altitude that there was significant overlap between them. The resulting model could not be measured accurately because of the lack of survey data and the inaccuracy of the camera’s internal GPS. As can be seen in Figure 39 the camera’s inaccurate GPS combined with the movement of the balloon creates a range of readings. In future modelling of such a large site the use of large directionally unique targets produced in Photoscan would significantly reduce error as would surveying to provide known ground

point georeferences.



Figure 37 - Asklepieion model looking Southeast

Asklepieion

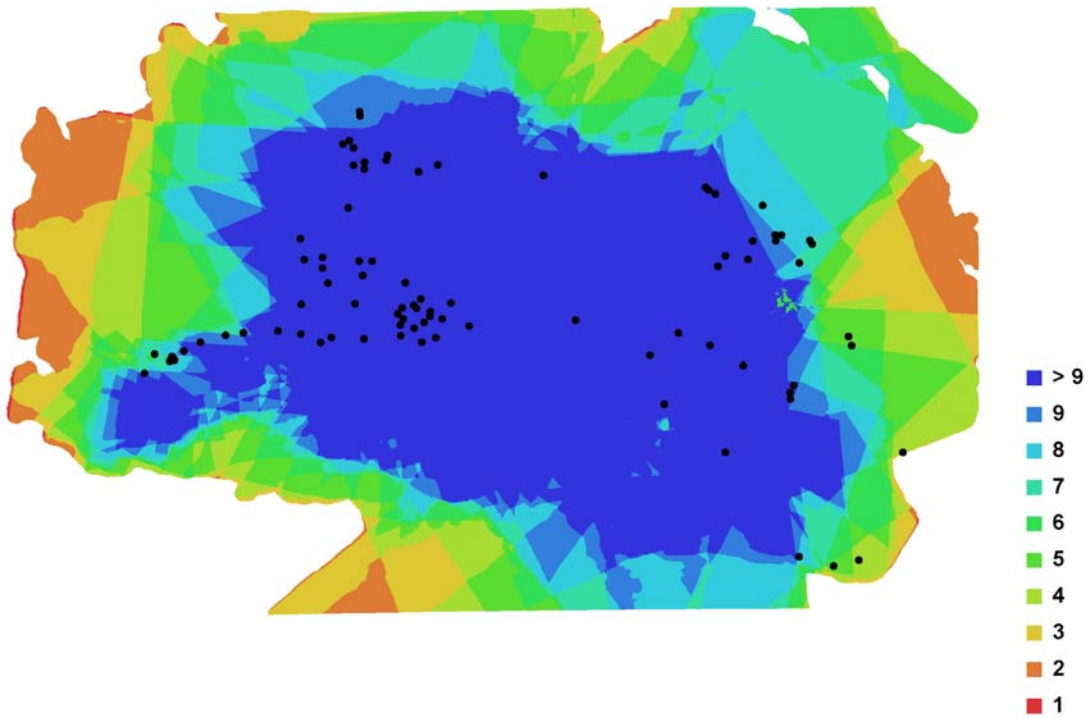


Figure 38 - Camera locations and image overlap: Asklepieion

Number of images: 86 Camera stations: 86
 Flying altitude: 22.29 Tie-points: 357159
 Ground resolution: 0.005 Projections: 1027024
 Coverage area: 6671. Error: 0.794774 pixels

Table 10 - Asklepieion Cameras

Camera Model	Resolution	Focal Length	Pixel Size	Precalibrated
Canon PowerShot G10 (6.1 mm)	4416 x 3312	6.1 mm	1.67953 x 1.67953 um	No

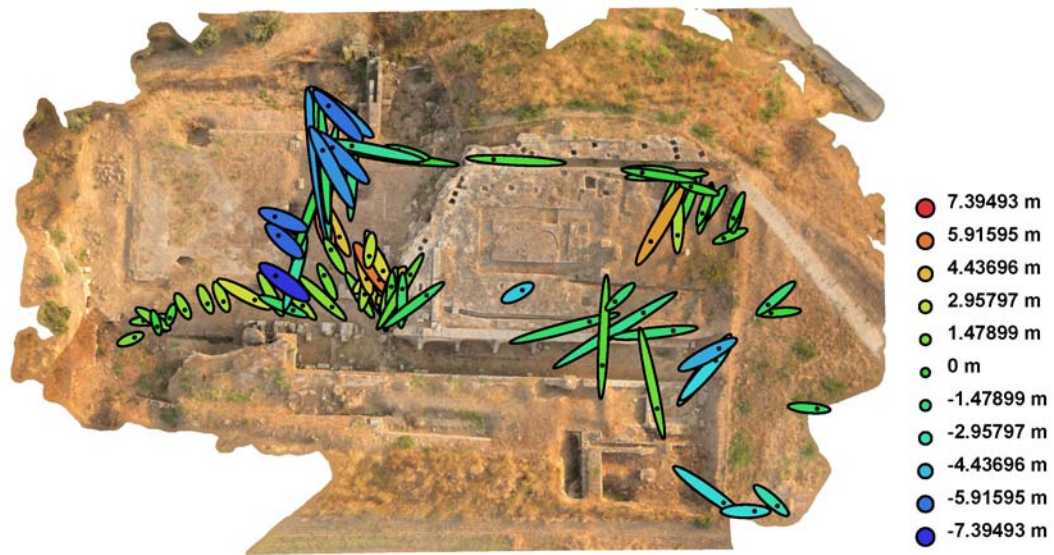


Figure 39 - Camera locations and error estimates: Asklepieion

Z error is represented by ellipse colour.

X,Y errors are represented by ellipse shape.

Estimated camera locations are marked with a black dot.

Table 11 - Average camera location error: Asklepieion

X error (m)	Y error (m)	Z error (m)	Total error (m)
2.405561	3.115297	2.902205	4.890255

Asklepieion – Digital Elevation Model

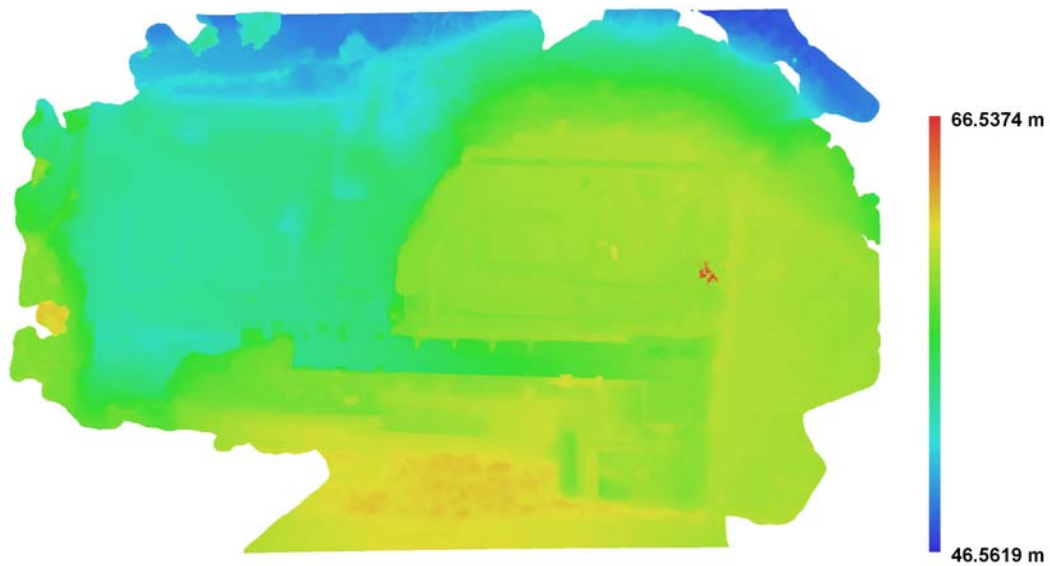


Figure 40 - Reconstructed digital elevation model.

Resolution: 0.0223861 m/pix

Point density: 1995.45 points per sq m: Asklepieion

4.4 – Fountain of the Lamps

“The city of Corinth possessed what must have been one of the most extensive underground water systems in the ancient world.” (Wiseman 1969, 75). In the summer of 1968 James Wiseman of Boston University and his team made what is perhaps the most significant discovery in this “underground city” (Wiseman 1969, 75); a marble Roman swimming pool dubbed “The Fountain of the Lamps” (Fountain of the Lamps), “part of a larger fountain-bath complex erected and refurbished during the Hellenistic and Early Roman periods” (Garnett 1975, 173). Although many artefacts were found in the fountain, the most significant was a collection of roughly 4,000 terracotta oil lamps. The lamps are thought to be votives; offerings to the gods (Garnett 2015, 410-412). The site consists of an underground bathing room with permanent wash basins; an underground fountain house; a network of water supply tunnels (and drains) to the bath, fountain and third room; a large outdoor courtyard with a swimming pool. (Wiseman 1972, 9). The entire complex is built into a naturally occurring grotto at the edge of a plateau.

The tunnels bringing water to the bath house, fountain house and pool are part of a complex of underground tunnels that extends for kilometres feeding numerous other fountains and homes in ancient times. The discovery of the site occurred contrary to what might normally be expected, with an upstream tunnel being found first, excavated towards the north (downhill) and leading first into one of the underground rooms and eventually into the pool area. (Wiseman recounts anecdotally that as they started to find the occasional lamp, he offered a reward of one drachma for every lamp a workman didn't break, not knowing of the trove they were about to come upon.) After the removal of many tons of soil and rock the site was documented, analysed and left untouched for decades.

During summer 2012 Wiseman gave a talk and tour of the Fountain of The Lamps. The tour and explanation of the site was made difficult in that, due to the lack of maintenance and continued flow of water through the site, there was a thick growth of reeds, bushes and fig trees, making most of the site difficult or impossible to see (Figure 41). In addition to their effect on visibility, all of these plants have been, and are, gradually dismantling the site with the growth of their roots. There was what appeared to be heavy erosion at the south end of the site where the smaller underground rooms are located. In the spring of 2013, Wiseman arranged for the Greek Ephorate to have the Fountain of the Lamps cleaned out and a pump put in to continuously remove water and arrangements were made for keeping the vegetation down (Figure 42). Evident in mid-August were four metre tall reeds filling the pool showing how difficult the battle to keep back nature in a moist site can be (Figure 43). There was, however, a considerable amount of the area that had not grown in because large sheets of gauze had been draped over it, allowing the Fountain of the Lamps to be seen as it is now.



Figure 41 - Fountain of the Lamps before cleaning

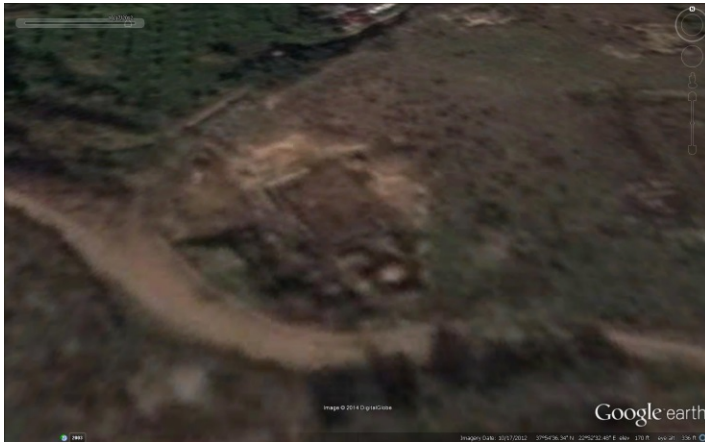


Figure 42 - Fountain of the Lamps immediately after cleaning



Figure 43 - Fountain of the Lamps overgrown again months after clearing

It seemed likely that if a site that had been excavated in the past had been thoroughly photographed during excavation, no matter how long ago, it might be possible to reconstruct in a three dimensional model. When this was suggested to Wiseman he informed me that during the five year excavation of the Fountain of the Lamps, thousands of photographs had been taken documenting the entire dig from start to finish.

With a series of modern photos of the complex, a 3D model as it currently exists was constructed (Figure 45). Wiseman was able to supply all of the photographs taken from 1968 to 1972 and once the features were understood, an effort to construct them as a model

of the site as it was in its final stages in 1972 was undertaken.

Obviously one cannot control how the past excavation photos were taken and of understandably they were not taken with a thought to what might be necessary 40 years later using unimagined technology. A contiguous series of shots taken in the same lighting, at the same time is unlikely. Some site directors of past excavations may have chosen to focus more on details rather than broader views, leaving the entire site to be done in two dimensional orthographic drawings.

Another obstacle was that photos might have been taken as the level of soil gradually reduced and that no contiguous shots might exist. This in fact was the case but was not an insurmountable obstacle. By cropping soil covered areas out of earlier photos, it was possible to employ them in the construction of the late excavation model. While one large comprehensive model of the entire site was not able to be produced, significant portions of the site were able to be successfully modelled showing that this is a viable method of recreating a site as it was when excavated. The key is through carefully choosing the photos with the most similar lighting and best overlap. While the modern model of the Fountain of the Lamps used 144 photos of the 145 taken, the main past excavation model used only nine photos of the thousands taken. As a result the model of the modern site is a fully rotatable 3D image while the 1972 Fountain of the Lamps model (Figure 44) is more of a relief which we can change the viewing angle of but not completely circleable. No surveyed points were available and so other report information about the model cannot be produced.

The model of the Fountain of the Lamps as it currently exists, was done more for practice with the technique but once the old and new models were built it became very clear that the

two could work together as a new form of tool capable of analysing the destruction that excavation combined with time can produce. What the models showed was that the cliff had collapsed, abbreviating the edge by approximately four metres, destroying a large part of the antechambers. Had the antechambers been reinforced back in the 1970s after excavation they would still be preserved. What the models provide is empirical evidence in the argument for cultural heritage management and preservation.

The initial intention of examining the Fountain of the Lamps was to be able to add to the record of the site, allowing researchers to measure layers that had been removed or revisit in three dimensions the site as it had been before its destruction. An archaeologist, during excavation, will try to record as much as possible but later discoveries or research can cause a need for refocusing, examining a portion of the site that was previously less studied.

Based on the results of comparing the before and after models, it is evident that photogrammetry is a tool that can be used to monitor over time the degradation of a site, giving us evidence for requesting funding for preservation, teaching us the processes involved in the aging of a completed archaeological excavation and warning us of rates of deterioration and displacement allowing us to intervene, should we see an increase in the rate. In presenting these results to Corinth Excavations Director- Guy D. R. Sanders, he suggested that this technology represents a low cost way to track changes in the columns of the Temple of Apollo, whose monolithic Doric columns are carved from pieces of fossiliferous stone which, with time and weather, will gradually wither away. Withering is acceptable or rather inevitable but if fissures start to form there are methods to deal with them if they can be noticed early enough. Concrete patching or steel banding as a temporary measure can prevent further damage and in some cases stabilize the object pending future

developments in preservation. Using photogrammetry can easily and inexpensively monitor these columns, spotting even the smallest changes in them. Other attempts at similar monitoring and/or comparison of deterioration have been done with success in quantifiably being able to monitor or revisit sites to study the ongoing entropy that they undergo (Fujii 2009, 24-133).

In future attempts at reconstructing past excavations it is advisable that any and all surveying data done originally be accessed and input into the model. Additionally, if there are portions of the site that are still intact, accessible and unaffected by erosion or other elements of time, these could be surveyed and those coordinates input into the model made with the historic photographs.

Although there is not much that can be done about a lack of overlapping photographs in older excavations, exploring the use of archival film footage might fill in gaps in the photographic record on a frame by frame basis.



Figure 44 - Fountain of the lamps after excavation in 1972



Figure 45 - Fountain of the lamps one year after clean up in 2012

4.2 – Features

In this section the documentation of significant, smaller scale features within sites will be described with mosaics, inscriptions and osteological excavations as examples.

4.2.1 - The Eutychia Mosaic

Mosaics are another of the more perishable of artefacts. Many are exposed to the elements, losing tesserae (the individual tiles used to construct them) to water and wind erosion, or are damaged by invasive plants and animals. Even ants can undermine and destroy a mosaic. Historically, in addition to destruction by earthquakes and other natural disasters, human destruction of mosaics played a significant role in their loss both in the distant past as well as following their rediscovery. Preservation and restoration of mosaics requires highly accurate recording of their original structure. With this purpose in mind photogrammetry can be a useful tool in the process. Mosaic preservation and restoration is one of the last areas of archaeology to adopt the use of photogrammetry as a documentation tool. This may be because of the perception that photogrammetry is a three dimensional tool while mosaics are perceived as being two dimensional. While there is abundant literature documenting more recent restorations and preservations of mosaics using traditional methods there are a few instances (Brutto 2015) (Işiklikaya 2008, 358-361) of photogrammetry being used in mosaic preservation and restoration.

Examples of botched restorations such as those housed in the Hatay Archaeology Museum in Turkey reinforce the need to not only photograph the initial condition of the mosaics but also to have accurate empirical data on their structures in order for them to have as close to

the original structure as possible when completed (BBC 2015). Traditionally in the study and preservation of mosaics they have been “documented by: photograph, description of their state of conservation and then measured” (Hamarnah et al. 2013, 141). Recording a mosaic with exacting measurements of the location of every tessera has been, until now with the advent of photogrammetry and laser scanning, impractical and prohibitively time consuming as it would each tessera to be traced by hand. As will be shown in the examples photogrammetry when applied to mosaics not only builds a large, thorough collection of photographs of the entire mosaic but also is able to provide an infinite number of measurements in order to meet exacting contemporary preservation standards.

Early photogrammetry of mosaics was done by O.Ajioka and Y.Hori at Ostia, Italy from 2008 with similar intentions to ours and the goal of supplanting the use of lasers with their bulk, high cost and lack of high definition photographic texture (Ajioka and Hori 2014).

The mosaic used in this example is known as the Eutychia (good luck) Mosaic. It consists of millions of tesserae; small square tiles of approximately 8mm cut from limestone and dolomitic limestone and in some areas augmented with glass.

Unearthed in 1933 by Oscar Broneer, the Eutychia Mosaic is a

“Severan mosaic in the South Stoa in [Ancient] Corinth, Greece, depict[ing] a victorious athlete and a seated, semidraped goddess. Holding an inscribed shield as well as a vessel from which water streams into a basin, she recalls two famous

Corinthian trademarks, the Aphrodite of Acrocorinth and the nymph Peirene...[and] was probably installed ca. 200 C.E.”

(Robinson 2012, 105)

Surrounding the central piece (Figure 46) which measures 1.30 x 1.27 m there are 12 squares with guilloche borders depicting birds in each of the four corners “a partridge, a parrot, a rooster [(Figure 47)], and a wading bird” while the “two intervening squares on each side contain rosettes and other floral designs with plain black backgrounds“. (Robinson 2012, 107) Surrounding this area are various panels of geometric patterns. On the east and west edges are larger multi-coloured pieces of marble (opus segmentatum)

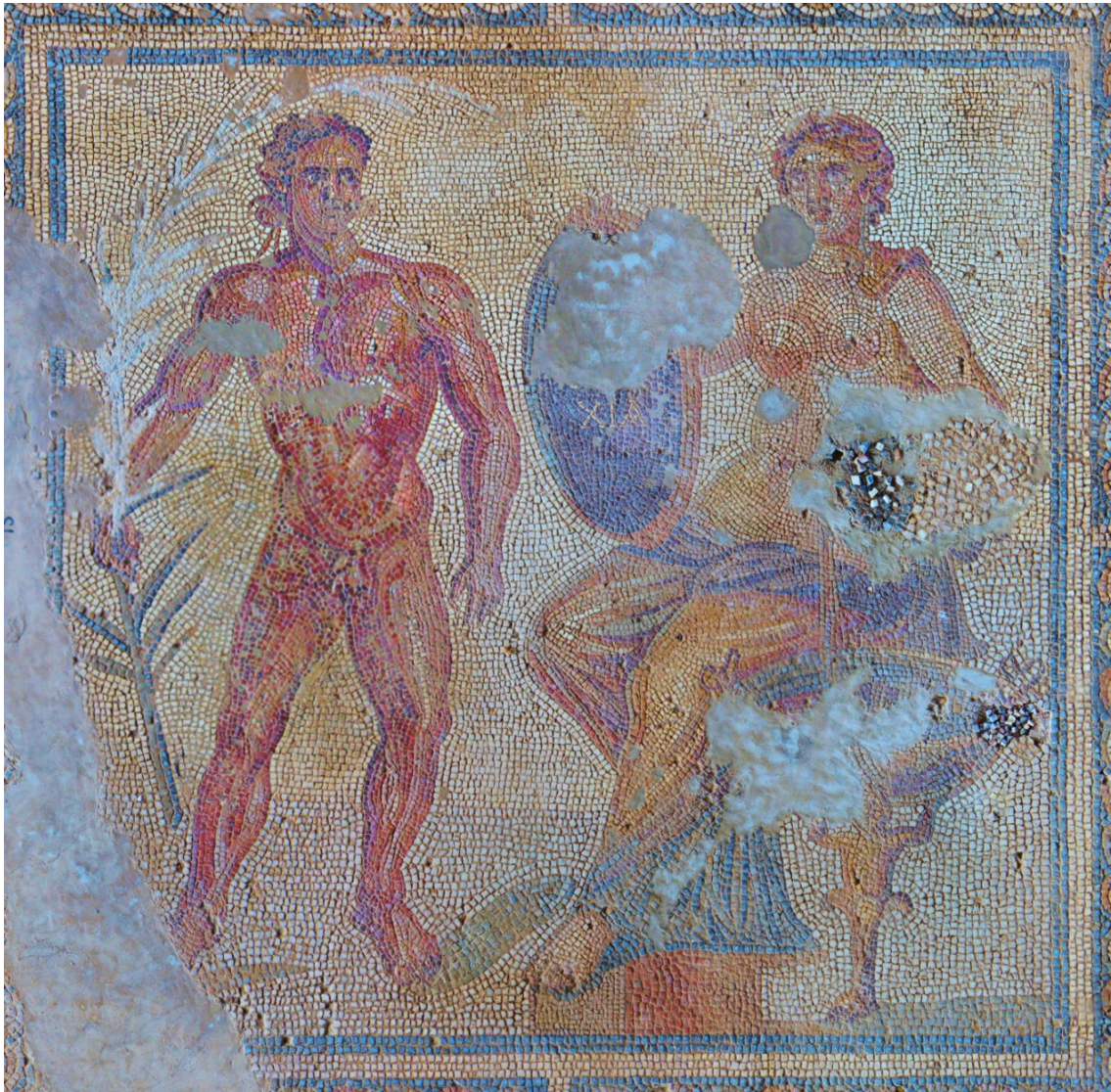


Figure 46 - Central panel of the Eutychia Mosaic



Figure 47 North East corner of central surround depicting a Rooster

The Eutychia Mosaic, although housed under a roof for many years, is in a building with glassless windows allowing the elements in. The greater threat to this work was that some of the ground beneath it was subsiding. The area in which the mosaic is housed has complex systems of underground waterways and wells leading from the Eastern end of the South Stoa down to the Peirene Fountain. It was correctly thought that some areas beneath the mosaic may be hollow. To a lesser degree there was also degradation simply due to dirt and other discolouration. Due to this ongoing damage and the significance of the mosaic, an

extraction and restoration is being undertaken under the direction of Guy Sanders by head conservator Nicol Anastassatou, conservators Spiros Armenis and Charis Delis with the aid of a grant from the Stockman Family Foundation. With the mosaic removed, the opportunity to excavate below its location was presented for the first time. In Summer 2015 excavation of the ground beneath the mosaic revealed an Hellenistic layer which included a grave, wells, coin hoards and pottery. The floor surface was then backfilled with piping installed to vent humidity from the wells in order to preserve the mosaic upon reinstallation.



Figure 48 - Floral pattern on south edge of central panel

In summer 2014 and 2015 James Herbst and the author photogrammetrically recorded the Eutychia Mosaic in Ancient Corinth. Although it might seem questionable to make a three dimensional model of a two dimensional subject there are a number of reasons why this is advantageous. The Eutychia Mosaic in particular has many subtle three dimensional aspects to it. There are different slopes to the floor as well as undulations and sunken areas which, upon completion of the restoration will not exist. Once a new substratum is built and the mosaic restored, the slope will have changed to accommodate inevitable moisture run-off and the undulations and sunken areas will be gone. The 3 dimensional modelling of the mosaic before and after will give us an idea of how those areas have changed. Another important reason to model the mosaic is that we can preserve accurate measurements of where each tessera is placed.

Photogrammetry of the mosaic in 2014 and 2015 was done for two distinct purposes; recording the original mosaic and accurately reinstalling the restored mosaic. However other purposes arose. Initially it was seen as a high quality, inexpensive way to record the original mosaic, progress on its removal and once restored, to be able to view and measure the differences. Although this was the initial intent, the restoration team soon found other uses for photogrammetry. They had used large transparent plastic sheets to do exact tracings to record the position of the patterns in the mosaic. Because of the extreme temperature shifts reaching over 40°C throughout the day the plastic sheets were experiencing expansion and contraction far beyond an acceptable level of variability. The photogrammetry exported to an orthophoto image provided a detailed record of the exact position, colour and shape of each of the tesserae. For the 2015 season, photogrammetry was used to guarantee the quality of the reinstallation which will be explained in the 2015 methodology.

4.2.1.A - In Situ Mosaic Recording Methodology (2014)



Figure 49 - Eutychia Mosaic in situ before removal

Markers were set up throughout the mosaic at points where parts of the image were missing so as not to block any tesserae. Permanent markers were mounted into the stone walls

which would not be affected by the removal operation. All of the points were then georeferenced. We constructed an apparatus which could span the rafters of the building with the camera mounted on it facing downward; the idea being that if we could maintain a more or less consistent distance from the floor the focal range could be kept fairly tight without having shots in which the tesserae were out of focus. We would then move the apparatus laterally on the rafters by about one metre which we had calculated would give us enough photographic overlap to be able to use in the photogrammetry. The apparatus was then slid along the rafters and the process repeated. Shutter release was achieved by remote control. At roughly two thirds through the process the batteries for the remote shutter release failed and we adjusted the camera so that it would shoot using a ten second delay. This technique worked well until, while trying to photograph some of the more damaged areas of the mosaic, we were forced to reach too far for the camera resulting in vibration of the apparatus that was not noticed until later viewing the photos. In order to reduce these flaws, I revisited the floor at the same time the next day and took a number of hand held photos of the areas that had been blurry. All of the photos were then fed into the Agisoft Photoscan software as well as the referenced coordinates. The resulting 3-d model accurately captured the undulations in the floor and was able to be exported to an orthophoto at a one to one scale.

The 2014 model used 190 of the 206 photographs input with fuzzy movement shots being excluded. The resulting model enabled us to produce ultrahigh resolution orthographic photos and accurate measurements of the exact location of the tesserae. Overall accuracy was very high within approximately 0.5 mm tolerances but a couple of targets were not as accurate, reducing overall accuracy to about 1 centimetre. Elevation above the model was consistently around 1.5 metres.

Eutychia mosaic

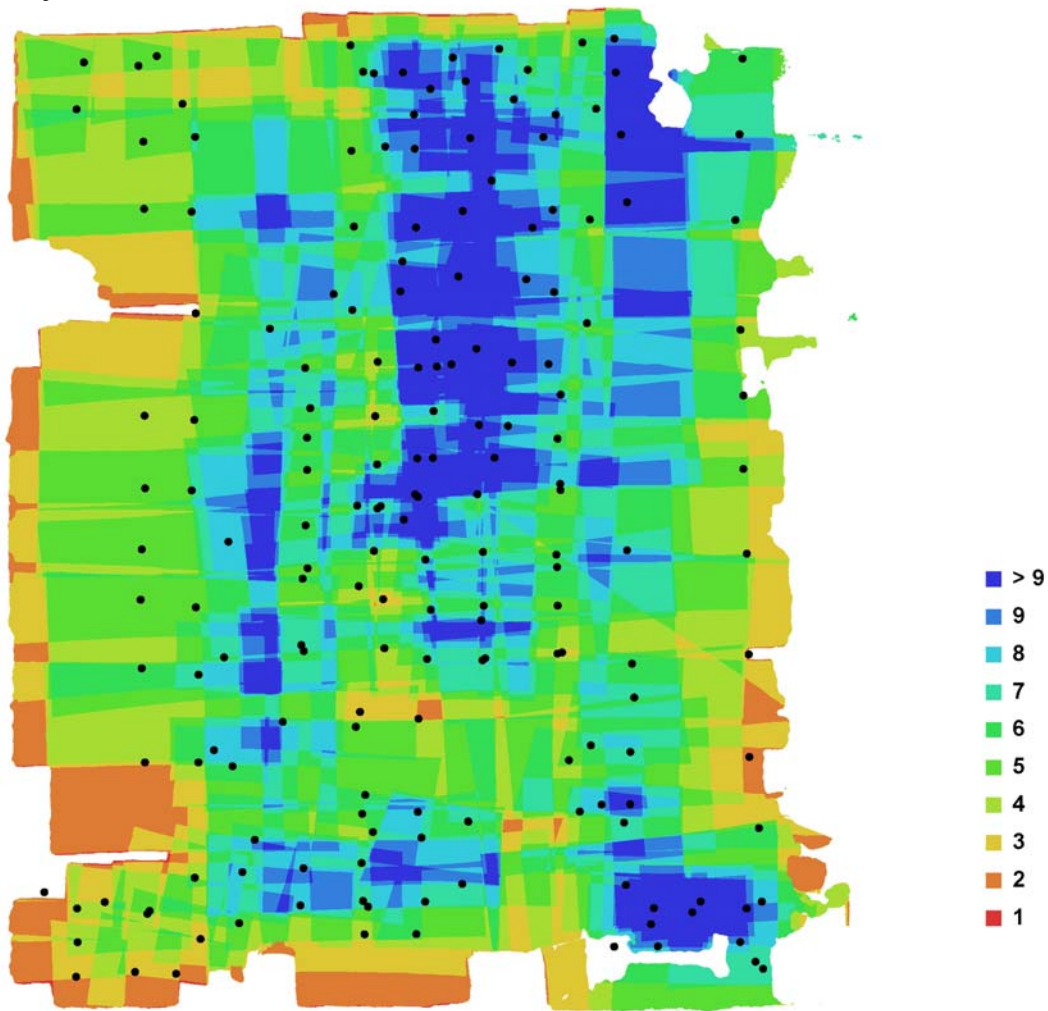


Figure 50 - Camera locations and image overlap: Eutychia mosaic

Number of images:	206	Camera stations:	190
Flying altitude:	1.35523 m	Tie-points:	2077677
Ground resolution:	0.000410337 m/pix	Projections:	5601657
Coverage area:	6.14702e-005 sq km	Error:	0.400565 pixels

Table 12 - Eutychia mosaic cameras

Camera Model	Resolution	Focal Length	Pixel Size	Precalibrated
SLT-A35 (18 mm)	4912 x 3264	18 mm	4.89089 x 4.89089 um	No
SLT-A35 (22 mm)	4912 x 3264	22 mm	4.89089 x 4.89089 um	No
SLT-A35 (20 mm)	4912 x 3264	20 mm	4.89089 x 4.89089 um	No
SLT-A35 (18 mm)	3568 x 2368	18 mm	6.73574 x 6.73574 um	No

Eutychia mosaic - Ground Control Points



Figure 51 - Eutychia Mosaic GCP locations

Table 13 - Eutychia mosaic control points

Label	X error (m)	Y error (m)	Z error (m)	Error (m)	Projections	Error (pix)
1	0.025157	-0.002939	-0.014374	0.029123	2	4.367580
2	-0.000000	-0.000000	0.000000	0.000000		
4	0.000000	0.000000	0.000000	0.000000		
5	-0.000000	-0.000000	0.000000	0.000000		
6	-0.001227	0.002006	-0.012580	0.012798	3	1.760596
7	-0.001118	-0.001243	0.005046	0.005316	5	4.540069
8	-0.001388	0.000353	0.006341	0.006501	8	10.066154

9	0.002076	0.002944	0.000713	0.003672	5	1.094785
10	-0.002756	0.003832	0.001489	0.004949	6	4.090523
11	-0.005964	-0.003602	0.005757	0.009038	4	3.036931
12	-0.001047	-0.005786	-0.006046	0.008434	7	4.507238
13	0.000623	-0.002759	-0.004551	0.005358	3	0.616719
14	-0.000373	-0.003214	0.010022	0.010531	13	1.852931
15	-0.001116	-0.000942	0.008497	0.008622	7	3.165652
16	-0.003191	0.000507	0.004306	0.005384	5	1.265597
17	-0.003204	0.001449	0.003504	0.004964	3	0.338496
18	-0.007870	0.004483	-0.001513	0.009183	8	1.308564
19	-0.000529	0.000321	0.008463	0.008485	8	1.156782
20	0.004047	0.000611	-0.014544	0.015109	4	1.866848
Total	0.006436	0.002574	0.007300	0.010067	91	3.935242

Eutychia mosaic - Digital Elevation Model

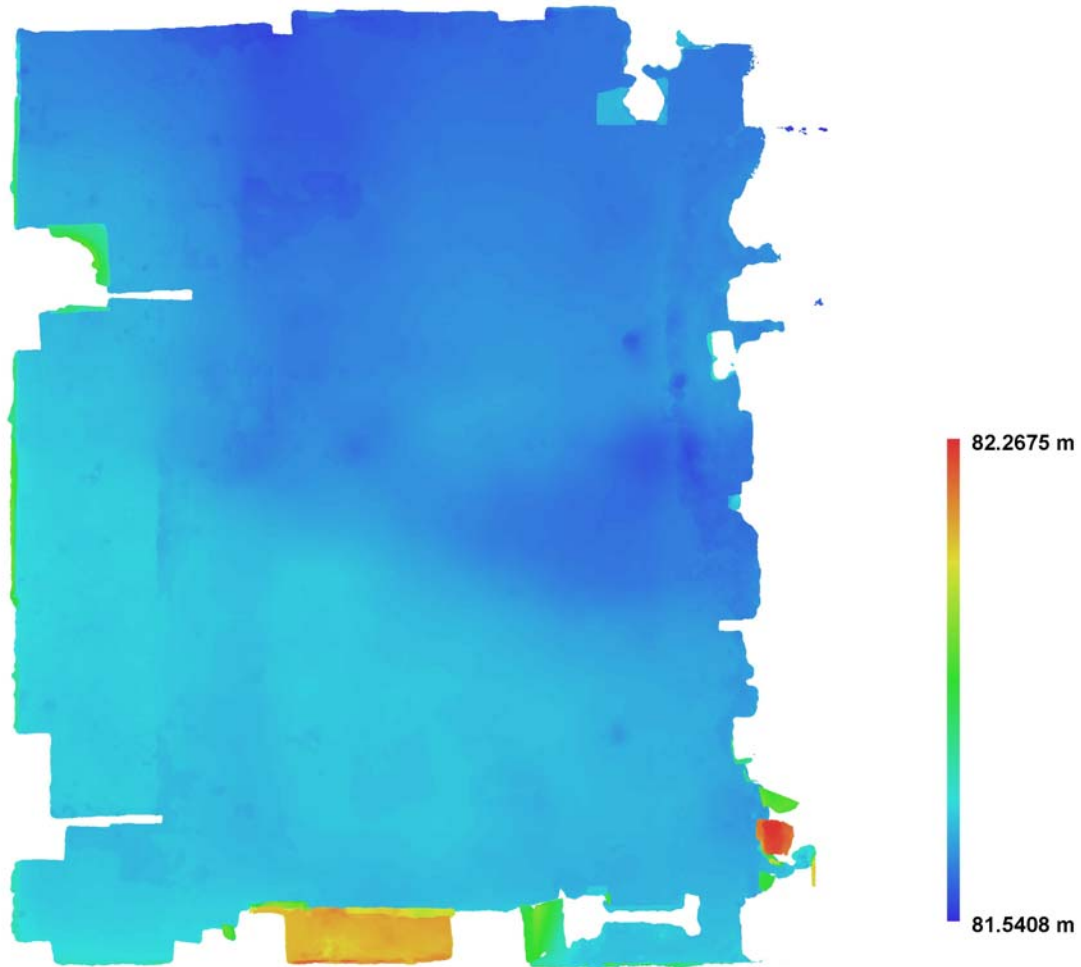


Figure 52 - Eutychia mosaic reconstructed digital elevation model

Resolution: 0.000820673 m/pix
Point density: 1.48477e+006 points per sq m

4.2.1.B - Mosaic Reinstallation Methodology (2015)

In order to facilitate the extraction of the Eutychia mosaic, head conservator Nicol Anastassatou determined 37 structurally strategic sections of the mosaic to be cut into separate pieces. Most sections were of a unique and uneven shape but were sectioned with maintaining structural integrity as the highest priority.

When the 37 separate sections of the mosaic were removed, one row of tessera was first extracted from between each of them. Gauze and cloth were then adhered to the surface using water soluble glue in order to keep all tesserae in place. The sections were then cut from the floor with a thick layer of concrete still attached beneath them. The sections were then flipped face down and conservators Charis Delis and Spyros Armenis meticulously removed the mortar substratum from each section. The end result was cleaned panels which depict the reverse image of the mosaic. It was these reverse panels that I was to use photogrammetry to record in order to facilitate their reinstallation.

To enable the reinstallation of the mosaic, a new and unprecedented method of installation was devised by Anastassatou. In museum situations mosaics have been mounted on aluminium honeycomb cored panels but never when placed in situ. (Getty Museum (n.d.)) This method was chosen in order to reduce the weight of each panel so that they could be manoeuvred by hand into position. The building in which they were being restored requires them to be passed over a 1.5 metre half wall and then taken to a lower floor area. If they were mounted onto concrete as was traditionally done, a crane would have been required. Anastassatou found a Greek supplier that was able to produce panels to an exacting standard, cutting them into precise shapes in order to fit them together within sub-millimetre tolerances. The panel supplier informed us that we needed to provide accurate

AutoCAD shape files. It is for this reason that photogrammetry was chosen in order to reproduce the exact shapes of the tesserae panels. Without such accuracy, reinstallation would not succeed due to the nature of the mosaic's original location in which it extends to the very edges of the interior of the stone building. Thus reinstallation requires that the same tesserae fit exactly within that space. The tesserae each measure approximately 8 mm square so it is within this tolerance that the panels have to fit.

Necessity required that the panels be photographed within the mosaic building as they were stored there and were difficult to move due to both their size and their fragility. The area provided for photographing was an uneven excavation surface under where the mosaic had originally been and which had been excavated in the preceding weeks. A large melamine board was ordered as a "stage" on which the panels could be consistently recorded. The melamine sheet arrived and was not rigid enough on its own to be put on an uneven surface. Conservators Charis Delis and Spyros Armenis, assistant site foreman Panos Kakouros and workers Michalis Vathis, Hecuran Coli, Marios Vathis and Tasos Tsogas constructed a wooden platform on which the melamine panel was placed. Ten unique targets, printed on clear adhesive sheets were placed around the perimeter of the board at regular intervals and James Herbst, site architect, directed the levelling of the platform with shims to a sub 1 mm tolerance using a total station. The location of each target was recorded in order to georeference and scale each panel once photographed and modelled.



Figure 53 - finished model showing Agisoft targets.

With smaller panels situated with the targets further away from them, angled shots were necessary in order to include the targets in the photographs. This resulted in photos in which there was blur at the limits of the depth of field. Changing the F-stop of the camera would have alleviated this problem but the lighting in the room precluded that option. (In retrospect instead of using ten targets we should have used twenty with closer spacing and

some more central ones that would show up when photographing smaller pieces. By doing so we would have consistently had eight to ten targets within the model range.)

The building in which the photogrammetry took place has glassless windows and is subject to changing lighting conditions. To maintain consistency of exposures gauze was placed over the windows and in spots where direct sunlight was a problem styrofoam sheets were erected. Although this produced a very uniform lighting, it did lengthen the exposure times to between 1/60th and 1/100th of a second, thus reducing the depth of field. A tripod would have been useful but a time element had to be considered in setup and execution. Firstly, the team moving the panels in and out of the room had to wait while each one was photographed. Hand held photography creates an advantage in this case in that it can be done with little time or setup. This minimized the amount of time the team were kept from performing other important work and their time is limited.

The second element requiring expediency was the temperature. Water is misted onto the mosaic surfaces to increase contrast and enhance the colours. The canvas backing is adhered with water soluble glue so the application of water was judicious to avoid tesserae detaching. At temperatures ranging between 36°C and 40°C the misted water evaporates quickly and can cause inconsistencies in the photographs resulting in unwanted variations in areas of the models.

The higher temperatures, however, were a compromise that had to be accepted as shooting later in the morning resulted in more even lighting. Coordination of the movement and storage of the panels was another concern with regard to timing but the team did an extraordinary job of moving panels in and out of the staging area despite their weight and

fragility.



Figure 54 – Moving of section T21; the central panel of the mosaic to be photographed. Conservators Charis Delis (far left) and Spyros Armenis (far right), assistant site foreman Panos Kakouros (second from right) and workers Michalis Vathis (rear left) and Hecuran Coli (rear right)

The first panel, T26, was brought in on a board and carefully slid onto the photo platform. 42 photographs were taken with appropriate overlap in order to ensure that the modelling software was able to use the parallax between photos to construct the model. The maximum number of targets possible were included in the photos in order to achieve proper scale. The mosaic panel was then measured to its extremes in a number of directions and left in place so that the first model could be made in Agisoft Photoscan, an orthophoto produced and measurements taken from it in Photoshop in order to check accuracy.

Results of the first measurements on the model were discouraging with discrepancies of five to ten millimetres due to various processing variations which I will now explain. This was a preliminary model and in consulting with James Herbst he advised an order of procedures including when to detect the markers, when to import coordinates and when to optimize cameras, that proved to be far more accurate. (see Appendix 1). Subsequent models had an error of 0.5 millimetres or less which, on an image of one to two and a half metres in breadth is acceptable for the purpose of the project. In total, close to 2000 photographs were used to produce the 37 models required.

Once the 3D models were completed, each was exported as an orthophoto at a scale of 0.0002 metres per pixel. Orthophotos were exported with an accompanying world file (a set of coordinates specific to the orthophoto) allowing them to be imported into Photoshop with coordinates and scale so that they could all be consistently and accurately measured.

In Photoshop the orthophotos were aligned as accurately as possible with southeast at the top left and using lines of tile within the mosaic to find the most vertical orientation. Each one was then trimmed along the edge of each tessera by Anastassatou and myself then given transparent backgrounds so that they could be matched as closely as possible in AutoCAD (Figure 55).

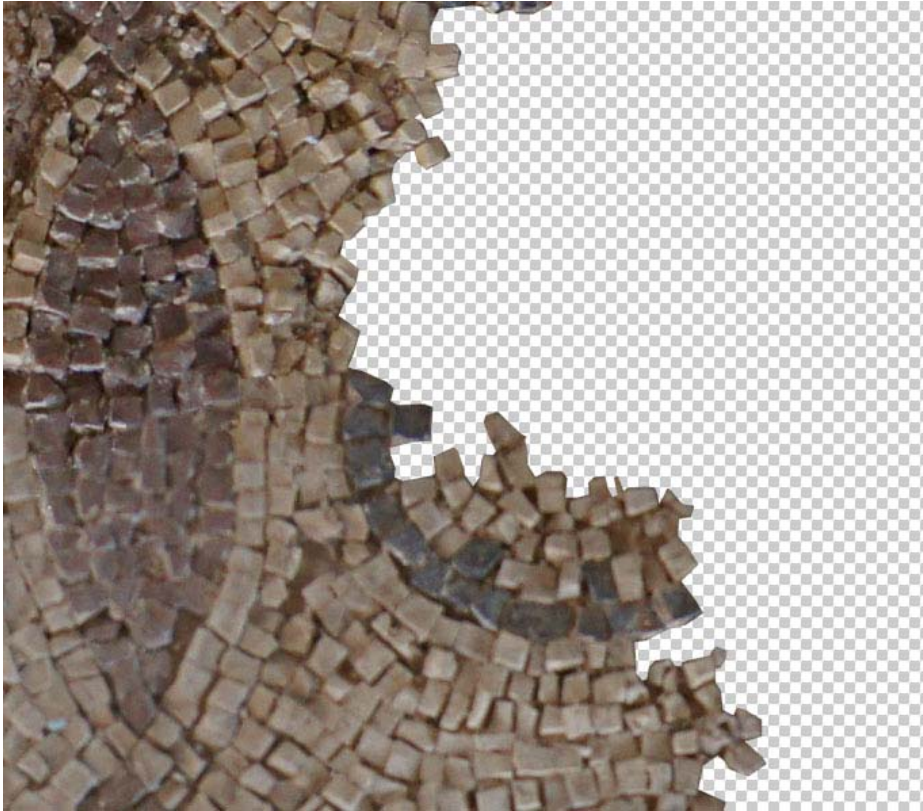


Figure 55 - Example of how the images were trimmed along each tessera's edge

Each panel was imported into AutoCAD using the MapDrafting/Insert Image command. The images were then arranged and aligned closely but leaving enough space to represent the single line of removed tesserae between them. The inaccuracy of the straight lines in the original manufacture of the mosaic meant that minor adjustments and compensations had to be made in order for both x and y axis to match to neighbouring panels. Once arranged, with each panel on a separate layer so that they could be turned off when not needed to avoid unnecessary software crashes, a new layer for the line drawings was created. Each line drawing was made one half tessera in from the outer edge of each panel. The arrangement of the panels allowed us to check the fit of the line drawings which represent what the cut honeycomb panels will be shaped like. Once all of the line drawings were completed and checked for compliance with the plan for their installation, they were sent to the panel manufacturer to cut the honeycomb panels.

Although we have used photogrammetry for a number of years in Ancient Corinth to document sites, objects and structures, giving us presentation materials and allowing for accurate site plans to be produced, this was the first time that, within critically accurate tolerances, photogrammetry was used to actively produce a product which would aid in conservation. It has proven itself to be a valuable, affordable and highly accurate tool in this process.

Eutychia mosaic T21

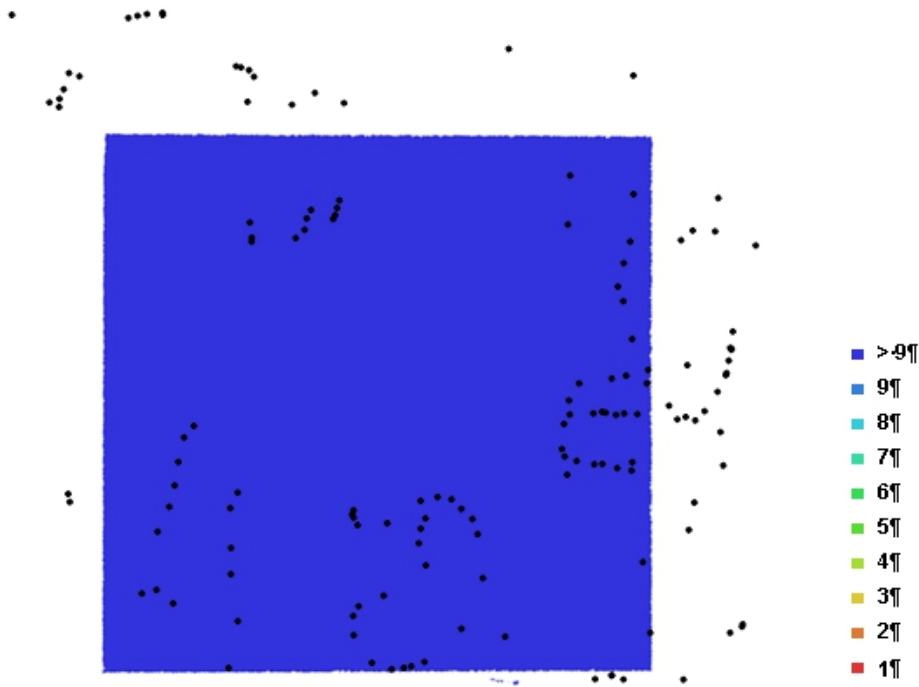


Figure 56 - Camera locations and image overlap for T21

Number of images:	146	Camera stations:	146
Flying altitude:	1.04227 m	Tie-points:	11579
Ground resolution:	0.000245397	Projections:	102591
m/pix		Error:	2.86432 pix
Coverage area:	1.97303e-006 sq		
km			

Table 14 - Mosaic section T21 cameras

Camera Model	Resolution	Focal Length	Pixel Size	Precalibrated
SLT-A35 (22 mm)	4912 x 3264	22 mm	4.89089 x 4.89089 um	No
SLT-A35 (20 mm)	4912 x 3264	20 mm	4.89089 x 4.89089 um	No
SLT-A35 (18 mm)	4912 x 3264	18 mm	4.89089 x 4.89089 um	No

Eutychia mosaic T21 - Ground Control Points



Figure 57 - Ground control points for Eutychia mosaic T21

Table 15 - Ground control points: T21

Label	X error (m)	Y error (m)	Z error (m)	Error (m)	Projections	Error (pix)
target 1	0.000487	0.001908	0.004704	0.005100	11	0.205192
target 2	-0.002892	0.000447	-0.000759	0.003023	26	0.663073
target 3	-0.005065	-0.000142	-0.002211	0.005528	21	1.267329
target 4	-0.002866	0.000844	-0.002551	0.003929	9	0.731046
target 5	-0.000946	-0.001494	0.001371	0.002238	7	1.054197
target 6	0.006275	-0.007460	0.003839	0.010477	9	1.568110
target 7	-0.000239	-0.000457	-0.000048	0.000518	27	1.270254
target 8	0.000823	0.003822	-0.002739	0.004773	37	1.051812
target 9	0.003255	0.001397	-0.002532	0.004354	12	0.908107
target 10	0.001169	0.001134	0.000928	0.001874	27	0.352447
Total	0.003089	0.002837	0.002559	0.004914	186	0.978511

Eutychia mosaic T21 – Digital Elevation Model

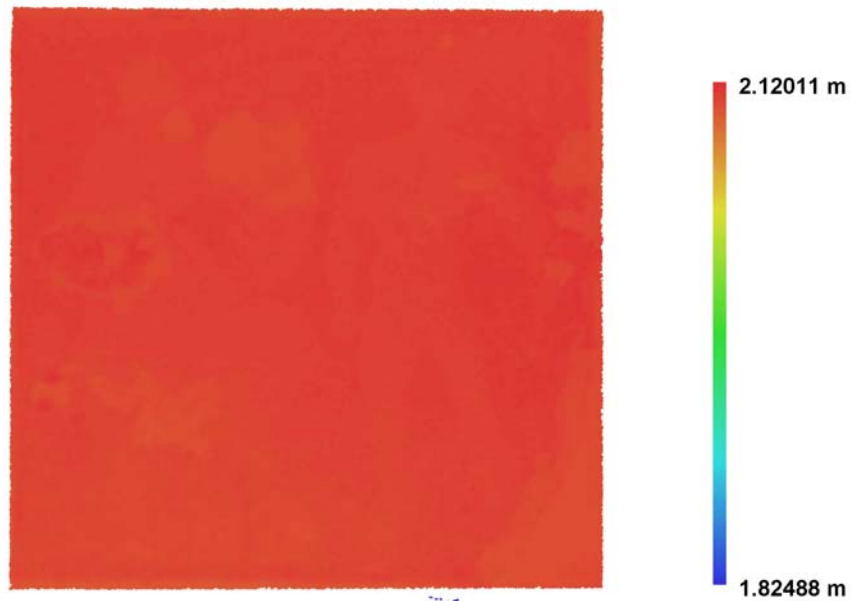


Figure 58 - Reconstructed digital elevation model of T21

Resolution: 0.000981587 m/pix
Point density: 1.03787e+006 points per sq m

IV.2.2 – Inscriptions



Figure 59 - Inscription in the Athenian Agora

Inscriptions are one of our most succinct tools in experiencing the thoughts, goals and priorities of past societies. They too are perishable, subject to erosion, natural disaster and human defacement both now and in the past. Recording inscriptions as well as making them accessible to multiple researchers has long relied on “rubbing”. Rubbing involves adhering paper to the inscription surface and using rubbing wax, charcoal or other soft drawing materials to rub the surface of the paper leaving pigment where the medium rubs against raised areas of the inscription. A long time genealogist, Elspeth Wallace, informed me that this practice has become extremely popular with genealogists in recording information from their ancestor’s headstones. A major drawback of rubbing is that it records a mainly two dimensional record of the inscription. Particularly with very worn inscriptions this two dimensional record leaves out subtle nuances and does not allow the viewer to look at those nuances at different lighting angles. Additionally, some inscriptions are found to have been carved over top of previous inscriptions. By working with different depths of incision it may be possible to discern two distinct messages. In their discussion on The University of Florida’s digital epigraphy and archaeology project Bozia et al. point out that 3D records of

inscriptions “can be visualized more effectively compared to 2D images, as they can be viewed from different angles, under different artificial lighting conditions, and in different zooming scales” (Bozia et al. 2012, 1).

A more sophisticated technique has been used in China for centuries using damp paper and pressing it with rabbit hair brushes to push the paper into depressions in the surface. (Berkeley.edu 2004). The technique of doing squeezes of inscriptions in Western archaeology has been practiced for more than a century (Tracy 2010, 6). It too involves pressing dampened, pliable paper into the undulations and crevices of the inscription. Once dry, the “squeeze” is a 3 dimensional image replica of the original inscription. Many researchers now choose not to do this technique or are prohibited due to its gradual destructive nature with some, according to Dimitri Nakassis, now using a technique called Reflectance Transformation Imaging (RTI).

RTI is done in a studio by placing the inscription face up with a camera mounted directly above and positioning multiple light sources in an approximate semi sphere around the object turning individual or multiple lights on for each photo and then comparing the photos for differences in light and shade in order to discern subtle variations in the surface that might otherwise not be seen. While effective, this technique is overly complex, expensive and has the severe limitation of the inscriptions being portable and able to be placed face up.

A major advantage of photogrammetry is its ability to capture subtle variations in a stone surface. On many Greek archaeological sites, there are countless stones incised with histories and information about the past. They, in their soft malleable stone have endured

thousands of years of exposure and erosion. Many are barely readable. As an experiment in how, by using photogrammetry, a moveable three dimensional image could be easily acquired, a well weathered inscription in the Athenian Agora had both the right amount of intact detail and the right amount of detail lacking to be a good candidate.

The inscription that chosen as an example was inscribed on a block of Hymettian marble (Ancient Agora number I 6954) (Figure 59) in 321 B.C. and currently situated in front of the Attalos Stoa in the Athenian Agora. It is a damaged and worn piece discovered while dismantling the Post-Herulian Wall at the southwest corner of the Library of Pantainos. The wear and damage made this piece a perfect candidate for photogrammetric enhancement (Meritt and Traill 1974, 345-346, number 494).

4.2.2.A - Inscription Methodology

After making a first modelling attempt and seeing that one could also view a reverse image of the inscription by looking at the back of the model, ArcGIS was chosen, with its ability to take a digital elevation model (DEM) and exaggerate the contours in order to enhance shallower portions of the inscription.

The inscription model was exported as a DEM and ArcGIS was able to give some of the more subtle, worn parts of the inscription greater depth and thus greater readability. Upon reflecting on the RTI technique it also seemed that using Hillshade in ArcGIS's Spatial Analyst could achieve what the RTI technique was attempting but with an infinite number of angles and rotations rather than twenty or thirty static lights. Using Hillshade in

combination with exaggeration of the DEM breathed new life into the heavily eroded inscription.

All 36 photographs were employed in the model with very similar distances from the inscription and so no depth of field issues to contend with giving it an accuracy of 0.748116 pixels.

As a remote sensing technique photogrammetry leaves the subject intact, opens new opportunities for recording inscriptions that have been off limits to researchers. According to Papadaki et al. (2015, 237) “[i]n some instances it is even not allowed to touch and tamper with the inscriptions, as they may be extremely fragile”. Photogrammetric recording of these inscriptions gives us the versatility to use the technique in the field where many of these inscriptions are in situ; large, on the ground, embedded into buildings or fragmented and in various collections. . An advantage of modelling inscriptions in three dimensions is that they may not be intact but rather a series of broken stones but our pieces in the model can be combined to produce a single readable stone.

Agora inscription

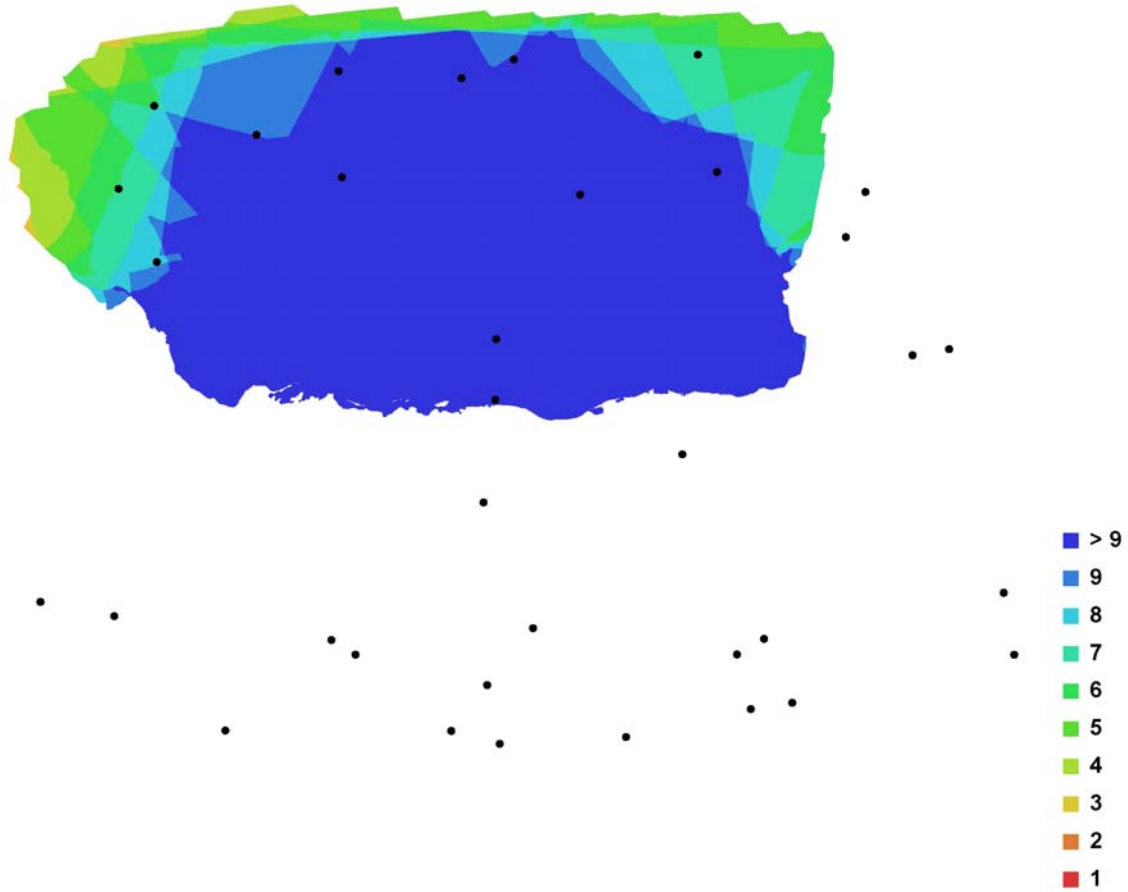


Figure 60- Camera locations and image overlap for Agora inscription

Number of images:	36	Camera stations:	36
Flying altitude:	0.213644 m	Tie-points:	56023
Ground resolution:	6.04221e-005 m/pix	Projections:	134549
Coverage area:	9.10053e-008 sq km	Error:	0.748116 pix

Table 16 - Agora inscription cameras

Camera Model	Resolution	Focal Length	Pixel Size	Precalibrated
SLT-A35 (50 mm)	4912 x 3264	50 mm	4.89089 x 4.89089 um	No
SLT-A35 (18 mm)	4912 x 3264	18 mm	4.89089 x 4.89089 um	No

Agora inscription – Digital Elevation Model

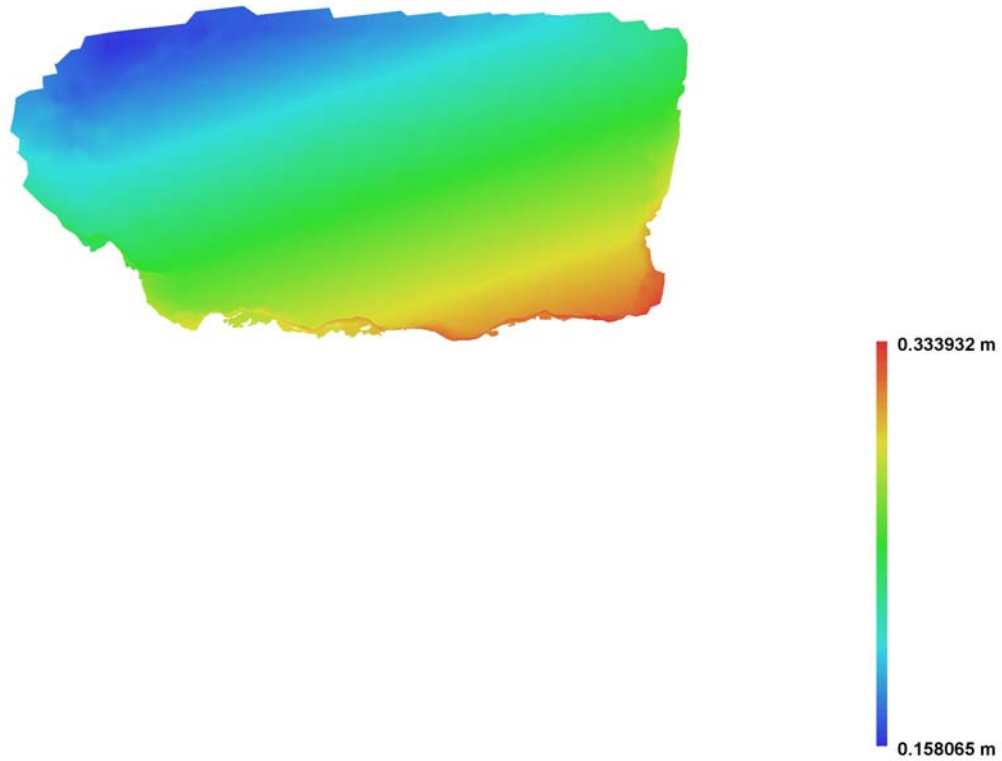


Figure 61 - Reconstructed digital elevation model of Agora inscription

Resolution: 0.000120844 m/pix

Point density: 6.84776e+007 points per sq m

4.2.3 – Osteology



Figure 62 - Model of Skeleton, Gietz, Poland produced from two 2008 photographs

Osteological documentation is complicated by a number of realities. Deterioration through climate, soil conditions, excavation or mishandling can result in a loss of diagnostic evidence. Photogrammetry can give us the most detailed accurate record of bones in situ before any of these factors affect what we can learn.

With regard to climate and soil conditions (too acidic or too alkaline), damage but not disruption may have been done to the bone so that it can still be unearthed in its original configuration Figure 62 is modelled from two photos taken without the intention of 3D modelling and illustrate what an in situ skeletal excavation looks like. It is only when attempting to remove the bone that it may fragment or crumble. For example, if bone is buried shallow or in an extremely cold environment, it may crack if at any time it is above the frost line in locations that experience sustained sub-zero temperatures (Liston 2007, 60; Todisco and Monchot 2008, 99). Even bones in regions that do not receive such temperatures on a regular basis can experience anomalies over decades, centuries or millennia meaning that even skeletal remains in Mediterranean sites may be subject to freezing damage given enough time, particularly “during the six specific cold events (8200,

6300, 4700, 2700, 1550 and 550 years BP)” that have affected the Mediterranean (Wanner et al. 2011, 3109).

Extraction of severely damaged bone can result in further damage or even destruction. During excavation, one tries to keep as much of the bone and thus the skeleton in situ, removing the earth around it in order to record its spatial relationships. During excavation the bones, their positions and their backgrounds are carefully photographed and drawn to keep an accurate record of their relation to each other and their surroundings. Some measurement is done in situ, however there is only so much that can be done within time constraints due to a limited field season, daily site closing times, variable lighting, and without interfering with the diggers. Drawings done on site are 2 dimensional and unable to record angles of the bone on a Z axis. The ability to create an accurate, accessible record of that bone combining the visual and quantitative aspects of it within the budgetary and time constraints of an excavation could add volumes to the story that it was able to convey.

Chapter 5 – Museum Objects

5.1 – Sculpture

For centuries the study of classical sculpture has been as important as that of ancient literary records for historians to understand the past. Methods of study, however, have been evolving with emerging technologies like photogrammetry and previous subjective methods based on style, often resulting in conflicting theories, “are now being supplemented, if not entirely replaced, by more "objective" criteria made possible by modern technological achievements” (Ridgway 1982, 155). Sculptures, particularly within the current context of repatriation and nationalism, rarely leave their countries of origin and so study is limited to those who are able to travel to such locations and have also succeeded in gaining permission to access those sculptures that they wish to study. Even with access, much of the study of sculpture is comparative in styles as well as details such as chisel shape, width and application. Sculptures being compared may be also be in pieces stored or exhibited at different locations. In some cases it may be that the goal is to determine if two partial pieces of sculpture in disparate locations are part of the same sculpture. Making pressings or casts to compare the two pieces has become very limited due to surface wear on the sculpture, controls relating to access and limited budgets.

With photogrammetry we can not only make two three dimensional models of two separate pieces; we are able to make them coexist within the same space either to compare them or, if they are thought to be from the same sculpture, finding common points, georeferencing each piece and virtually joining them as one. The benefit is not only in being able to verify the origins of given pieces but to be able to show what a completed piece would have looked like. In their 2003 work on reuniting sculptures of the Parthenon digitally, Stumpf

et al. see the use of digital models as not only good for the aforementioned reasons but also as a tool to create “realistic reconstruction of damaged or lost parts in virtual space, thus bringing us one step closer to the unattainable dream of seeing the Parthenon as it once stood” (Stumpf et al. 2003, 3).

In the summer of 2015 I was asked by Catherine Vanderpool if I could do a 3d model of a bust of Julius Caesar that was going to be temporarily removed from a case in the archaeological museum of Ancient Corinth. One great advantage of modern photogrammetry is that there can be little or no setup so such spontaneity is possible. Vanderpool’s request was that in addition to the often unavailable bust being modelled in 3d, that I photograph and model an arm housed in the Ephorate’s Apotheke (warehouse) and see if it could be matched and modelled with a torso in one of the main galleries of the museum. Vanderpool acknowledged that the bust did not belong to the armoured torso.

The bust of Caesar (Ancient Corinth Museum: S 2771) is carved from fine-crystal white marble and dates from the first century A.D. and was unearthed by Burt Hodge Hill in 1933. The torso (Ancient Corinth Museum: S 1081A) fashioned in a similar stone depicting a leather cuirass (armour) over top of a tunic, dates from the second century A.D. The cuirass is “decorated in relief with gorgoneion at center top, below two winged Nikai adorning a trophy in the center” (ASCSA.net, n.d.). (For more on these pieces see Ridgway, 1981)

5.1.1 - Julius Caesar Bust Methodology

The bust was moved to the conservation lab from its display case in the museum and positioned on a grounded post by conservator Spyros Armenis in order to elevate it from the desk surface and allow undercutting in the model. A large set of small scale targets were printed and placed around the base and table surface. No adhesives were applied to the bust and Armenis performed some detail clean-up on it before photography began.

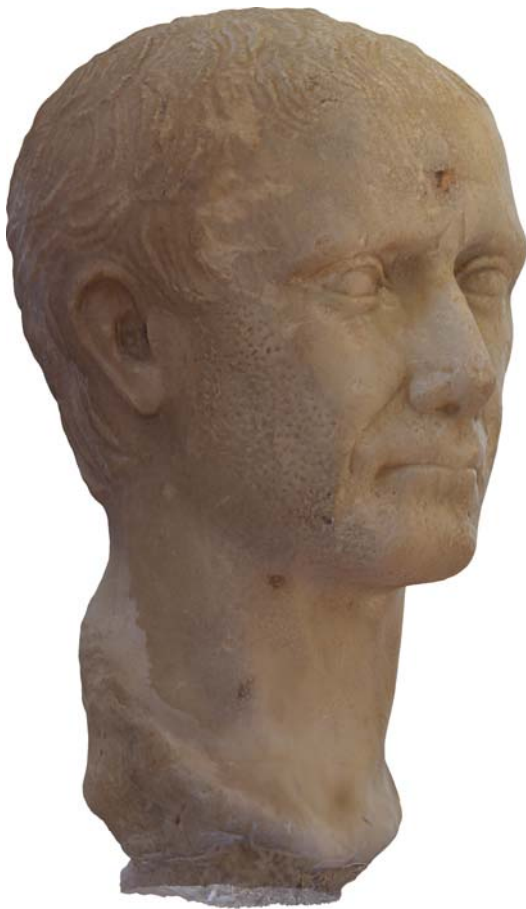


Figure 63 – 3D model of bust of Julius Caesar - Ancient Corinth Museum: S 2771

170 photos were taken; a large number for such a small object but justifiable in order to capture all of its nuances and also to obtain clear views from multiple angles of every nuance that could be hidden in complex curves, under the chin, nose, ears and in the eye

sockets. (There is always, however, the temptation to over-photograph when the subject is not completely accessible.) As mentioned in the lighting section of General Methodology, natural light coming through windows can change so shooting has to be accomplished fairly quickly. In addition, when shooting angles that included the bright windows or overhead lighting, exposures were being affected. The solution was to cover as many angles as possible while avoiding having those elements in the shots.

The model used all of the 170 photos submitted and combined with alignment of the 15 targets used resulted in an accuracy of around 1.9 pixels which is relatively low when compared to other close range objects. This may be attributable to the problem of depth of field in the images. While this may not result in as much of a quantifiable model as others, the photos applied did result in a highly detailed texture.

5.1.2 - Julius Caesar Torso and Arm Methodology



Figure 64 - Roman Torso (Ancient Corinth Museum: S 1081A)

The torso presented three challenges. The first was that it is situated just inches from the gallery wall. Attaining an all-round cohesive 3d model seemed unlikely but, by shooting many angles of shots from against the wall and using a ladder I was able to produce a presentable model with smaller gaps in the back than expected.



Figure 65 - Roman Torso Model (Ancient Corinth Museum: S 1081A)

Another challenge was the multidimensionality of the torso. All of its nooks and crannies could easily result in occlusions and so care had to be taken in shooting multiple angles of each area where there were concavities.



Figure 66 - Roman Arm

The third challenge, or rather limitation, was that as it was an open museum with spectators and there were no permissions to place targets and get a correct scale for the model. Interestingly the resulting model, due to the fact that it was shot using the same camera, lens and settings, was of the same corresponding scale as both Caesar's bust and arm.

Vanderpool and I had to locate the arm in the Ephorate's Apotheke, position it in the best makeshift area for lighting, stable surfaces and uncomplicated backgrounds and use small items to place it on so as to elevate it from the surface. When an object is sitting on a surface, the underside cannot be photographed and the surface becomes part of the object.

In order to integrate the two pieces of sculpture, each was modelled and then markers were

placed in both models at common points with matching numbers. Upon merging the models the option of using common targets was chosen and resulted in a relatively good fit between the two parts.

The Torso model used 215 of the 245 photographs taken and the arm model used 92 out of 114 photographs. In both cases the awkwardness of the photographic situation resulted in a number of photographs being rejected. The final model used only 307 of the 359 photographs input, in part due to the number of different focal lengths I used to access the complexity of the sculpture.

Associating the disparate sculpture parts has clear advantages when pieces of a single sculpture are in different locations and collections. It will allow us to view these sculptures as they once were, even allowing us to print 3d replicas of reunited objects or producing single portable pieces in order to test fit against other sculptural elements to see if they match.



Figure 67 - 3D model of Roman torso with arm relocated

Roman Torso

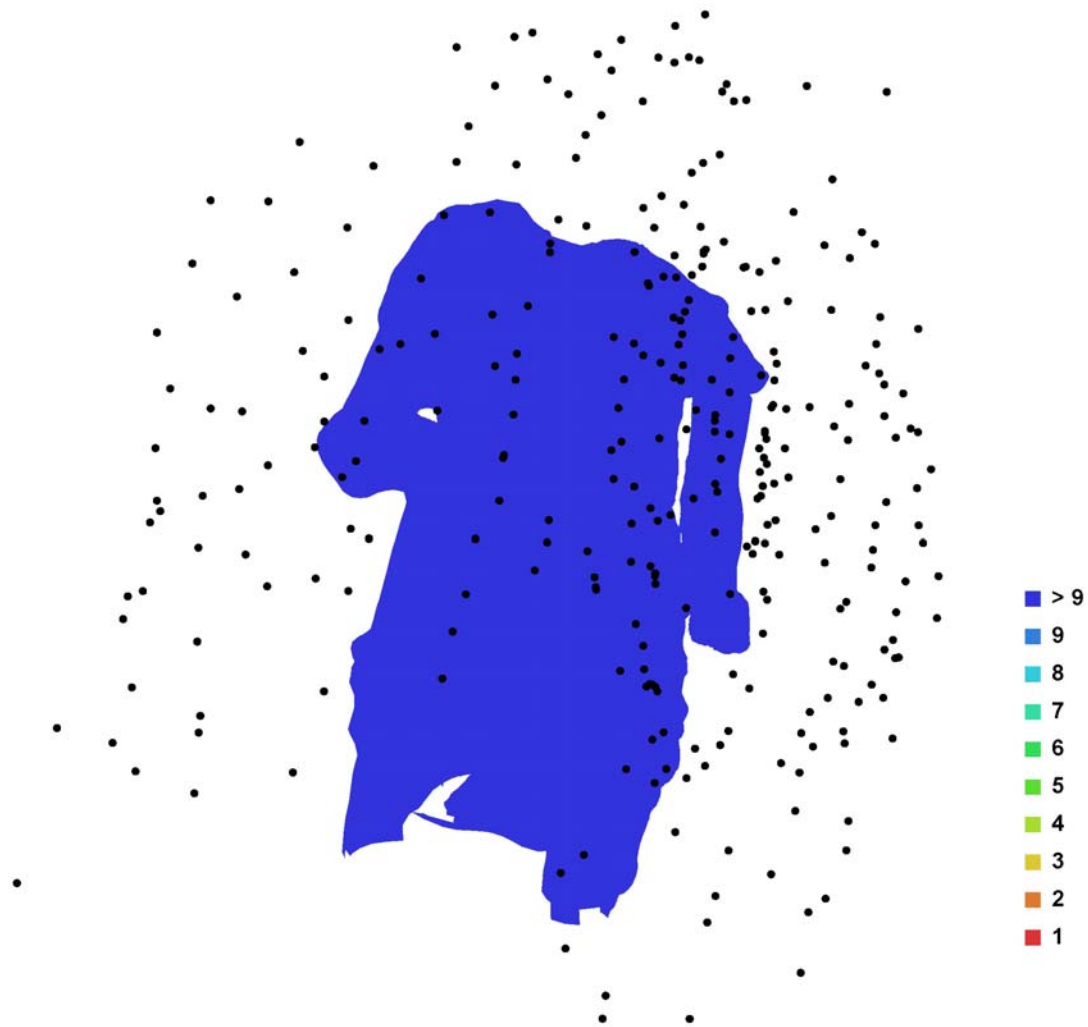


Figure 68 - Camera locations and image overlap for torso joined with arm

Number of images:	359	Camera stations:	307
Flying altitude:	3.82503 m	Tie-points:	75445
Ground resolution:	0.000742327 m/pix	Projections:	232160
Coverage area:	6.19543e-005 sq km	Error:	1.37489 pix

Table 17 - Joined torso cameras

Camera Model	Resolution	Focal Length	Pixel Size	Precalibrated
SLT-A35 (18 mm)	4912 x 3264	18 mm	4.89089 x 4.89089 um	No
SLT-A35 (20 mm)	4912 x 3264	20 mm	4.89089 x 4.89089 um	No
SLT-A35 (26 mm)	4912 x 3264	26 mm	4.89089 x 4.89089 um	No
SLT-A35 (28 mm)	4912 x 3264	28 mm	4.89089 x 4.89089 um	No

Camera Model	Resolution	Focal Length	Pixel Size	Precalibrated
SLT-A35 (30 mm)	4912 x 3264	30 mm	4.89089 x 4.89089 um	No
SLT-A35 (40 mm)	4912 x 3264	40 mm	4.89089 x 4.89089 um	No
SLT-A35 (18 mm)	4912 x 3264	18 mm	4.89089 x 4.89089 um	No
SLT-A35 (50 mm)	4912 x 3264	50 mm	4.89089 x 4.89089 um	No
SLT-A35 (55 mm)	4912 x 3264	55 mm	4.92071 x 4.92071 um	No
SLT-A35 (35 mm)	4912 x 3264	35 mm	4.93792 x 4.93792 um	No
SLT-A35 (22 mm)	4912 x 3264	22 mm	4.89089 x 4.89089 um	No
SLT-A35 (20 mm)	4912 x 3264	20 mm	4.89089 x 4.89089 um	No
SLT-A35 (30 mm)	4912 x 3264	30 mm	4.89089 x 4.89089 um	No
SLT-A35 (28 mm)	4912 x 3264	28 mm	4.89089 x 4.89089 um	No

Roman Torso - Digital Elevation Model

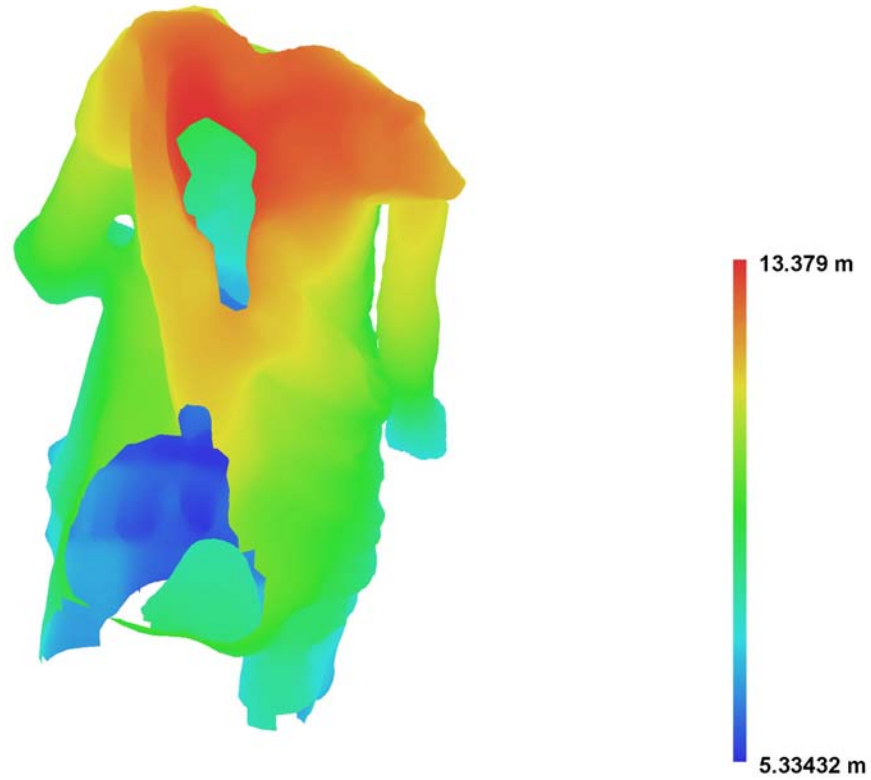


Figure 69 - Reconstructed digital elevation model of combined arm and torso

Resolution: 0.00562591 m/pix
Point density: 31594.8 points per sq m

5.2 - Small objects



Smaller objects can range from débitage to some of the most significant finds of coins, bones, jewellery and other artefacts. Capturing the nuances of these objects has always been difficult and up until the present, illustration has been used to accentuate those nuances, pronounce curves and corners, and enhance depths in order to appreciate the minutia of the object far better than with what a photograph can imply. These illustrations are enormously time consuming and while they do accomplish their task, are influenced by the subjectivity and style of the artist.

Photogrammetry of smaller objects does not have to be done in full three dimensions but

can be topical, using two models to show either side of an object such as a coin or an earring. In a set of jewellery that I illustrated for Stymphalos, Volume One: The Acropolis Sanctuary, the most difficult; ne impossible task was to capture the curvature profile of golden ring bands. The light angles and intensities of the photographs were unable to capture the nuances of the curves and I had to illustrate them with my best estimation of their geometry as the originals were 8,000 kilometres away.

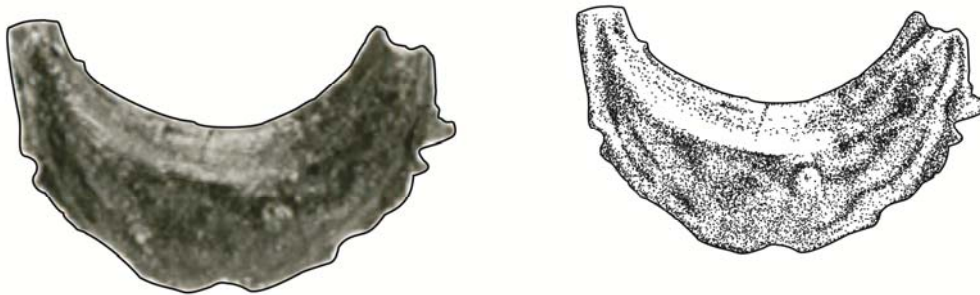


Figure 70 - Photograph of earring from Stymphalos and illustration of same

While good lighting is important, many of these shortcomings can be overcome using photogrammetry. We can make an accurate 3 dimensional model and then, within our software, literally split a piece in half showing the exact cross section of the band. This may seem a miniscule and unnecessary detail but to archaeologists such details can be very important. Such a cross section can be diagnostic in that the same producer or process might result in that cross section over and over again, allowing us with other excavated rings to ascertain stratigraphic relativity, dating, local associations and trade routes.

The cataloguing of coins is always a two dimensional process. Subtleties that might be missed with one very good light angle can be seen in a slightly different one. Using photogrammetry we are able to keep a record of every curve on the surface of a coin to be comparatively studied into the future. In addition, exported DEMs can be compared to see

if two coins have come from the same mint despite their differences in wear and damage. As with engravings, we can exaggerate the features on the surface of the coin, seeing things that we otherwise would not and being able to compare the now accentuated features with ease.

5.3.1 - Pottery Methodology

As an example of how a smaller piece can be modelled I chose an oinochoe pouring vessel from Ancient Corinth. The oinochoe was shot outside under a covered area providing diffused natural light. It was raised from shooting surface to prevent the modelling software from blending the oinochoe with the table top.

All 38 of the photographs taken were accepted into the model and resulted in a fairly comprehensive representation of the jug and an accuracy error of 0.65 pixels.



Figure 71 - Photogrammetric model of an oinochoe

The resulting models not only create a lasting 3D record of the object but also, if georeferenced, can be exported in orthophotos of different standard viewpoints in order for illustrators to create the expected profiles. As with the example given of jewellery, the ceramic can also be sectioned to show profiles of parts such as the handle allowing the model to be more diagnostic.

5.3.2 – Bone Methodology



Figure 72 - Photogrammetric mesh of a skull

In addition to the relevance of photogrammetry to the excavation documentation process it also presents opportunities with regard to the study of bones. While some collections are unavailable for study due to finances, distances or other limitations there is also the loss of data due to repatriation. With repatriation these bones and the further knowledge we could

have gained from them can be lost forever. By using photogrammetry, exact 3d replicas of individual bones or entire skeletons can be produced and, we can now print 3d replicas that not only give us the visual representation of the original but also the textural element that is an intrinsic part of osteological study. In bone fragments it is easier to size, sex or identify by feel than by visual. Recreations from photogrammetric models will allow us to do this with remains that have long left our hands.

Traditionally cast reproductions were done of bones but by using photogrammetry and 3d printing we can reduce time and cost as well as not having to directly physically interact with the bones as is the case in casting. “Combined with medical imaging systems like CT Scanners and MRIs, 3D printers can create accurate models of bones, allowing physical anthropologists to rapidly share data across the globe” (Wilder 3-D Imaging Lab 2008).

As an example of the effect achieved by modelling bone a skull stored in Ancient Corinth was used. Lighting was natural in a well diffused covered outdoor area. The skull was not suspended and modelling did result in its “adhesion” to the table surface. A major goal in this process was to be able to capture the subtle nuances, trauma and pathologies of the skull in a way that would be diagnostic in the model. To achieve this “textural” recording; beyond just being able to do craniometric measurements, 44 photographs, 43 of which were used by the program, were taken with as diverse a set of angles as possible. From previous experience learned from shooting a cow scapula outdoors with a highly complex background and its disastrous results, the backgrounds for the skull were kept as simple as possible.



Figure 73 - Cow scapula illustrating the perils of complex backgrounds

Chapter 6 - Summary of Techniques and Results

In all of the previous examples of archaeological photogrammetric recording and modelling we have seen a broad variety of challenges and solutions. Each is a learning process and has its own unique requirements but there are essential lessons to be learned from all and applied to future models.

Moving forward, the broad range of subjects and photographic methods employed for these models have provided excellent examples of the levels of accuracy that can be achieved in a model and of how to avoid a lack of accuracy. Shutter speeds should be kept above 1/100th of a second when possible. Focal range should be kept as high as possible with the proper choice of lens; in the case of the Sony A35 used in many of these examples, an 18mm focal length is optimum, particularly for achieving adequate overlap. One of the most important factors in photo documentation is keeping the F-stop as high as possible, meaning that the aperture of the lens is as small as possible, thus achieving the greatest depth of field. In order to accommodate these objectives and in view of some of the difficult lighting conditions encountered, a monopod will do so while minimizing setup and maintaining mobility.

The following table is a statistical summary of the modelling examples used in this thesis. Errors in metres are only provided in cases where georeferencing was done. The error in metres for the Asklepieion stands out as being far greater than the others in that it was not done with georeferenced markers on the ground but rather used the GPS positioning in the aerial camera. As a contrast, the result for section T21 of the Eutychia mosaic with its sub-

millimetre accuracy is in part due to careful surveying of the markers as well as the improvements in modelling technique suggested by James Herbst. Pixel error data is more comprehensive and is at its most accurate in cases where a large depth of field did not take place. The Agora inscription, skull, oinochoe, skeleton and the site at Thebes all relied on very direct photos with little use of oblique ones. Caesar's bust however, did involve oblique angles in order to capture all of its detail. Cropping of those photos in areas where blur occurs would significantly increase its accuracy.

Table 18 - Model statistical summary

	error m	error pixels	Photos	cameras	Markers	Tie Points	Dense Cloud Points	3d Model Faces
Thebes	0.024625	0.691223	324	308	15	884297	older model	269,539
Frankish Structures	0.188689	0.779176	121	115	27	202,734	18,312,814	1,220,057
Frankish Structures with Drone	1.144564	1.0414	257	257	0	31666	5,348,773	1,074,108
Asklepieion	4.890255	0.794774	86	86	0	357159	13,927,368	2,785,456
FOL 2012	na	1.45	145	144	0	33,927	2,696,553	41,398
FOL 1972	na	na	9	3	0	976	228,483	179,999
Mosaic Full	0.010067	3.935242	206	90	20	2,077,677	97,726,765	17,529,997
Mosaic T21	0.004914	0.978511	146	146	10	11,579	6,117,993	1,242,314
Caesar's Bust	na	1.9	170	170	15	12,900	1,847,793	372,777
Arm	na	1.2	114	92	4	23,669	3,176,777	638,738
Torso	na	1.4	245	215	4	51,776	21,972,809	68,587
Combined Torso & Arm	na	1.3	359	307	4	75,445	25,135,420	707,325
Inscription	na	0.748116	36	36	4	56,023	older model	21,365,478
Skull	na	0.45	44	43	0	129,484	8,064,106	1,612,817
Skeleton in situ	na	na	6	6	4	2,278	1,082,541	189,413
Oinochoe	na	0.65	38	38	0	26,949	4,089,432	641,440

The introduction of unique sizeable targets in Agisoft Photoscan; version 1.1.6 has added considerable accuracy to the modelling results compared to the bottle caps that we once used. They have provided the ability to instantly recognize all of our targets rather than having to manually assign them and the software is now better able to align the photos as a

result. While similar lighting, equipment and photo techniques, surveying and even subject matter were used to photograph the Eutychia mosaic in 2014 and 2015, a major difference was the use in 2015 of the Photoscan produced unique targets resulting in an accuracy of 0.004914 metres in 2015 versus that of 0.010067 metres with the previously surveyed handmade targets in 2014. The sub-millimetre accuracies achieved in 2015 are similar to those produced by Koutsoudis et al. (2013, 6) using Photoscan to model an Ottoman monument in Xanthi, Greece. In their testing of multiple 3D modelling software suites Schonig and Heidemann (2015, 456) find that it is “clear that PhotoScan exhibits exceedingly few deviations to the ground truth”. With the results of the Eutychia mosaic the models produced have reached a very high level of accuracy given the size of the project so at this point greater accuracy is not a concern when due diligence is observed. Further improvements in modelling therefore, are less dependent on increases in accuracy and would benefit more from increased image quality both at the photographic level with photographic equipment developments producing more detailed images with greater image stabilization for low lighting conditions and at the software level with more photorealistic representations once textures are applied.

Online documentation of photogrammetric methodology using Agisoft Photoscan is scant, vague and much of the progress that has been made in the accuracy, quality and even the visual appeal of the models we have produced over the past four years has been a result of trial and error; producing better photographs and better models with each project.

The numbers in the table do not tell the whole story. While it is imperative in larger subjects to have a larger number of photographs and greater modelling complexity, some of the most

impressive results have been with the least number of photos. With as little as two photos we can achieve a presentable, if not quantifiable model reinforcing the fact that the purpose of the model is the guiding factor in what techniques are used to achieve it.

Chapter 7 - Conclusions

While photogrammetry was and is considered to be a method of capturing large scale landscapes, quantifying them and giving them dimensions, its increased ease of use and accessibility has introduced it to new areas of study. Within archaeology, it has begun to be used for mapping whole sites but this ease and accessibility is now reducing the scale and budget of the projects that are able to take advantage of it. A digital duct tape; modern photogrammetry is finding many more uses as we explore new areas of archaeology that have not previously seen the advantage of it. The ability to almost infinitely reduce the scale of what is being photogrammetrically documented geometrically multiplies the technique's subject matter. For Edouard Deville, the modelling of the Rocky Mountains was a lofty goal. In the contemporary archaeological environment with its academic challenges, photogrammetry represents the ability to capture the subtle nuances of all aspects of an archaeological site at virtually no cost; an equally lofty goal.

What the examples in this thesis have shown is that it is essential to consult with the archaeologists, conservators or other scholars requesting that 3D modelling be done in order to tailor the work to the results needed.

Photogrammetry has enormous potential in that it can be applied to various aspects of archaeological field work, documentation, public information, museum work and academic publication. Depending on the purpose of the model, different techniques can be applied to achieve the appropriate results. Compound these challenges with shrinking budgets and photogrammetry could become what is possibly the most powerful tool to arrive in the

archaeologist's arsenal since the trowel.

Moving forward with the techniques learned in the examples in this thesis the primary goal will be to continue to increase the predictability and accuracy of the models. Raising interest and awareness of the possibilities of 3D modelling will inevitably lead to new opportunities and an even broader variety of subject matter. A new project already on the horizon is to model an ancient musical instrument housed in the archaeological museum of Ancient Corinth in order to provide a CNC (computer numerical control) wood crafter with a digital model with which to make an exact recreation so that it might be played to show visitor what an instrument like that might have sounded like.

As 3d photogrammetry becomes more accepted and utilized, so too will 3D printers which are plummeting in price and the combination of these two technologies represents many remarkable possibilities. In teaching, being able to supply students with replicas of artifacts being studied and significantly reducing the cost of type specimens will enhance the learning process and allow greater engagement with students. In museums being able to allow visitors more of a hands-on experience handling replicas makes for a more immersive experience. Even the ability to preserve the record of artifacts of all sizes that might foreseeably be put in jeopardy by some of the radical groups currently destroying portions of our shared world heritage allows for not only the continued study of such artifacts but more importantly, CNC machined exact recreations.

Possible applications of photogrammetry continue to arise. As with any technology, the future can be difficult to predict but the direction that photogrammetry has been moving

in is clear; it is increasingly accessible to those with less training and small budgets, broadening its possible application in documenting all aspects of the dense Mediterranean archaeological record, preserving data for use now and by future generations.

Sources Cited

Ajioka, O., Hori, Y., Application of SFM and Laser Scanning Technology to the Description of Mosaics Piece by Piece, The International Archives of the Photogrammetry, Remote Sensing and Spatial Information Sciences, Volume XL-5, 2014
ISPRS Technical Commission V Symposium, 23 – 25 June 2014, Riva del Garda, Italy

Albertz, J., Meydenbauer, A., Pioneer Of Photogrammetric Documentation Of The Cultural Heritage, Proceedings 18th International Symposium CIPA 2001

ASCSA.net, Corinth Object: - S 1081A – ASCSA.net, Retrieved November 19, 2015 from <http://corinth.ascsa.net/id/corinth/object/s%201081a?q=references%3A%22Corinth%3APublication%3ARidgway%2C+Hesperia+50.4%2C+1981%22&t=&v=icons&p=1&sort=rating+desc%2C+sort+asc&s=18>

ASCSA.net, Corinth Object: - S 2771 – ASCSA.net, Retrieved November 19, 2015 from <http://corinth.ascsa.net/id/corinth/object/s%202771?q=s2771&t=&v=icons&sort=&s=1>

ASCSA.net., Corinth Monument Asklepion, Retrieved October 28, 2015, from <http://corinth.ascsa.net/id/corinth/monument/asklepion?q=&t=monument&v=table&sort=&s=17>

BBC, Turkey: Investigation over 'ruined' Roman mosaics, <http://www.bbc.com/news/blogs-news-from-elsewhere-32582162>

Berkeley.edu, What is Rubbing?, 2004, <http://www.lib.berkeley.edu/EAL/stone/rubbings.html>

Bouras, Ch., Particular difficulties in the conservation and study of Greek historical monuments, *Photogrammetria*, Volume 30, Issues 3–6, June 1975, Pages 99–105

Bozia, E., Barmpoutis, A., Wagman, R.S., 'The First Online 3D Epigraphic Library', In *Proceedings of CIEGL12: 14th International Congress of Greek and Latin Epigraphy*, Humboldt University, Berlin, 27 - 31 Aug, 2012.

Bradley, R., “Repeating the unrepeatable experiment” in *Material Evidence: Learning from Archaeological Practice* Edited by Robert Chapman and Alison Wylie, Routledge 2015, pp 23-41

von Brevern, Jan, *Intermédialités : histoire et théorie des arts, des lettres et des techniques / Intermediality: History and Theory of the Arts, Literature and Technologies*, n° 17, 2011, p. 53-67

Birrell, A *Survey Photography in British Columbia 1858-1900, The Past in Focus: Photography & British Columbia, 1858-1914, Winter 1981/82*

Collier, O., 2002. “The Impact on Topographic Mapping of Developments in Land and Air Survey: 1900-1939”, *Cartography and Geographic Information Science*, 29(3): 155-174.

Dimitriadis, G., Ampatzidis, D., Scale error inconsistencies in classical geodetic networks via GNSS baselines, *South-Eastern European Journal of Earth Observation and Geomatics*, Issue Vo3, 2014

Doyle, F., 1964. "The Historical Development of Analytical Photogrammetry", *Photogrammetric Engineering*, XXX(2): 259-265.

El-Hakim, S., Beraldin, J.A., Picard, M., Cournoyer, L., Surface Reconstruction Of Large Complex Structures From Mixed Range Data – The Erechtheion Experience, *The International Archives of the Photogrammetry, Remote Sensing and Spatial Information Sciences*. Vol. XXXVII. Part B5. Beijing 2008

Garnett, K.S., "Variety as Roman Lamp Forms Follow Function" *Proceedings of the Balkan Light 2015*, 16-19 September 2015, Athens, Greece, pp.405-412

Garnett, K.S., Late Roman Corinthian Lamps from the Fountain of the Lamps, *Hesperia: The Journal of the American School of Classical Studies at Athens*, Vol. 44, No. 2 (Apr. - Jun., 1975), pp. 173-206, Published by: [The American School of Classical Studies at Athens](http://www.jstor.org/proxy/lib.uwaterloo.ca/stable/147586)
Article Stable URL: <http://www.jstor.org/proxy.lib.uwaterloo.ca/stable/147586>

Getty Museum, Roman Mosaics from Tunisia,. (n.d.). Retrieved November 13, 2015, from http://www.getty.edu/museum/conservation/partnerships/roman_mosaics/

Hamarneh, C., Mjalli, A.M., Al-Balawneh, M., Documentation of Mosaic Tangible Heritage in Jordan, *Annual of the Department of Antiquities of Jordan* 01/2008; 52

Hodder, I., (1997). 'Always momentary, fluid and flexible': towards a reflexive excavation methodology. *Antiquity*, 71, pp 691-700.

Hodder, I., Hutson, S., *Reading the Past: Current Approaches to Interpretation in Archaeology*, Cambridge University Press 2003

Hodder, I., Shanks, M., Alexandri, A., Buchli, V., Carman, J., Last, J., Lucas, G., (eds) *Interpreting Archaeology: Finding Meaning in the Past*. Routledge, 1995

Işiklikaya I. "Comparison of Conventional and Photogrammetric Documentation of Mosaics at the Agora of Perge" in Aïcha Ben Abed, Martha Demas, and Thomas Roby (ed) *Lessons Learned: Reflecting on the Theory and Practice of Mosaic Conservation*, the Getty Conservation Institute, pp. 358-361, 2008

Koutsoudis, A., Vidmar, B., Ioannakis, G., Arnaoutoglou, F., Pavlidis, G. and Chamzas, C., Multi-image 3D reconstruction data evaluation., *Journal of Cultural Heritage*, 15(1): 73–79, 2014.

Konecny, G., 1985. "The International Society for Photogrammetry and Remote Sensing - 75 Years Old, or 75 Years Young", *Keynote Address, Photogrammetric Engineering and Remote Sensing*, 51(7), pp 919-933.

Fussell, A., "Terrestrial Photogrammetry in Archaeology" *World Archaeology*, Vol. 14, No. 2, Photogrammetry/Miscellany (Oct., 1982) , pp. 157-172

Lucas, G., *Critical Approaches to Fieldwork: Contemporary and Historical Archaeological Practice*, Routledge 2001

Liston, M.. "Secondary Cremation Burials at Kavousi Vronda, Crete: Symbolic Representation in Mortuary Practice". *Hesperia: The Journal of the American School of Classical Studies at Athens* 76.1 (2007): 57–71.

Marinov, B., FH-KA - Master course Photogrammetry 2003, University of Karlsruhe, http://www.uacg.bg/filebank/acadstaff/userfiles/study_en_425_Karlsruhe_photo_L0_jpg.pdf

Meritt, B., Traill, J., *The Athenian Agora XV. The Athenian Councillors*. Princeton 1974. pp 345-346

Ministry of Culture and Sports | Thebes (Ministry of Culture and Sports | Thebes)

http://odysseus.culture.gr/h/3/eh351.jsp?obj_id=2459

Moullou, D., "The project "Development of Geographical Information Systems on the Acropolis of Athens". *Managing scientific questions of documentation "Acropolis Restoration News 10*, 2010, 12-15

Moullou, D., Mavromati, D., 2007. Topographic and photogrammetric recording of the Acropolis of Athens. *Proc. Of XXI International CIPA Symposium*, 1-6 October, Athens, Greece, 515-520

Moysiadis, A., Perakis, K.,, " The potential of conventional surveying, photogrammetry and laser scanning in monuments of cultural heritage documentation", *Proceedings of the 3rd International CEMEPE & SECOTOX Conference Skiathos*, June 19-24, 2011, pp. 1291-1296

Papadaki, A. I., et al. "Accurate 3d Scanning Of Damaged Ancient Greek Inscriptions For Revealing Weathered Letters." *ISPRS-International Archives of the Photogrammetry, Remote Sensing and Spatial Information Sciences 1* (2015): 237-243.

Pfaff, C.A., "Archaic Corinthian Architecture, ca. 600 to 480 B.C.", *Corinth*, Vol. 20, *Corinth, The Centenary: 1896-1996* (2003), pp. 95-140, Published by: American School of Classical Studies at Athens
Stable URL: <http://www.jstor.org/stable/4390719>

Ridgway, *Sculpture from Corinth*, *Hesperia: The Journal of the American School of Classical Studies at Athens*, Vol. 50, No. 4, *Greek Towns and Cities: A Symposium* (Oct. - Dec., 1981), pp. 422-448

Ridgway, Brunilde S. 1982. The Study of Ancient Sculpture. *American Journal of Archaeology* 86:155-157

Robinson, B., "Good Luck" from Corinth: A Mosaic of Allegory, Athletics, and City Identity, *American Journal of Archaeology*, Vol. 116, No. 1 (January 2012), pp. 105-132

Published by: [Archaeological Institute of America](#)

Article DOI: 10.3764/aja.116.1.0105

Article Stable URL: <http://www.jstor.org/stable/10.3764/aja.116.1.0105>

Roebuck, C., The Asklepieion and Lerna, Corinth, Vol. 14, The Asklepieion and Lerna (1951), pp. iii-xi+xiii+1-173+175+177-182, Published by: American School of Classical Studies at Athens

Shanks, M., Hodder, I., "Processual, Postprocessual, and Interpretive Archaeologies" in Hodder et al (eds) 1995, pp 3-29.

Schöning J. and Heidemann G. 2015, Evaluation of Multi-view 3D Reconstruction Software in Azzopardi G and Petkov N. (eds) *Computer Analysis of Images and Patterns*. 16th International Conference, CAIP 2015, Valletta, Malta, September 2-4, 2015, Proceedings, Part II, Lecture Notes in Computer Science, Volume 9257, pp 450-461

Smith, T., Plantzos, D., *A companion to Greek art* (Blackwell companions to the ancient world; 90). Malden, MA; Oxford: Wiley-Blackwell., 2012

Snodgrass, A.M., 1987: *An archaeology of Greece: the present state and future scope of a discipline*, University of California Press, Berkeley

Stumpf, J., Tchou C, Hawkins, T., Martinez, P., Emerson, B., Brownlow, M., Jones, A., Yun, N., and Debevec, P., Digital Reunification of the Parthenon and its Sculptures, 4th International Symposium on Virtual Reality, Archaeology and Intelligent Cultural Heritage, VAST (2003)

D. Arnold, A. Chalmers, F. Niccolucci (Editors)

Schenk, T., *Introduction to Photogrammetry*, Department of Civil and Environmental Engineering and Geodetic Science, The Ohio State University, 2005

Symeonoglou, S., *The Topography of Thebes from the Bronze Age to Modern Times*. Princeton University Press, Princeton, 1985

Todisco, D., Monchot, H., Bone Weathering in a Periglacial Environment: The Taya ra Site (KbFk-7), Qikirtaq Island, Nunavik (Canada), Arctic, VOL. 61, NO.1 (MARCH 2008) P. 87-101

Tsingas, V., Liapakis, C., Xylia V., D. Mavromati, Moullou D., Grammatikopoulos L., Stentoumis, C, "3d Modelling of the Acropolis of Athens using balloon images and terrestrial Laser Scanning" *The International Archives of the Photogrammetry, Remote Sensing and Spatial Information Sciences*. Vol. XXXVII. Part B5. Beijing 2008, 1101-1106)

Verhoeven, G., Doneus, N., Doneus, M., & Štuhec, S. (2013). From pixel to mesh: accurate

and straightforward 3D documentation of cultural heritage from the Cres/Lošinj archipelago. In Z. Ettinger Starčić & D. Tončinić (Eds.), *Izdanja hrvatskog arheološkog društva* (Vol. 30, pp. 165–176). Presented at the Istraživanja na otocima, Zagreb: Hrvatsko arheološko društvo - Lošinjski muzej.

Wanner, H., Solomina, O., Grosjean, M., Ritz, S.P., Jetel, M., Structure and origin of Holocene cold events, *Quaternary Science Reviews*, Volume 30, Issues 21–22, October 2011, Pages 3109-3123, ISSN 0277-3791,
<http://dx.doi.org/10.1016/j.quascirev.2011.07.010>.
(<http://www.sciencedirect.com/science/article/pii/S0277379111002149>)

Wilder 3-D Imaging Lab Wilder 3-D Imaging Lab, 2008, Texas A&M University - Center for Maritime Archaeology and Conservation,
<http://nautarch.tamu.edu/WilderLab/3dprinting.shtml>

Williams, C., Frankish Corinth: An Overview, *Corinth*, Vol. 20, Corinth, The Centenary: 1896-1996 (2003), pp. 423-434

Wiseman, J., Excavations in Corinth, the Gymnasium Area, 1967-1968, *Hesperia: The Journal of the American School of Classical Studies at Athens*, Vol. 38, No. 1 (Jan. - Mar., 1969), pp. 64-106
Published by: [The American School of Classical Studies at Athens](#)
Article Stable URL: <http://www.jstor.org.proxy.lib.uwaterloo.ca/stable/147640>

Wiseman, J., [Remote Sensing in Archaeology](#)
New York, NY : Springer 2007

Wiseman, J., The Gymnasium Area at Corinth, 1969-1970, *Hesperia: The Journal of the American School of Classical Studies at Athens*, Vol. 41, No. 1 (Jan. - Mar., 1972), pp. 1-42
Published by: [The American School of Classical Studies at Athens](#)
Article Stable URL: <http://www.jstor.org.proxy.lib.uwaterloo.ca/stable/147475>

Wolf, P., Dewitt, B., Wilkinson, B.: Elements of Photogrammetry with Applications in GIS, Fourth Edition. [Introduction to Analytical Photogrammetry](#), Chapter (McGraw-Hill Professional, 2014), AccessEngineering

Sources consulted but not Cited

Aguilera, D. G.; Lahoz, J. G., Virtual Archaeological Sites Modelling Through Low-Cost Methodology

[Survey Review](#), Volume 42, Number 317, July 2010 , pp. 300-315(16)

Bahadir Ergun [Creating A 3D urban model by terrestrial laser scanners and photogrammetry techniques: a case study on the historical peninsula of Istanbul](#)

Proc. SPIE 6618, 66180H (2007); <http://dx.doi.org/10.1117/12.720988>

Ducke, B., Score, D., J., Reeves, Cultural Heritage Multiview 3D reconstruction of the archaeological site at Weymouth from image series Oxford

Archaeology, Janus House, Osney Mead, OX20ES, Oxford, UK

M. Brunetti, M. Callieri, B. Pizzo, C. Montani, P. Pingi, and R. Scopigno [Using 3D scanning to monitor wood deformations and to evaluate preservation strategies](#) Proc. SPIE

6618, 66180E (2007); <http://dx.doi.org/10.1117/12.726169> Online Publication Date: Jul 16, 2007

J. N. Green, P. E. Baker, B. Richards and D. M. Squire, [Simple Underwater Photogrammetric Techniques](#) , Archaeometry, Volume 13, Issue 2, August 1971, Pages: 221–232, Article first published online : 23 AUG 2007, Volume 13, Issue 2, August 1971, Pages: 221–232, Article first published online : 23 AUG 2007,

Fabio Bruno, Stefano Bruno, Giovanna De Sensi, Maria-Laura Luchi, Stefania Mancuso, Maurizio Muzzupappa From 3D reconstruction to virtual reality: A complete methodology for digital archaeological exhibition
Journal of Cultural Heritage, Volume 11, Issue 1, January–March 2010, Pages 42-49

Proceedings 18th

International Symposium CIPA 2001 Potsdam (Germany), September 18 - 21, 2001

Albrecht Meydenbauer – Pioneer of Photogrammetric Documentation of the Cultural Heritage

Jörg Albrecht

Proceedings 18th International Symposium CIPA 2001

Image Credits

Figure 1 - Aerial Photogrammetry (Marinov 2003, 2)

Figure 2 - Close Range Photogrammetry (Marinov 2003, 3)

Figure 3 <http://www.uh.edu/engines/durer1.gif>

Figure 14 -

<http://ascsa.net/id/corinth/image/digital%202013%200403?q=herbst&t=image&v=list&sort=&s=1>

Figure 8- General Plan © YSMA Archive

http://www.ysma.gr/static/images/6_4_GIS_KatopsiGEN.jpg

Appendix 1 – Tutorial

For those who are going to use photogrammetry to model a mosaic, here is a summary of the steps we used to model the Eutychia mosaic which you may find useful. To the best of my knowledge there is not such a tutorial available for the photogrammetry of mosaics using latest version of Agisoft Photoscan; version 1.1.6.

The first step in working on such a complex model is to organize your photographs in an orderly and easily referenced manner. It is important to remember that Photoscan uses absolute referencing of the photo's location when building the model so a consistent location must be chosen. In our example, photos of each tesserae panel were stored in individual folders named T1, T2, etc. which were in turn housed in a folder called Eutychia within Dropbox. Each model was stored in the root of Eutychia folder. Another folder within Eutychia was used to store untrimmed orthophotos and a final folder was used to store the trimmed orthophotos and the resulting model and AutoCAD drawing. Photo sets ranging from 35 to 114 photos were individually loaded and modelled.

First the align photos command was used on the photos with no coordinates entered, producing a sparse point cloud. Settings for this step were Accuracy: High and Pair Selection: Generic. The default Tie Point Limit of 40000 and Key Point Limit of 1000 were used.

Once the sparse cloud was created, the Detect Markers command was used. In some cases all ten markers were found while in others as few as five were. For smaller panels the more remote markers were not found or lack of focus made accurate placement of them

unreliable. Tesserae panels ranged from approximately one metre square to 1.5 metres by 2.5 metres. The marker coordinates surveyed by James Herbst were then imported and in cases where no marker had been found, those coordinates were used to make a new marker. Most markers then appeared on the photos as confirmed location flags while others formed the “smoking points” that Photoscan uses to denote suggested locations for markers. Each of these smoking points, sometimes in the hundreds, then had to be individually adjusted into place over the center of each target. Once every flag was in place, averaging between 80 to 200 per model, the cameras (photos) were optimized. The Dense Cloud was then constructed.

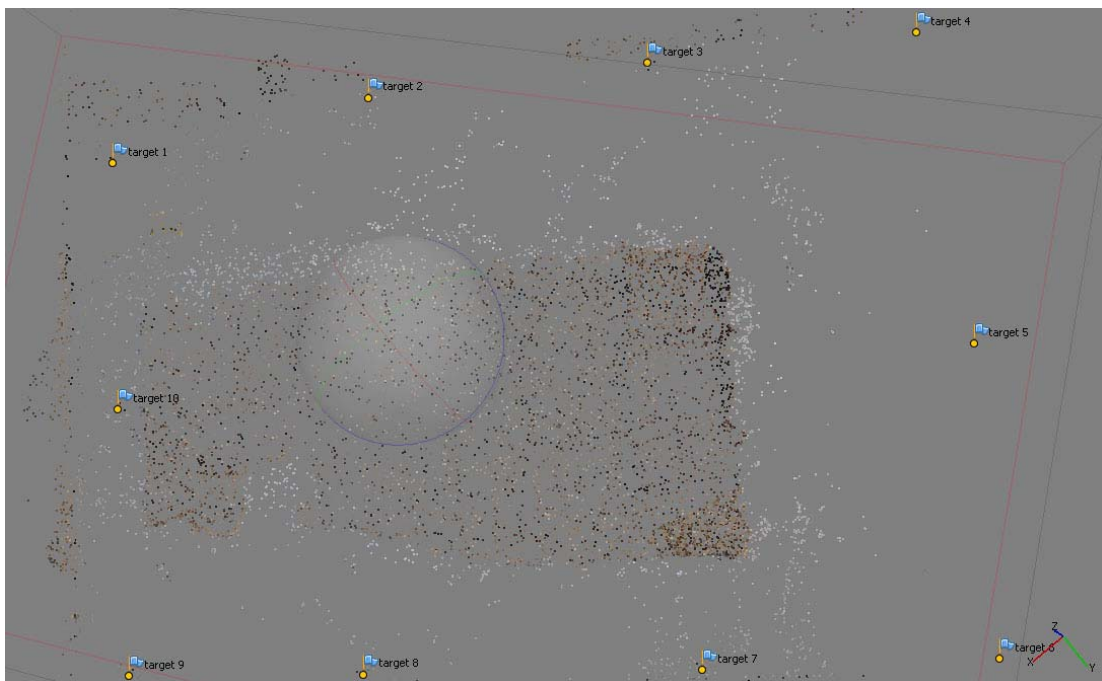


Figure 74 - Sparse point cloud of a mosaic panel showing georeferenced targets

Dense clouds on these panels took as little as one half hour to as much as six hours to build. (Done one at a time there would not have been enough time during my four week stay to complete the project so I used remote desktop to access two machines that I had built at the University of Waterloo. These machines already had the photos loaded via Dropbox so I was able to run multiple models simultaneously.) Through experimentation we found that

using medium quality instead of high or ultra-high on the dense clouds made no difference to the accuracy of the measurements and saved a significant amount of time. Depth filtering was set to Aggressive.



Figure 75 - Dense point cloud of mosaic panel

The dense cloud was then used to produce a mesh; millions of triangular vector lines joining three, three dimensionally located points at a time. This also took a considerable amount of time per model; from 15 minutes to three hours. The mesh was produced with Surface Type: arbitrary, Source Data: dense cloud and Face Count set at High (1,227,449).

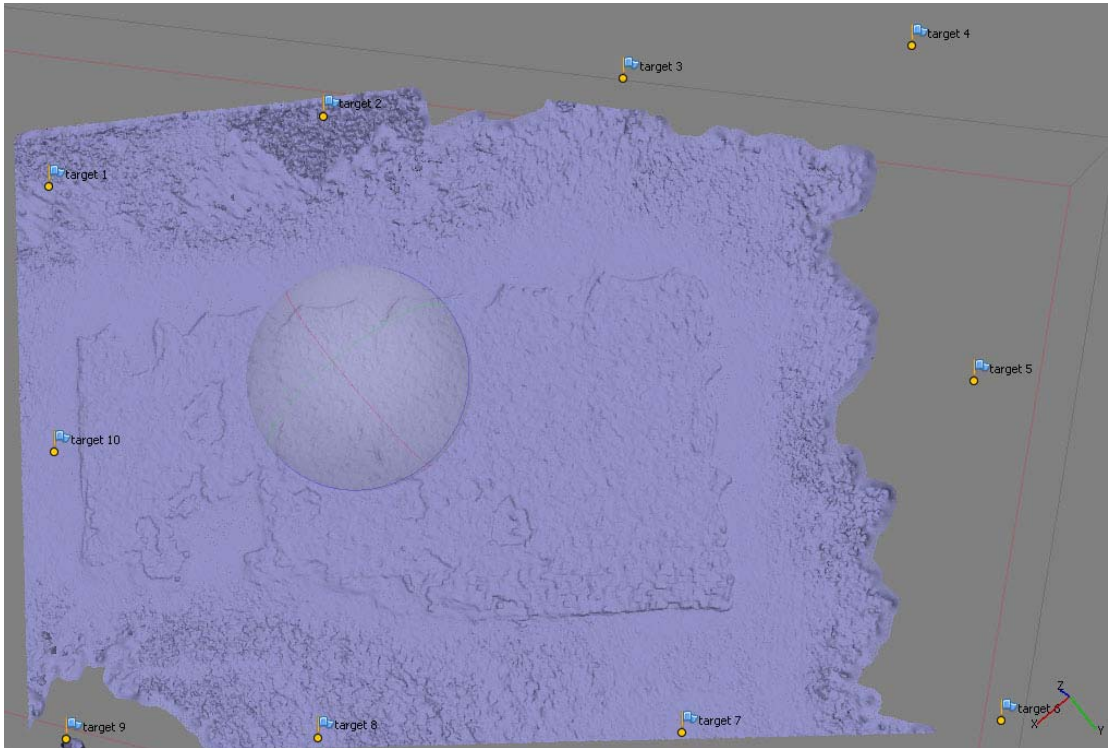


Figure 76 - Mesh applied to mosaic panel

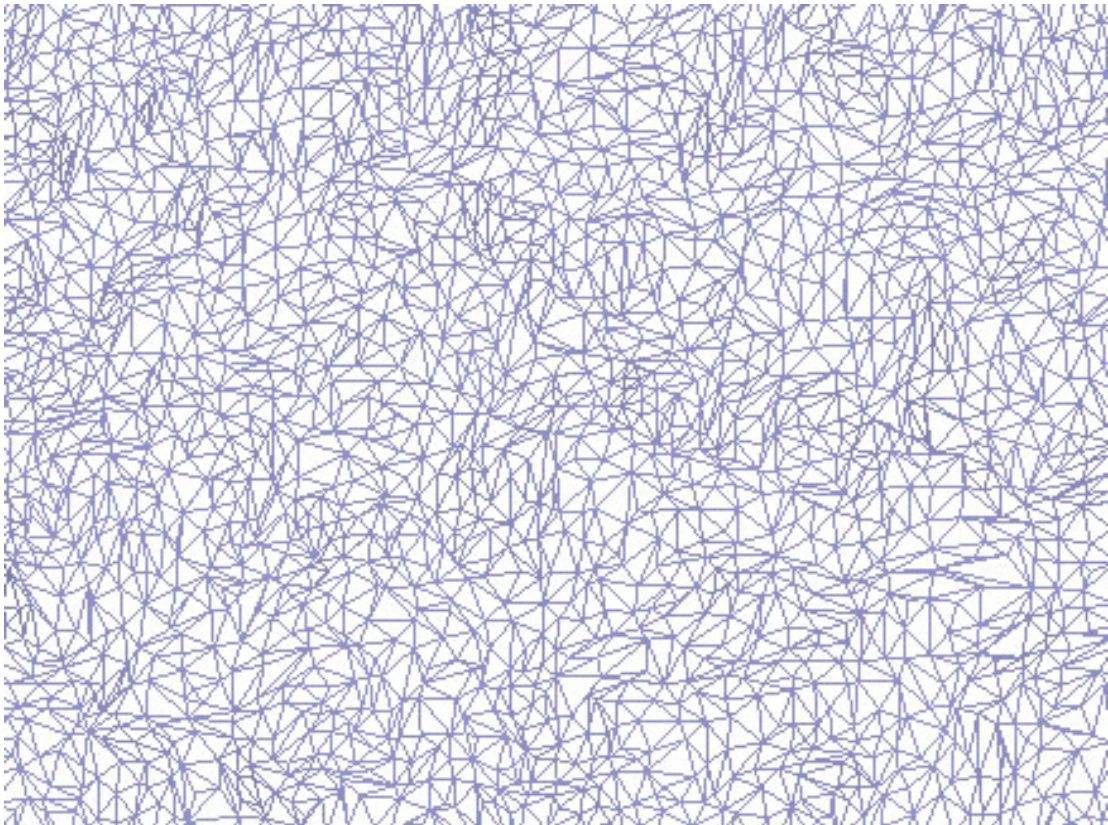


Figure 77 - Closeup of mesh showing points joined by triangles

Once the mesh was constructed, texture was applied, “draping” the 3d mesh with elements of the photos used to construct the model, giving it a life like quality. Mapping Mode was generic, Blending Mode was “mosaic” and Texture Size/Count was set at 4096 X 4 to avoid pixilation and give the individual tessera clarity for use during the Photoshop trimming process.

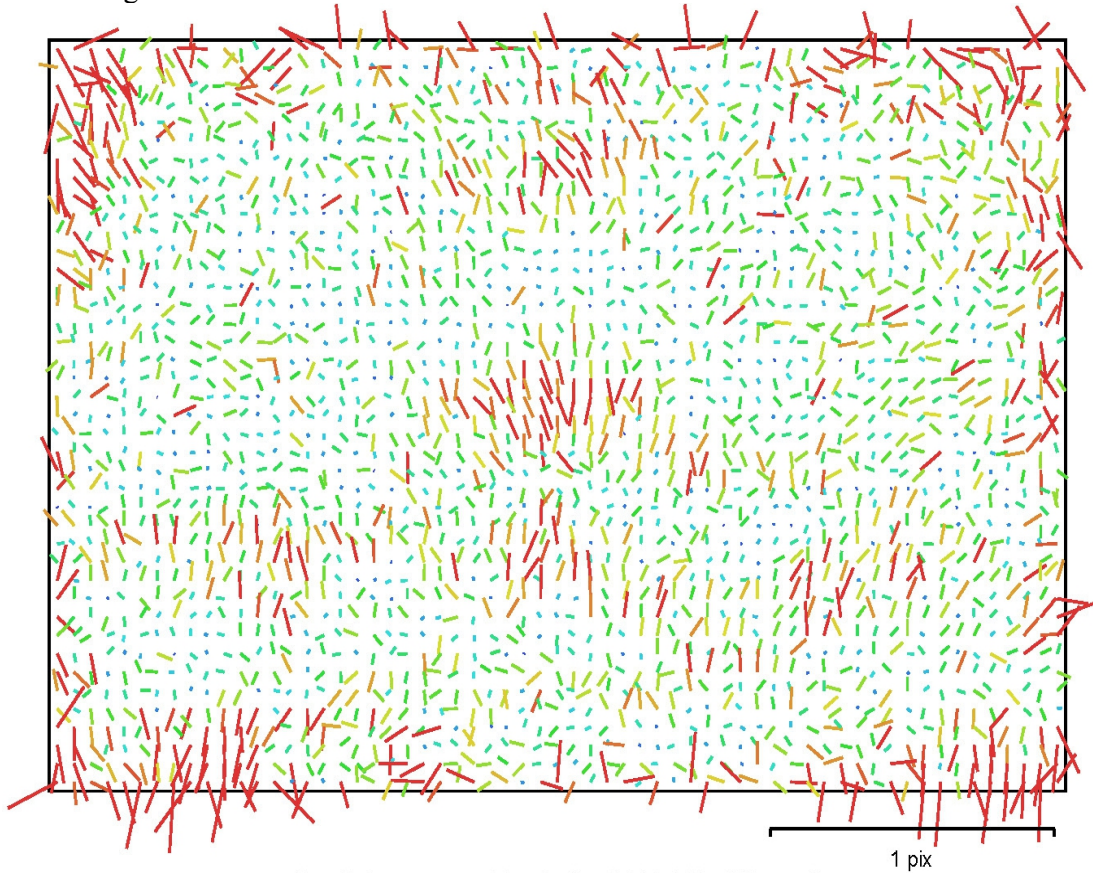
The preceding steps and settings were achieved through a trial and error process and worked best for our needs and the nature of our photos and models. Variations on these may better suite other user’s projects.

Appendix 2 – Camera Calibrations

Calibration of cameras between the sparse cloud and dense cloud stages of processing has proven to significantly improve the accuracy of results. The following pages are reports on the calibration for each of the georeferenced models.

For each model there is a calibration page for each focal length used. In models that are made from two joined chunks there is a set of calibrations for each chunk and so specific focal lengths will be seen multiple times.

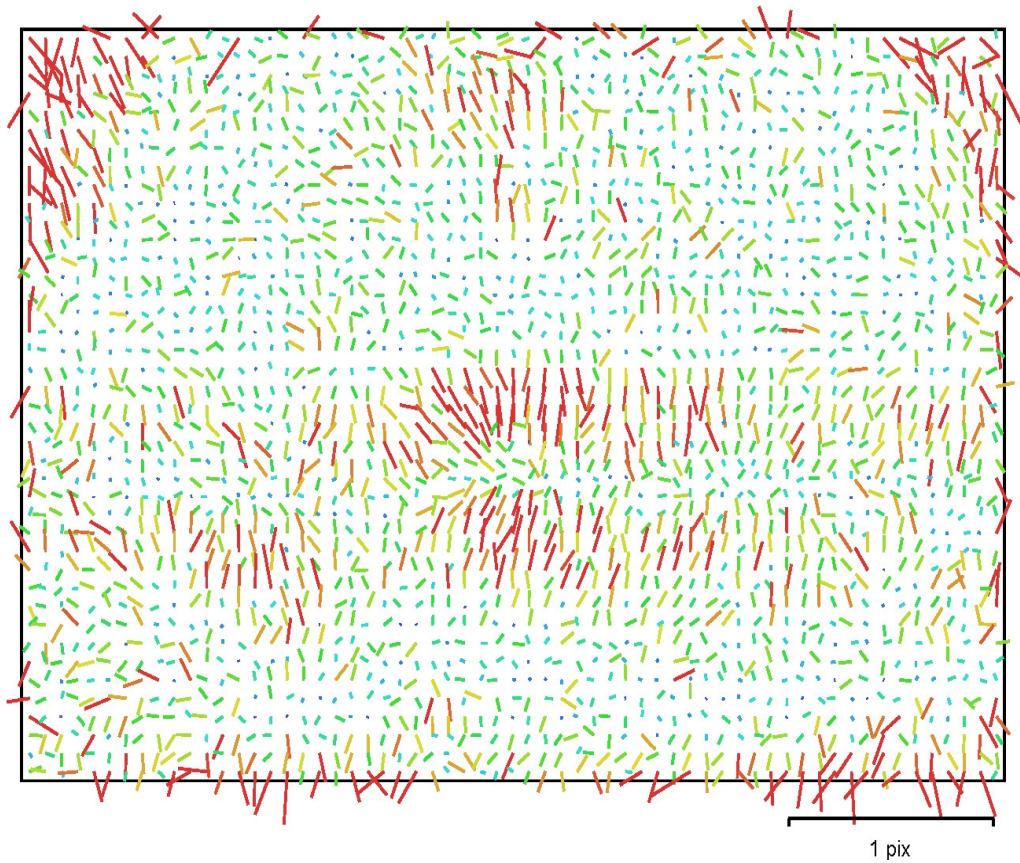
Thebes Original



SLT-A35 (18 mm)

Type:	Frame	K1:	-0.0899512
Fx:	3795.41	K2:	0.0215929
Fy:	3795.41	K3:	-0.000144522
Cx:	2440.07	K4:	0
Cy:	1619.95	P1:	0
Skew:	0	P2:	0

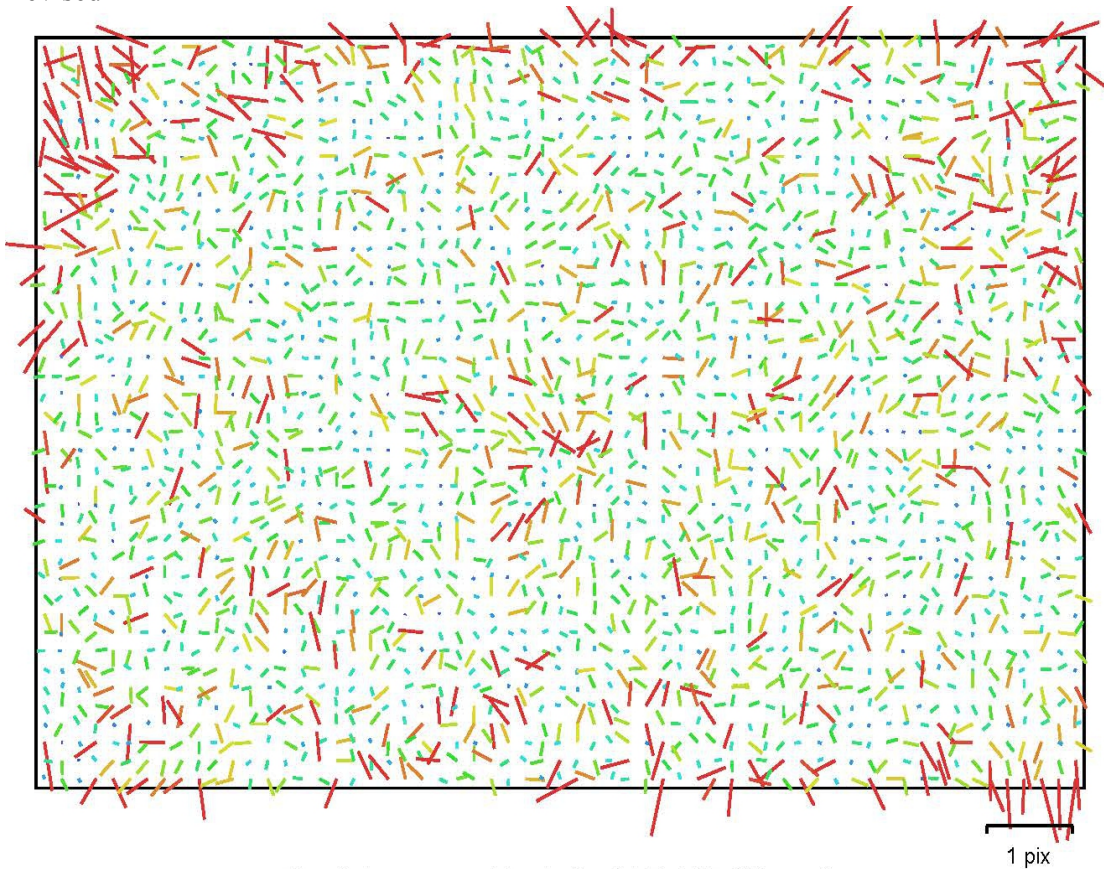
Thebes Original



SLT-A35 (18 mm)

Type:	Frame	K1:	-0.0921161
Fx:	3804.89	K2:	0.0303829
Fy:	3804.89	K3:	-0.0095383
Cx:	2442.33	K4:	0
Cy:	1610.61	P1:	0
Skew:	0	P2:	0

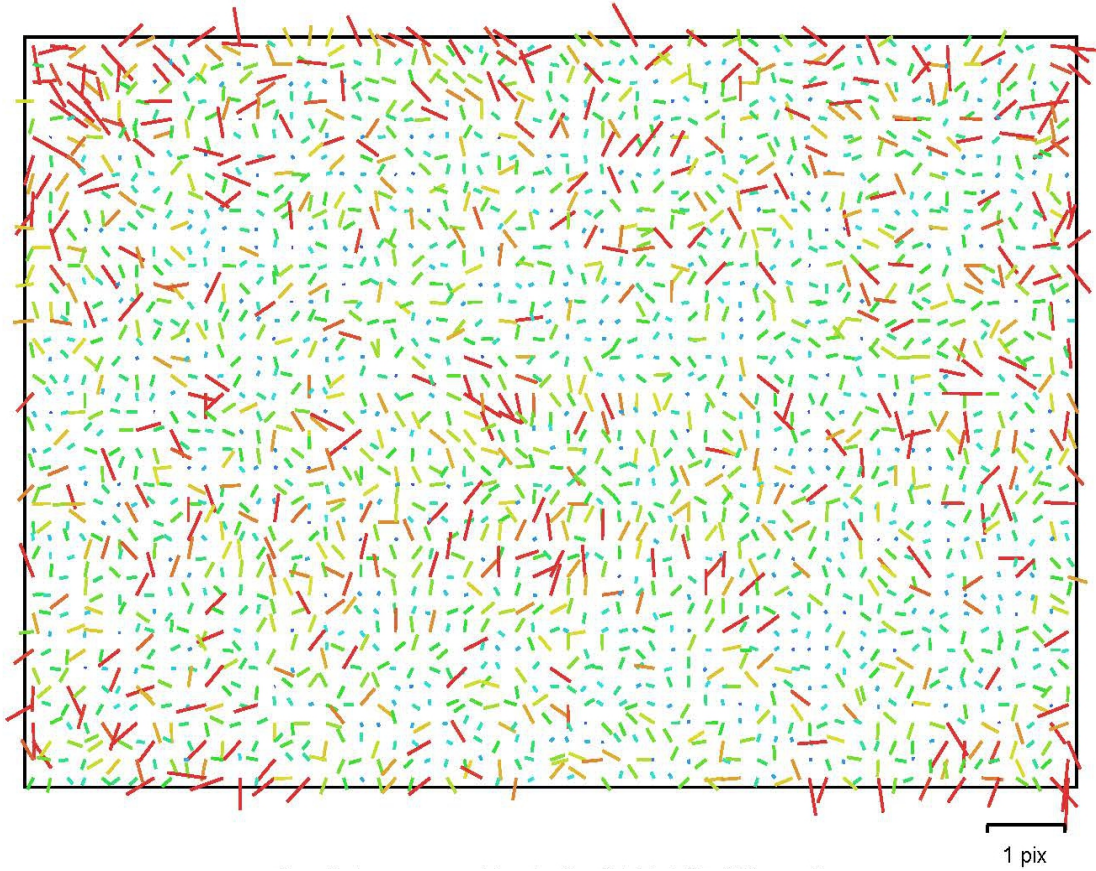
Thebes
Revised



SLT-A35 (18 mm)

Type:	Frame	K1:	-0.0896934
Fx:	3799.86	K2:	0.0238875
Fy:	3799.86	K3:	-0.00350264
Cx:	2442.84	K4:	0
Cy:	1620.47	P1:	0
Skew:	0	P2:	0

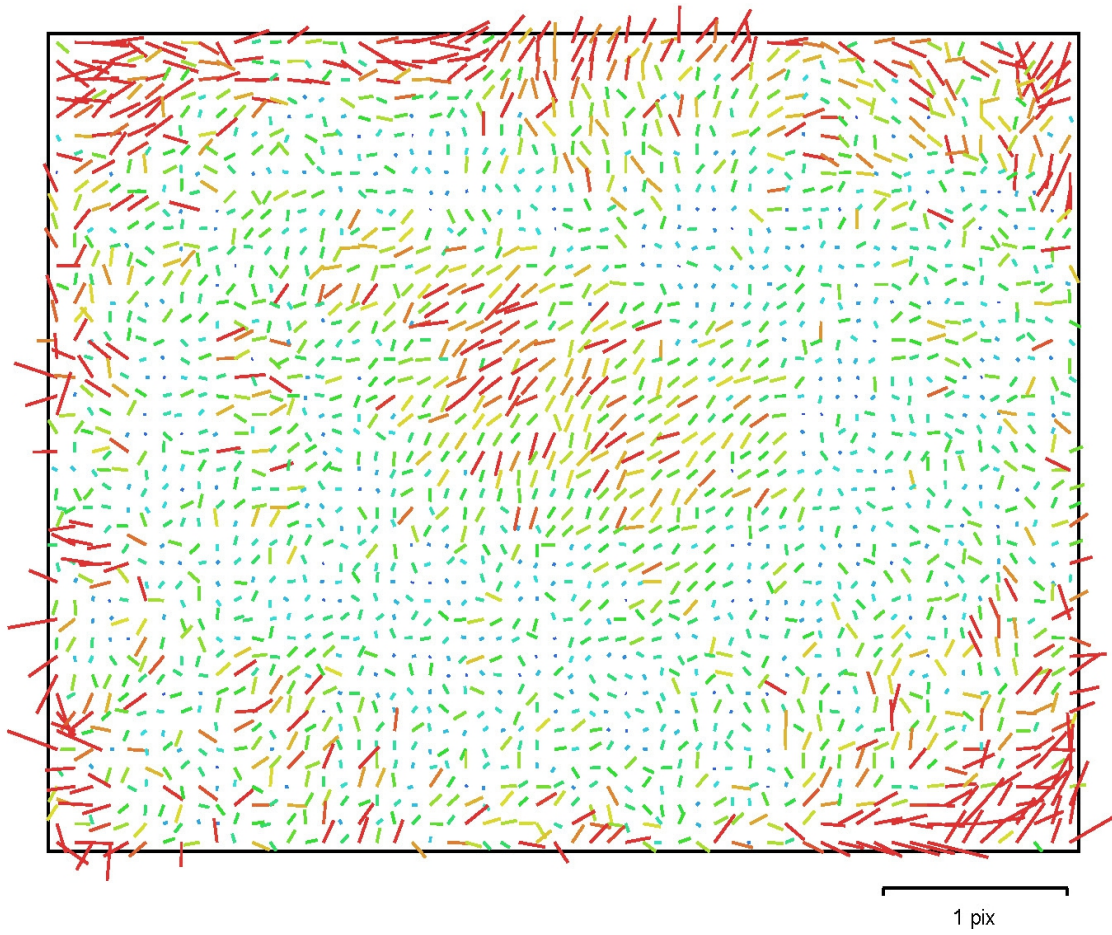
Thebes Revised



SLT-A35 (18 mm)

Type:	Frame	K1:	-0.0924974
Fx:	3802.94	K2:	0.0310593
Fy:	3802.94	K3:	-0.00981446
Cx:	2442.44	K4:	0
Cy:	1611.35	P1:	0
Skew:	0	P2:	0

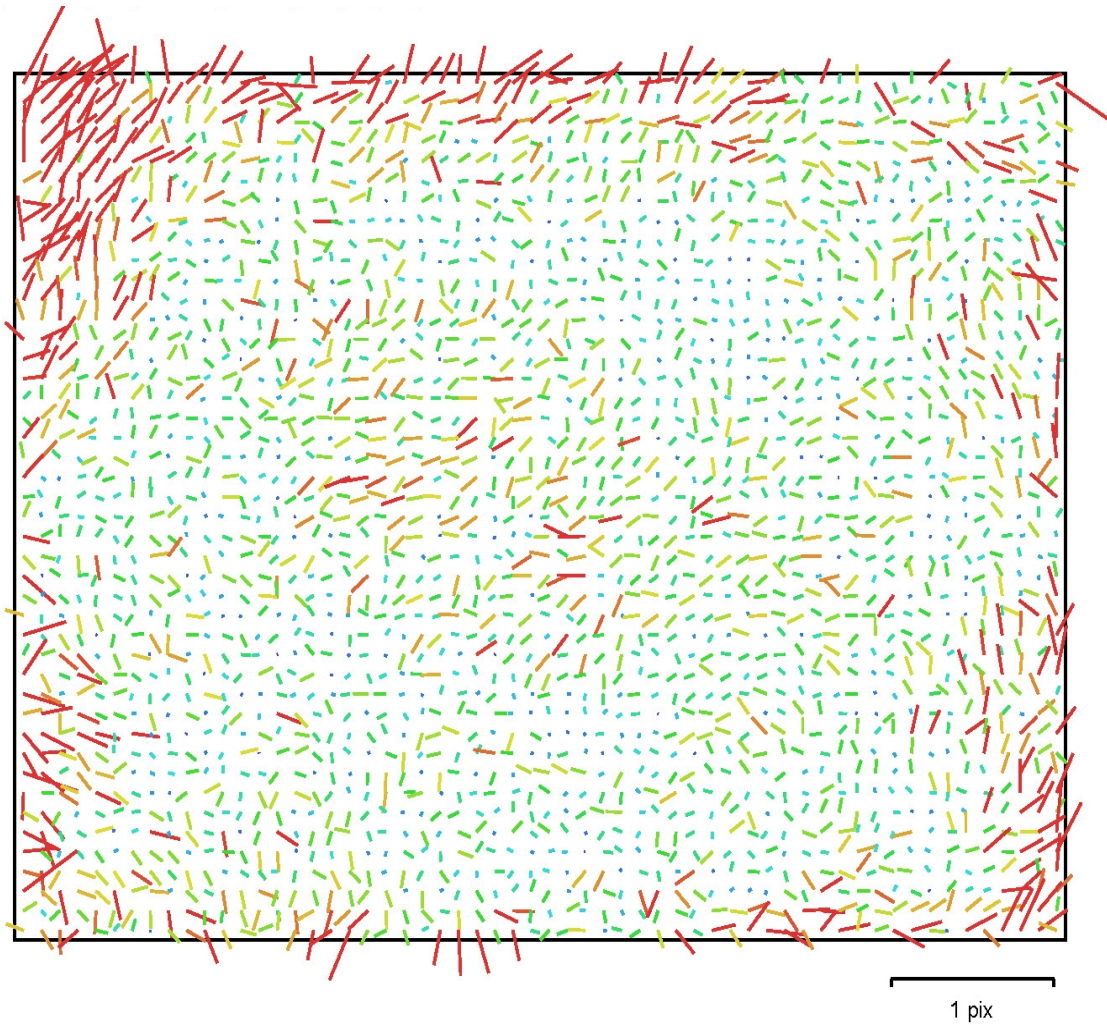
Asklepieion



Canon PowerShot G10 (6.1 mm)

Type:	Frame	K1:	-0.155112
Fx:	3722.45	K2:	0.145725
Fy:	3722.45	K3:	-0.0404956
Cx:	2226.31	K4:	0
Cy:	1594.1	P1:	0
Skew:	0	P2:	0

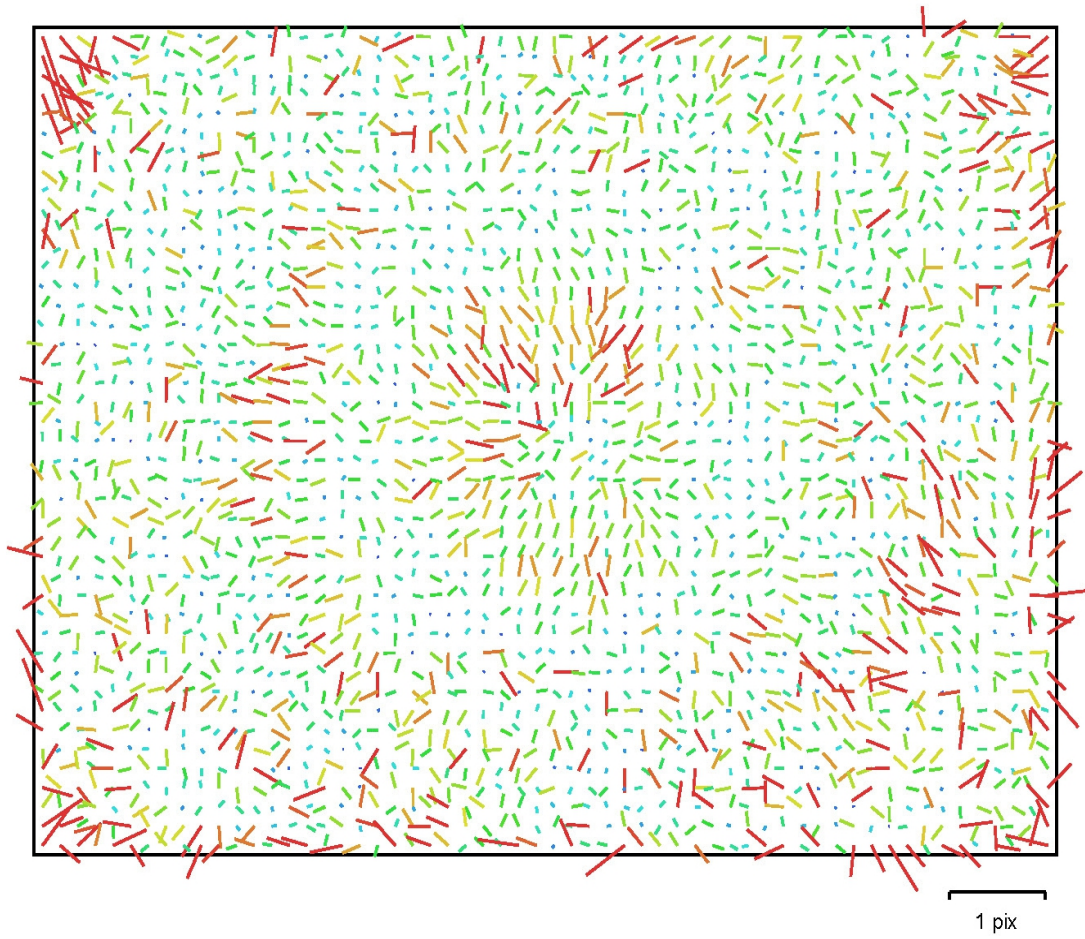
Frankish Area Calibrations



Canon PowerShot G10 (6.1 mm)

Type:	Frame	K1:	-0.153806
Fx:	3717.02	K2:	0.144135
Fy:	3717.02	K3:	-0.0392664
Cx:	2237.94	K4:	0
Cy:	1594.32	P1:	0
Skew:	0	P2:	0

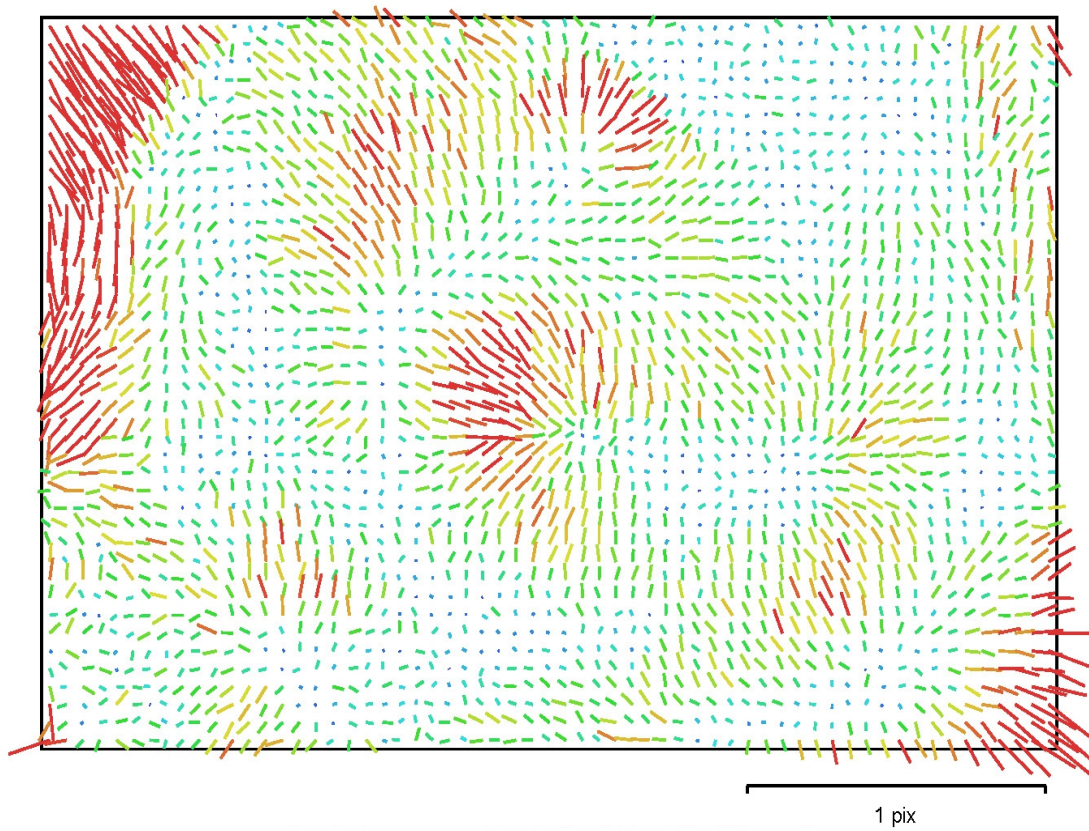
Frankish Drone



FC300X

Type:	Frame	K1:	-0.131832
Fx:	2326.66	K2:	0.107672
Fy:	2326.66	K3:	-0.0148997
Cx:	1998.97	K4:	0
Cy:	1503.92	P1:	0
Skew:	0	P2:	0

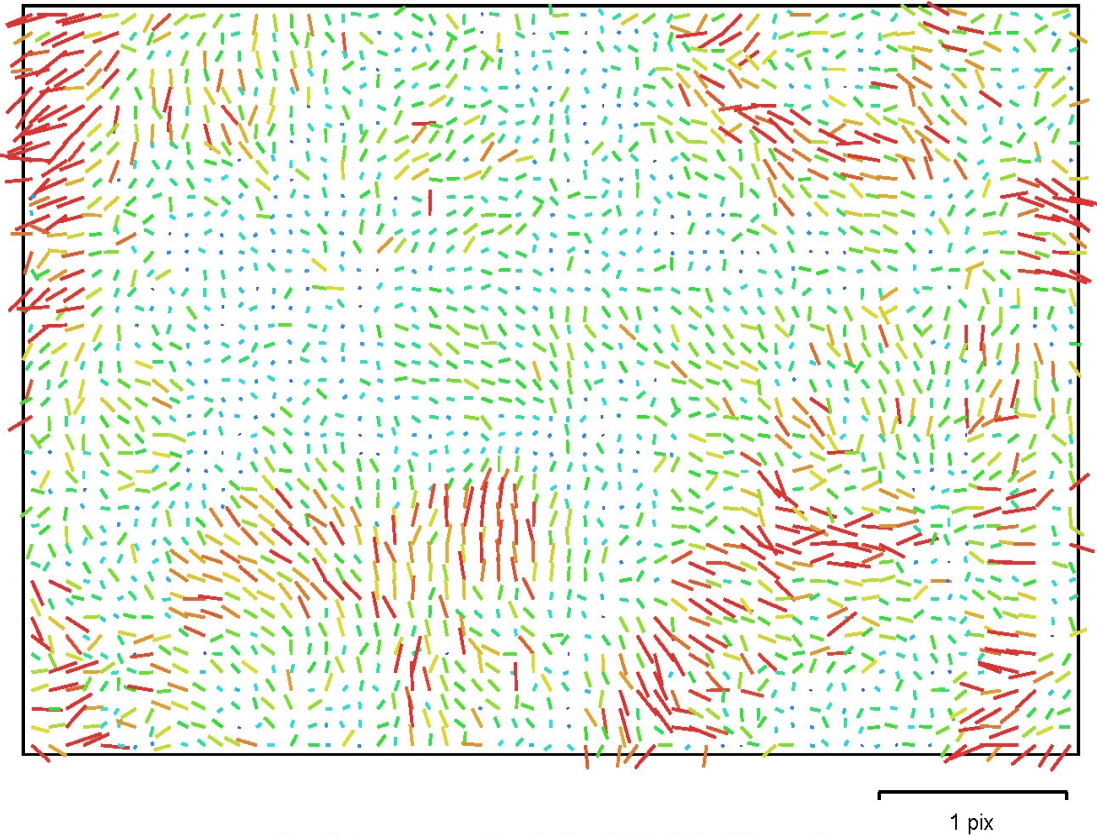
Eutychia Mosaic in Situ



SLT-A35 (18 mm)

Type:	Frame	K1:	-0.0885226
Fx:	3799.19	K2:	0.0192773
Fy:	3799.19	K3:	0.00125199
Cx:	2461.28	K4:	0
Cy:	1605.5	P1:	0
Skew:	0	P2:	0

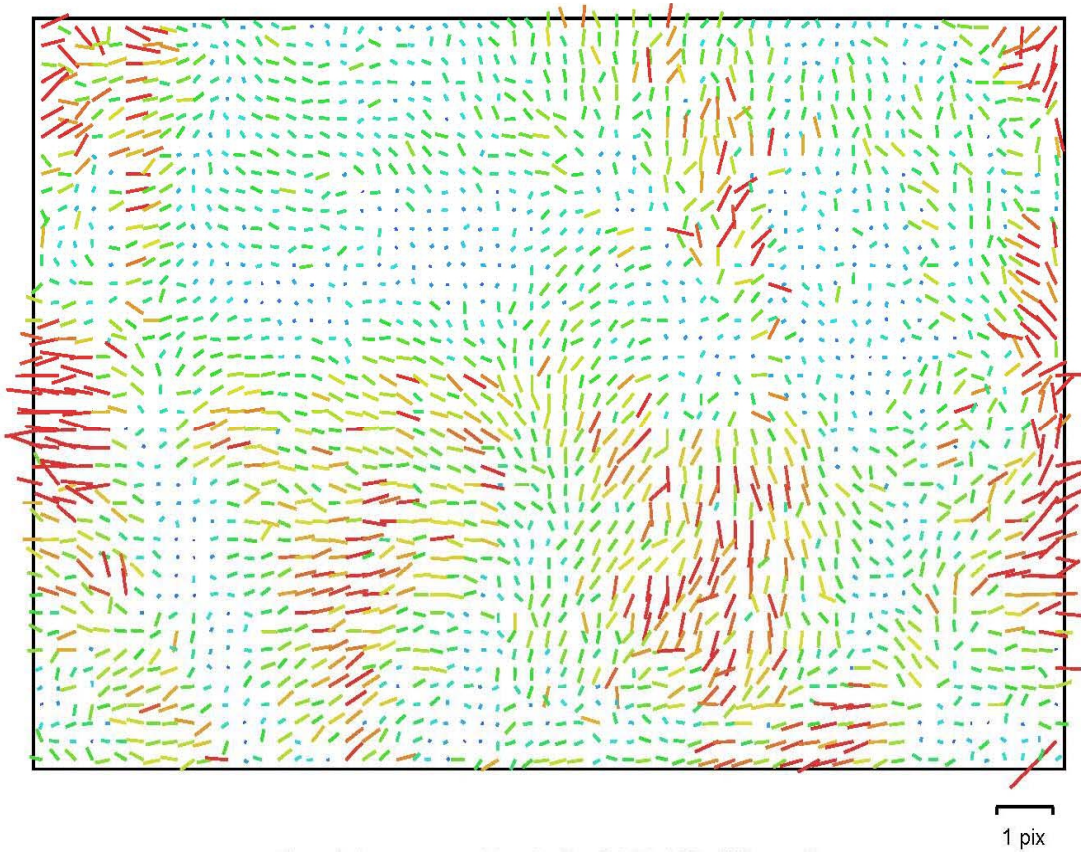
Eutychia Mosaic in Situ



SLT-A35 (22 mm)

Type:	Frame	K1:	-0.0677018
Fx:	4464.58	K2:	0.0084267
Fy:	4464.58	K3:	0.00825321
Cx:	2467.35	K4:	0
Cy:	1600.12	P1:	0
Skew:	0	P2:	0

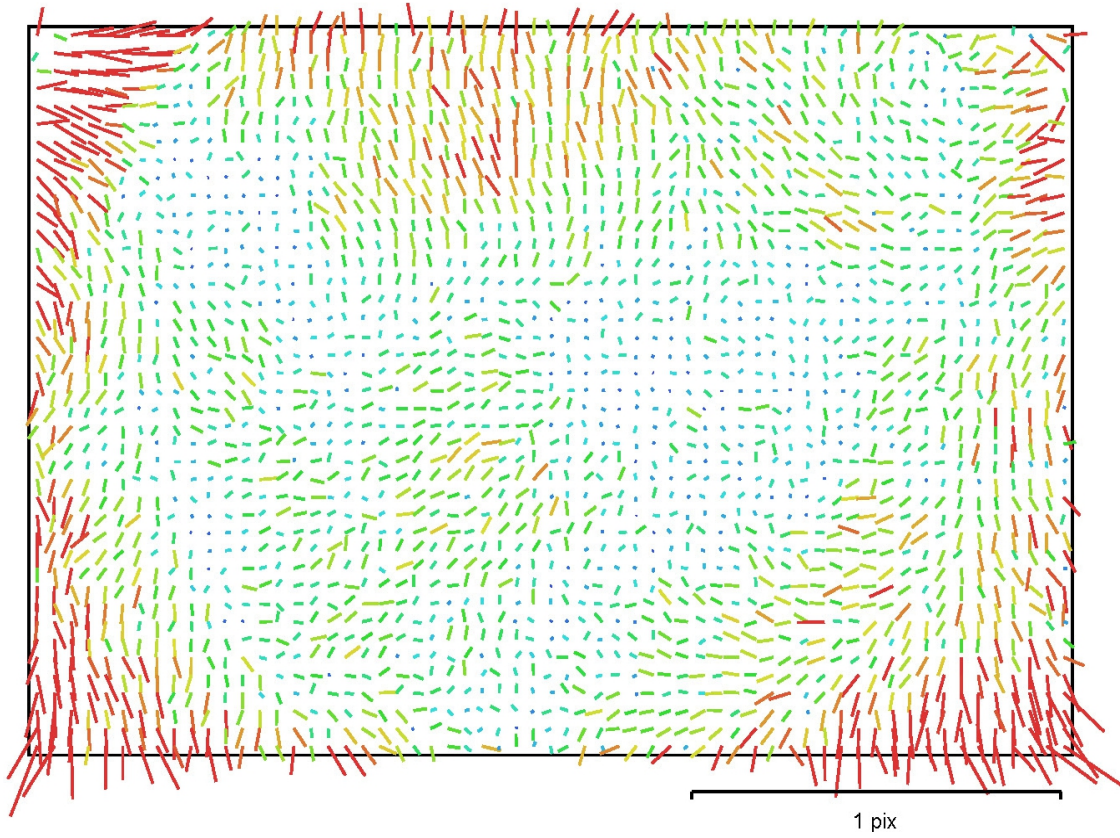
Eutychia Mosaic in Situ



SLT-A35 (20 mm)

Type:	Frame	K1:	-0.0624713
Fx:	4016.85	K2:	-0.0276877
Fy:	4016.85	K3:	0.034484
Cx:	2453.2	K4:	0
Cy:	1567.83	P1:	0
Skew:	0	P2:	0

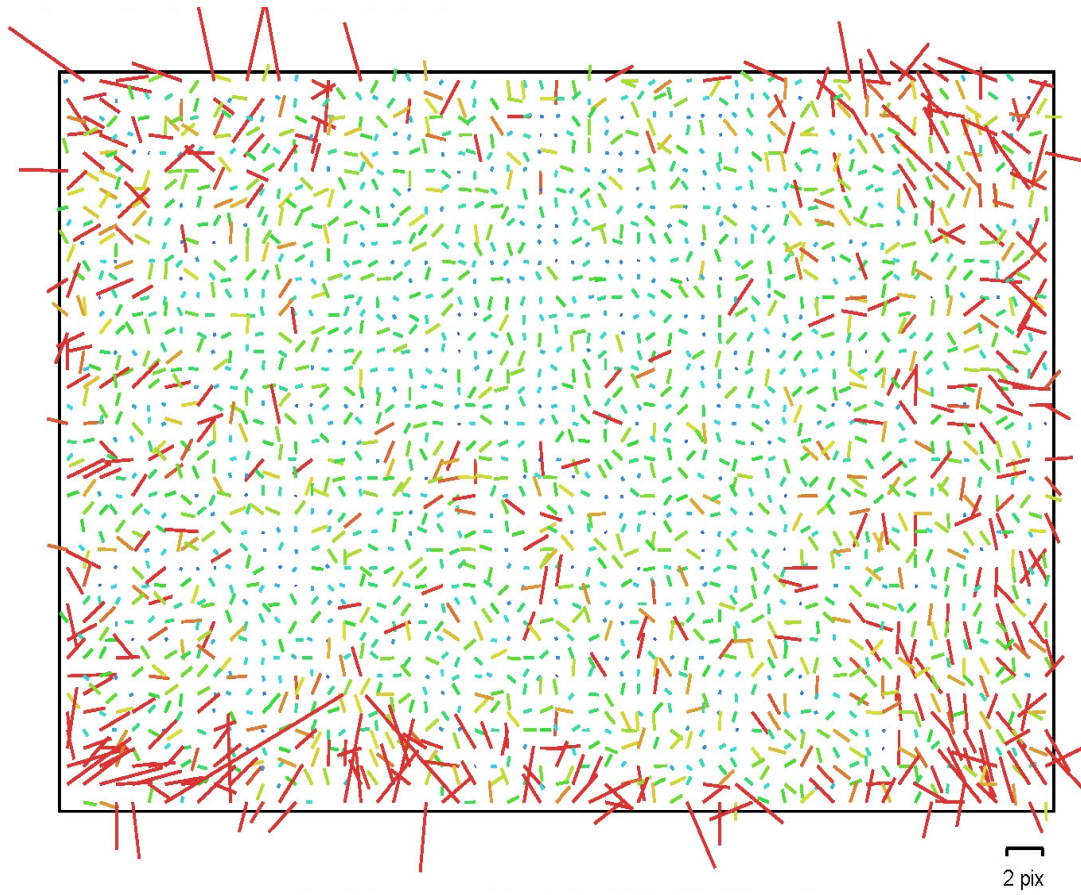
Eutychia Mosaic in Situ



SLT-A35 (18 mm)

Type:	Frame	K1:	-0.0927848
Fx:	2773.87	K2:	0.0165341
Fy:	2773.87	K3:	0.005752
Cx:	1790.39	K4:	0
Cy:	1154.45	P1:	0
Skew:	0	P2:	0

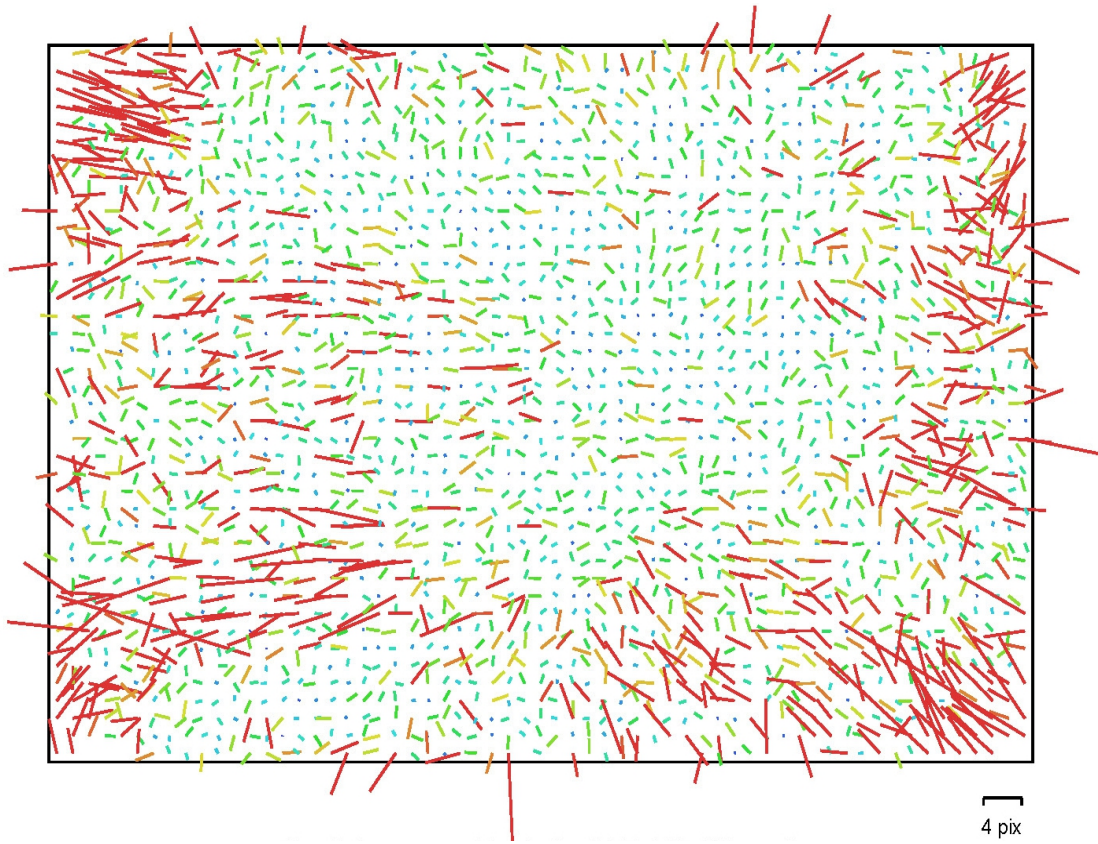
Mosaic Panel T21



SLT-A35 (22 mm)

Type:	Frame	K1:	-0.0660693
Fx:	4485.27	K2:	0.00887514
Fy:	4484.04	K3:	-0.0178609
Cx:	2421.44	K4:	0
Cy:	1595.56	P1:	-0.000663983
Skew:	-0.885399	P2:	0.000797499

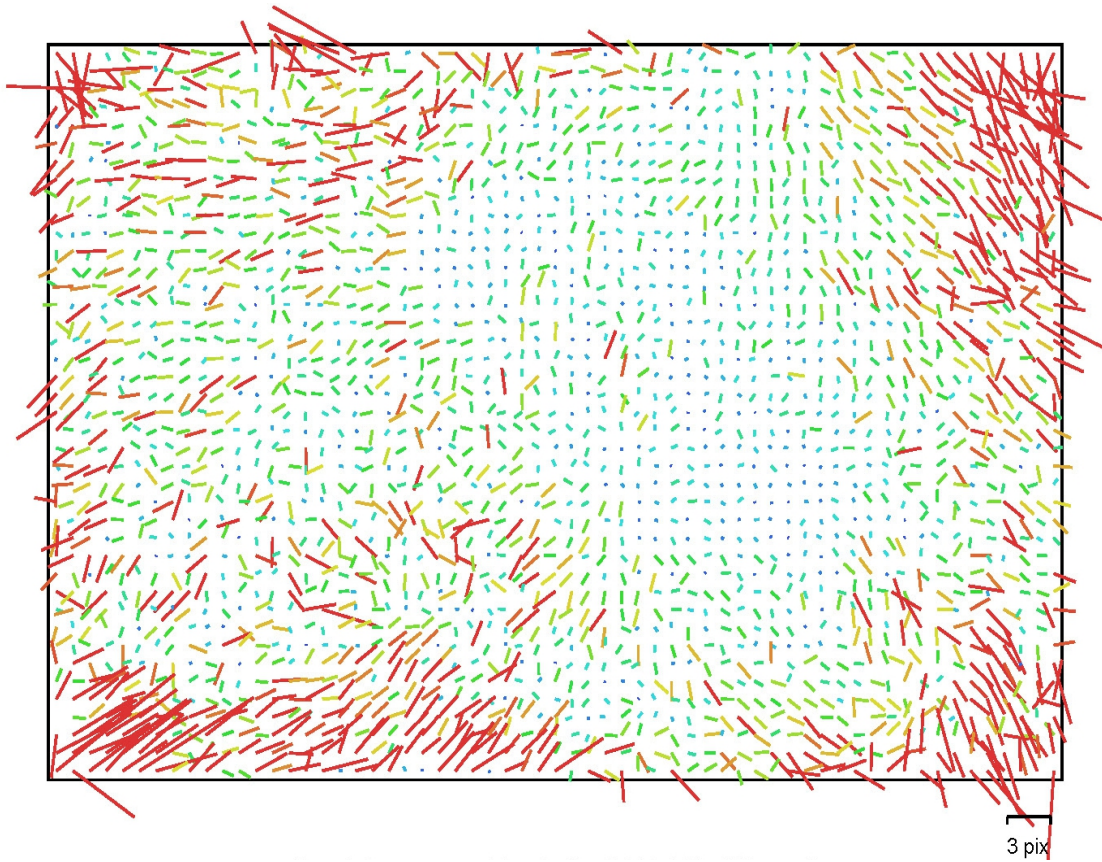
Mosaic Panel T21



SLT-A35 (20 mm)

Type:	Frame	K1:	-0.0911318
Fx:	4159.33	K2:	0.0923436
Fy:	4155.45	K3:	-0.14553
Cx:	2419.42	K4:	0
Cy:	1571.31	P1:	-0.000822365
Skew:	7.46766	P2:	0.000898115

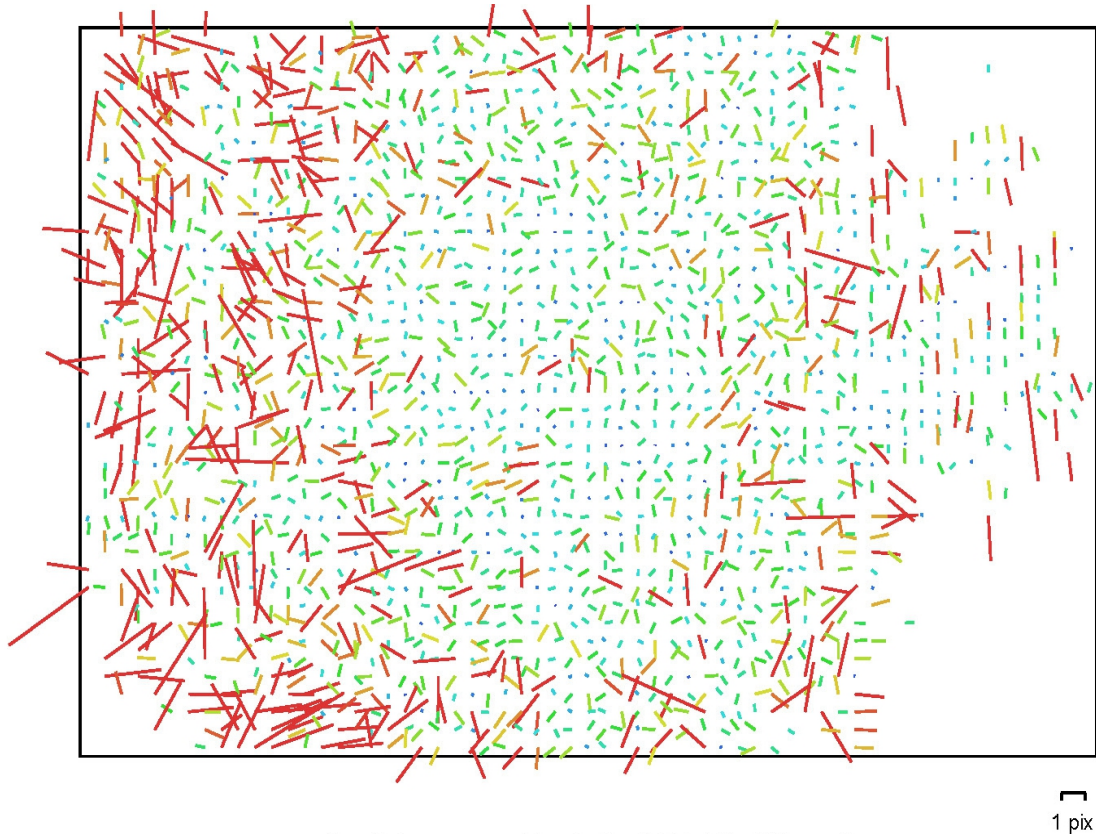
Mosaic Panel T21



SLT-A35 (18 mm)

Type:	Frame	K1:	-0.0934452
Fx:	3880.5	K2:	0.0517113
Fy:	3859.6	K3:	-0.0433097
Cx:	2462.94	K4:	0
Cy:	1600.5	P1:	-0.0010034
Skew:	5.01107	P2:	0.00137286

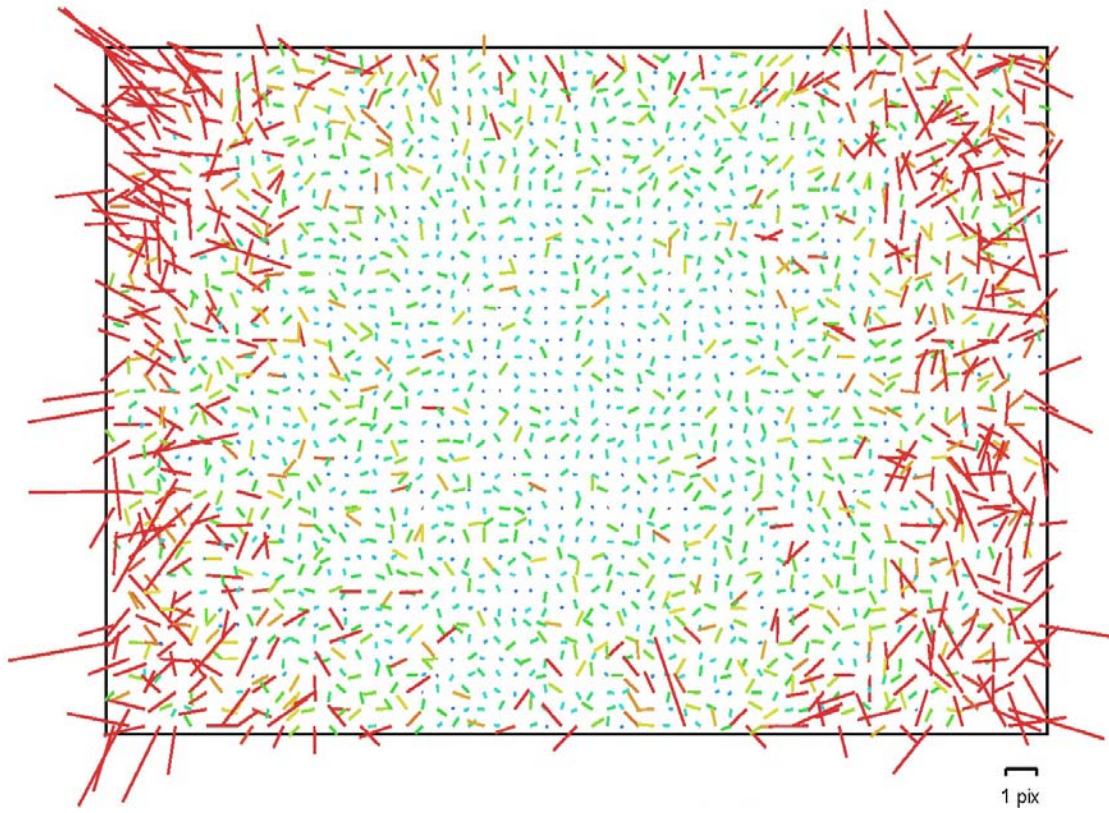
Roman Arm and Torso Joined



SLT-A35 (18 mm)

Type:	Frame	K1:	-0.0916979
Fx:	3737.65	K2:	0.000344673
Fy:	3737.65	K3:	0.0211433
Cx:	2437.75	K4:	0
Cy:	1638.72	P1:	0
Skew:	0	P2:	0

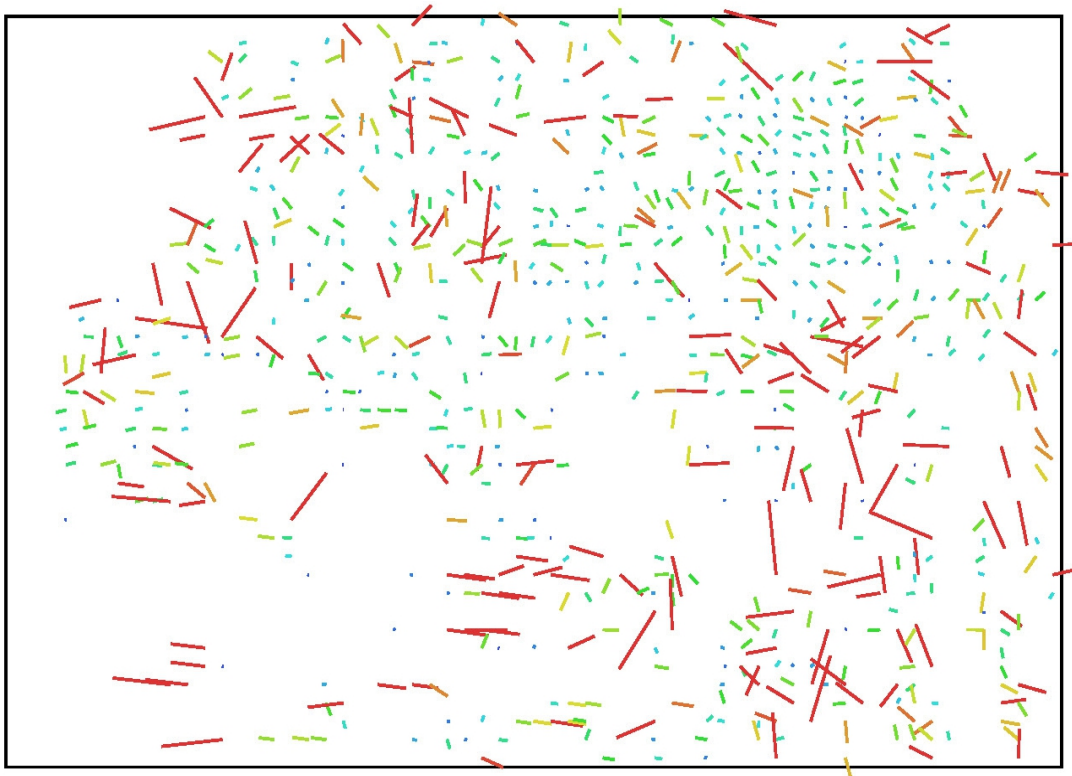
Roman Arm and Torso Joined



SLT-A35 (20 mm)

Type:	Frame	K1:	-0.0932763
Fx:	3969.91	K2:	0.0144348
Fy:	3969.91	K3:	0.0136291
Cx:	2430.44	K4:	0
Cy:	1633.5	P1:	0
Skew:	0	P2:	0

Roman Arm and Torso Joined

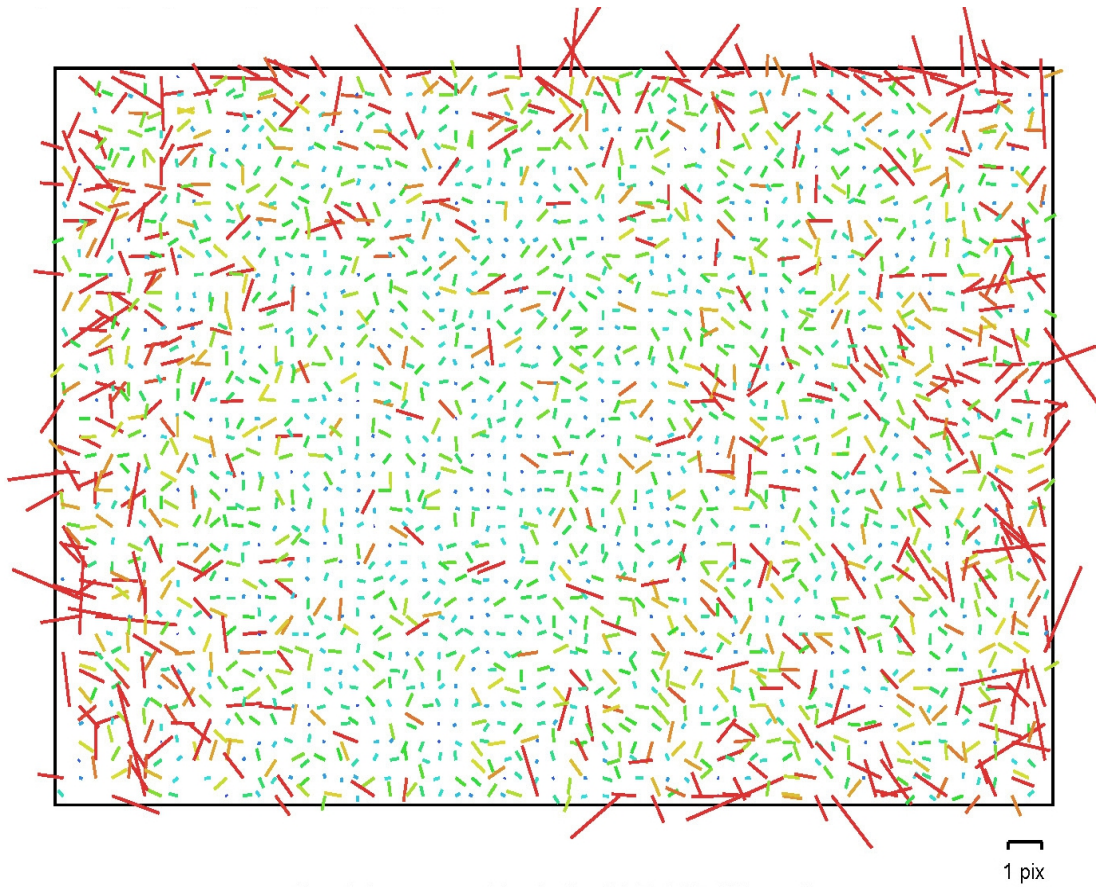


2 pix

SLT-A35 (26 mm)

Type:	Frame	K1:	-0.0850101
Fx:	5220.79	K2:	0.151797
Fy:	5220.79	K3:	-0.343401
Cx:	2435.34	K4:	0
Cy:	1647.43	P1:	0
Skew:	0	P2:	0

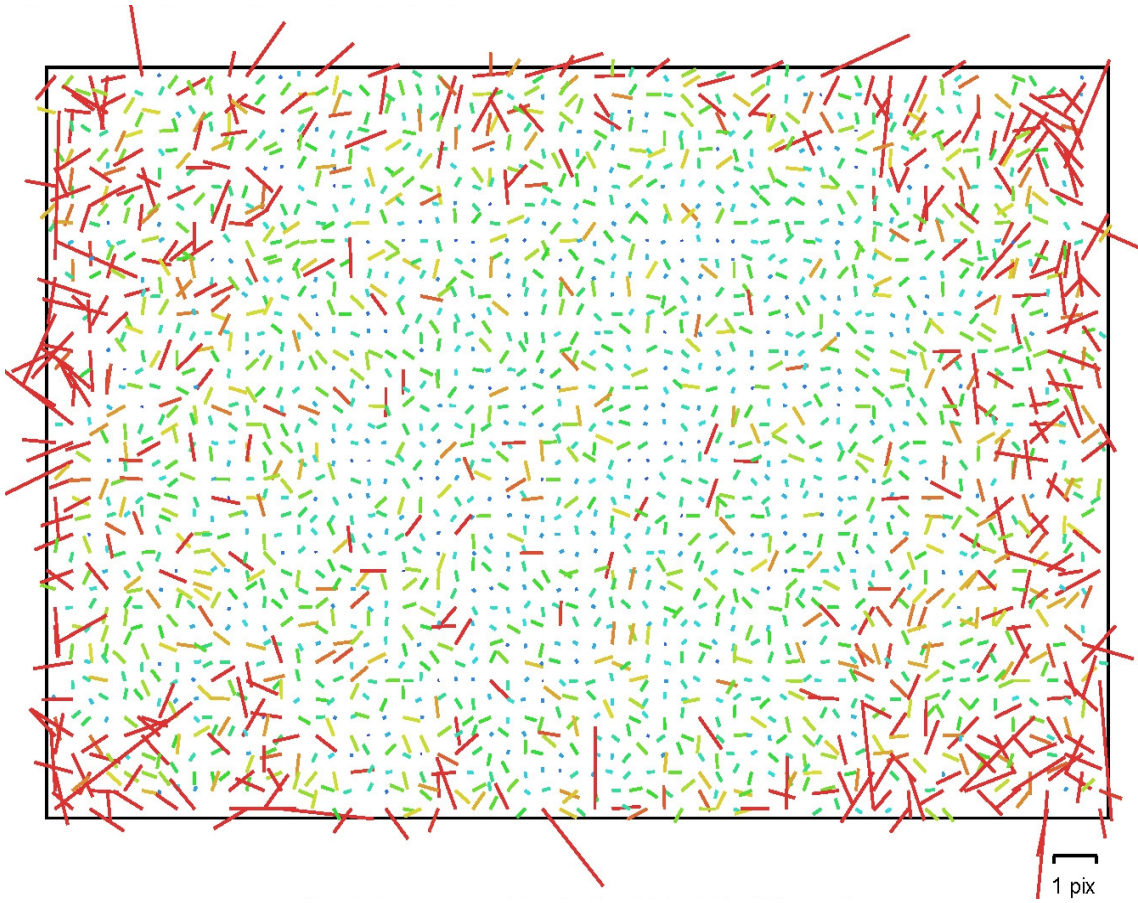
Roman Arm and Torso Joined



SLT-A35 (28 mm)

Type:	Frame	K1:	-0.0477599
Fx:	5840.41	K2:	-0.0288413
Fy:	5840.41	K3:	0.0636707
Cx:	2426.77	K4:	0
Cy:	1628.35	P1:	0
Skew:	0	P2:	0

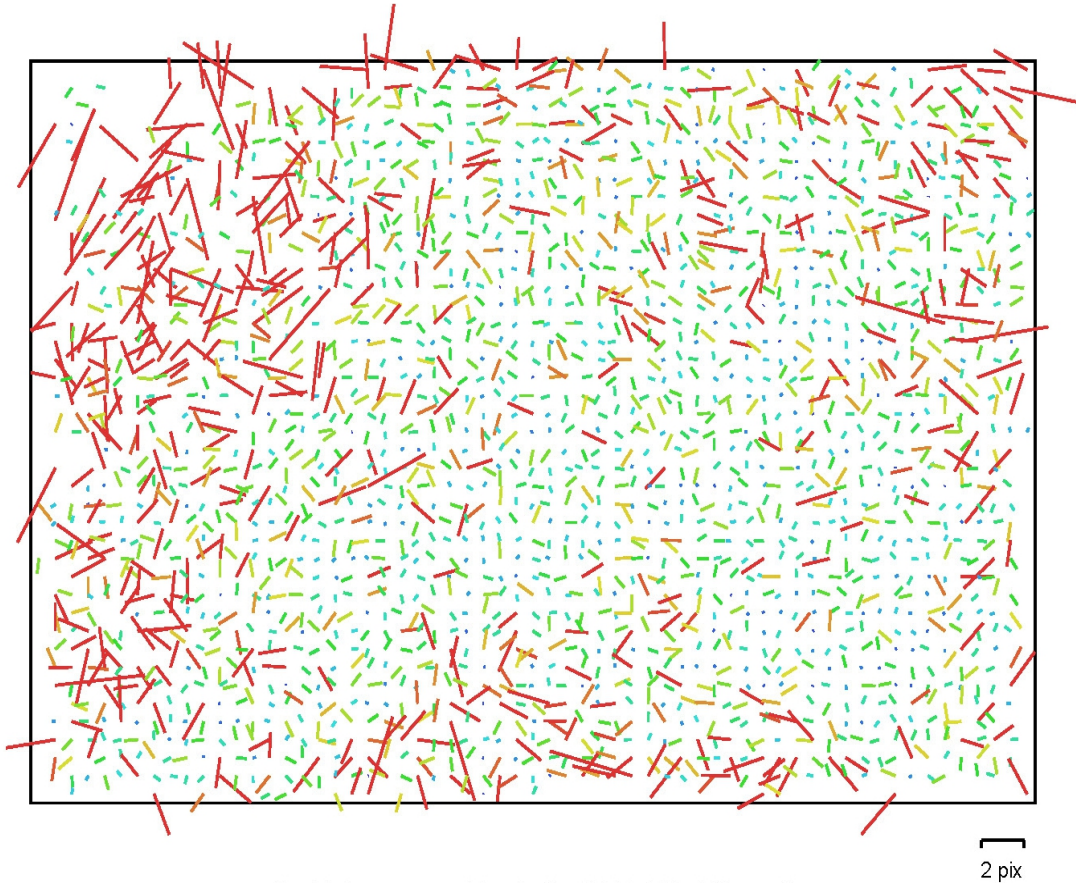
Roman Arm and Torso Joined



SLT-A35 (30 mm)

Type:	Frame	K1:	-0.045132
Fx:	6478.07	K2:	0.0824749
Fy:	6478.07	K3:	-0.320522
Cx:	2413.52	K4:	0
Cy:	1602.95	P1:	0
Skew:	0	P2:	0

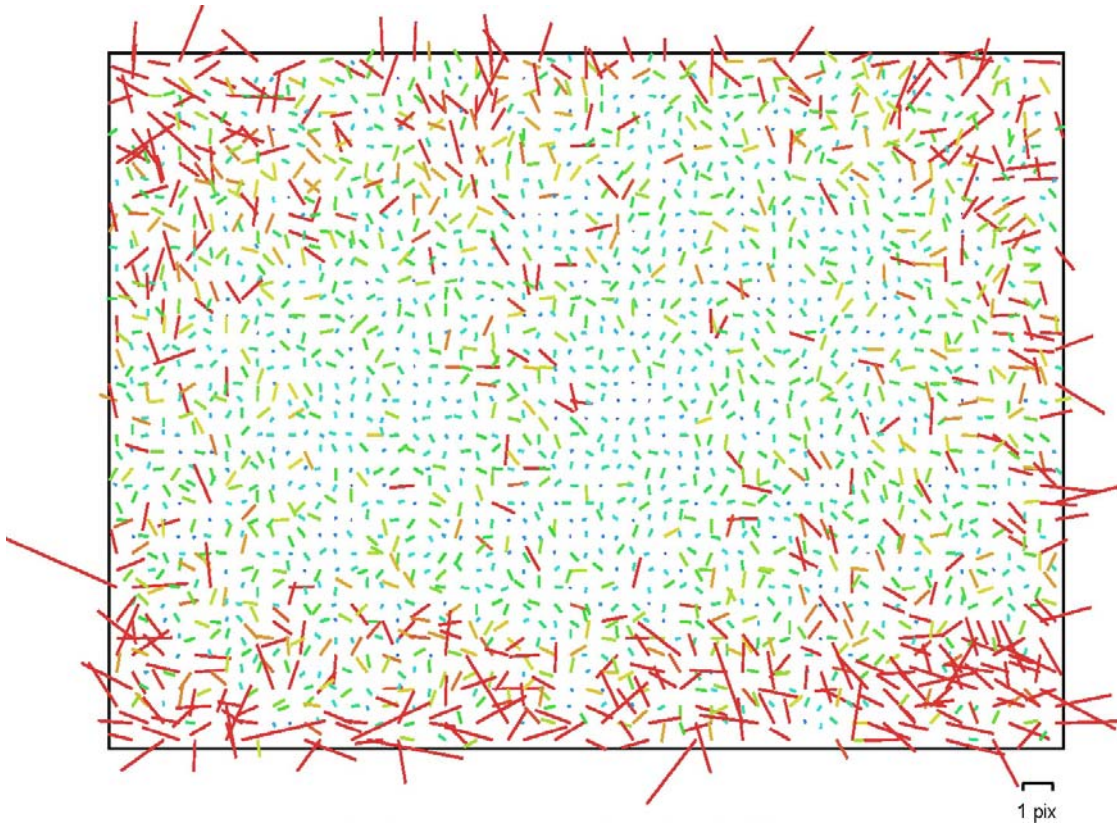
Roman Arm and Torso Joined



SLT-A35 (40 mm)

Type:	Frame	K1:	0.00170438
Fx:	8046.77	K2:	-0.265772
Fy:	8046.77	K3:	0.820653
Cx:	2430	K4:	0
Cy:	1651.02	P1:	0
Skew:	0	P2:	0

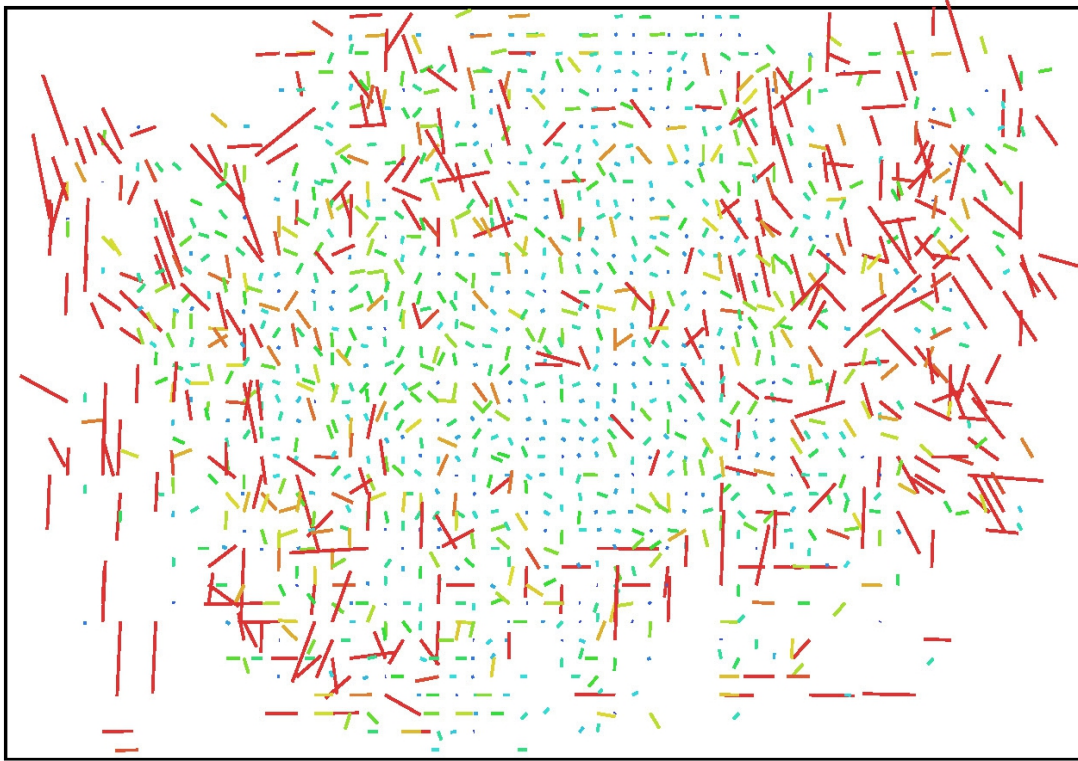
Roman Arm and Torso Joined



SLT-A35 (18 mm)

Type:	Frame	K1:	-0.110799
Fx:	3680.57	K2:	0.0465731
Fy:	3680.57	K3:	-0.0202267
Cx:	2445.54	K4:	0
Cy:	1630.9	P1:	0
Skew:	0	P2:	0

Roman Arm and Torso Joined

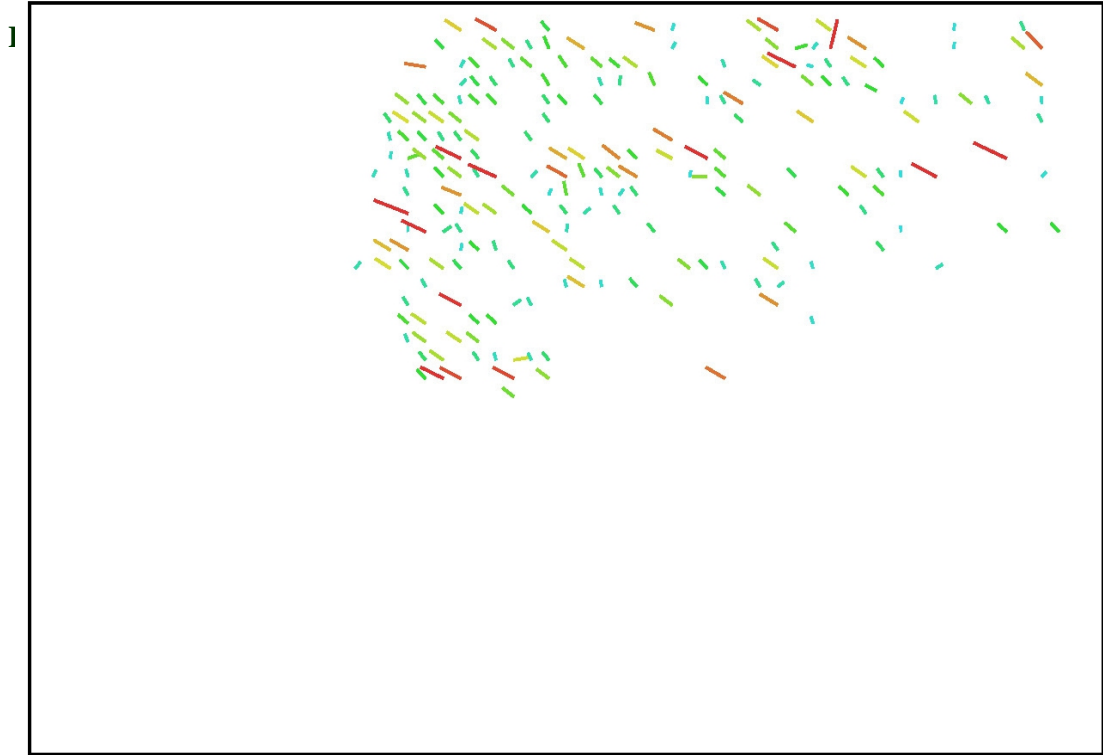


2 pix

SLT-A35 (50 mm)

Type:	Frame	K1:	0.0367359
Fx:	10138.5	K2:	-1.01415
Fy:	10138.5	K3:	7.77143
Cx:	2442.21	K4:	0
Cy:	1560.74	P1:	0
Skew:	0	P2:	0

Roman Arm and Torso Joined



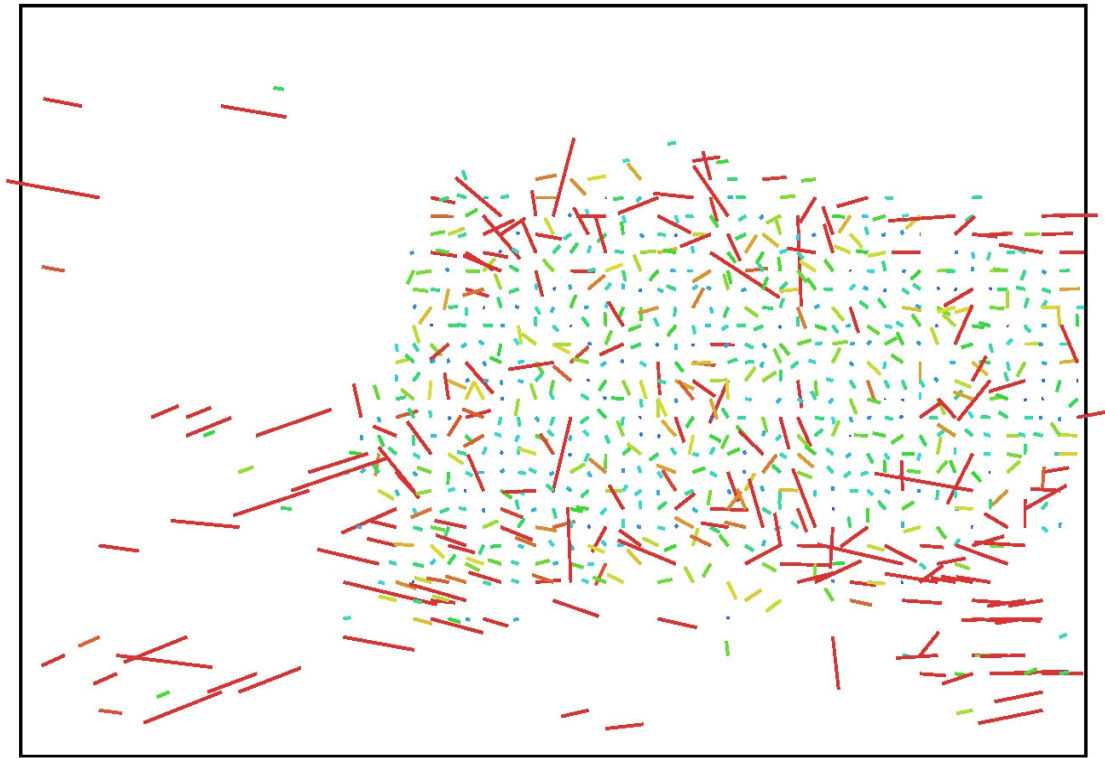
3 pix

SLT-A35 (55 mm)

Type:	Frame	K1:	-0.00318606
Fx:	10840.3	K2:	-0.366396
Fy:	10840.3	K3:	4.43797
Cx:	2517.66	K4:	0
Cy:	1664.44	P1:	0
Skew:	0	P2:	0

Photogrammetry in Mediterranean Archaeology

Roman Arm and Torso Joined



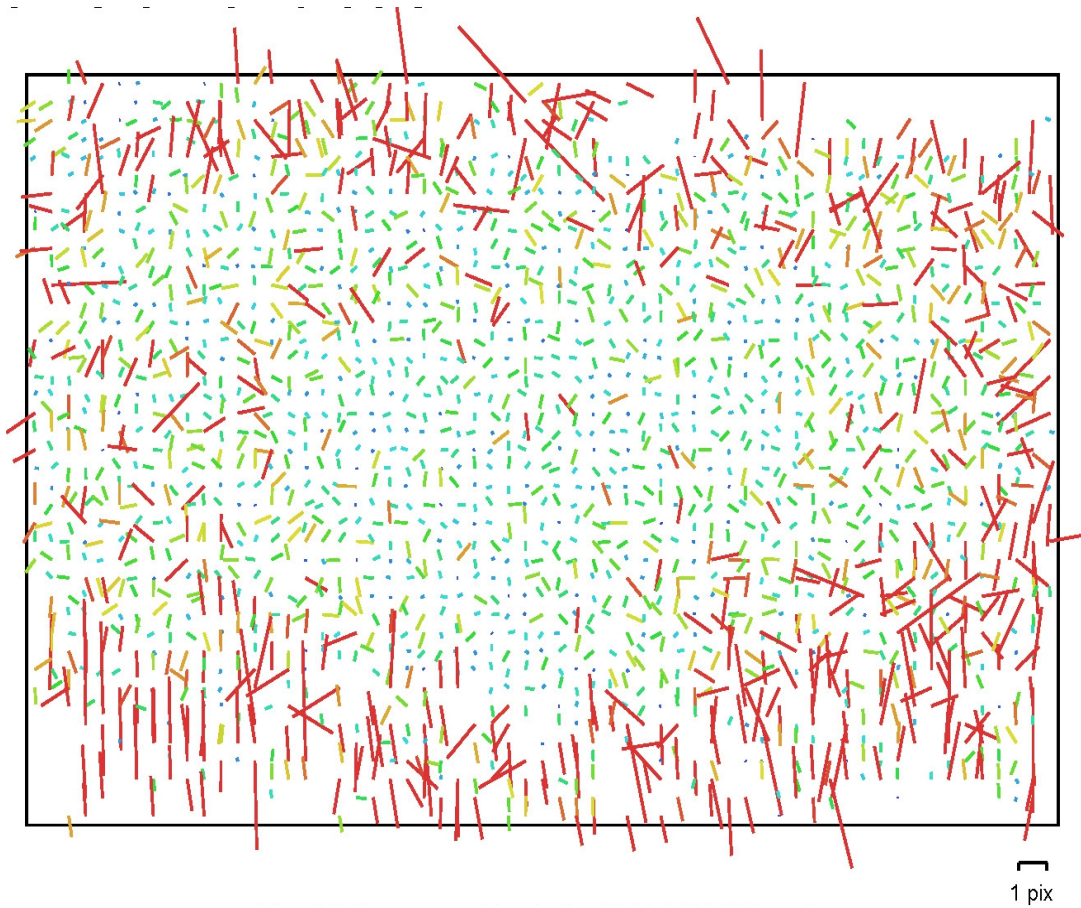
1 pix

SLT-A35 (35 mm)

Type:	Frame	K1:	0.0456366
Fx:	6857.75	K2:	-0.982845
Fy:	6857.75	K3:	2.60202
Cx:	2399.56	K4:	0
Cy:	1629.59	P1:	0
Skew:	0	P2:	0

Photogrammetry in Mediterranean Archaeology

Roman Arm and Torso Joined

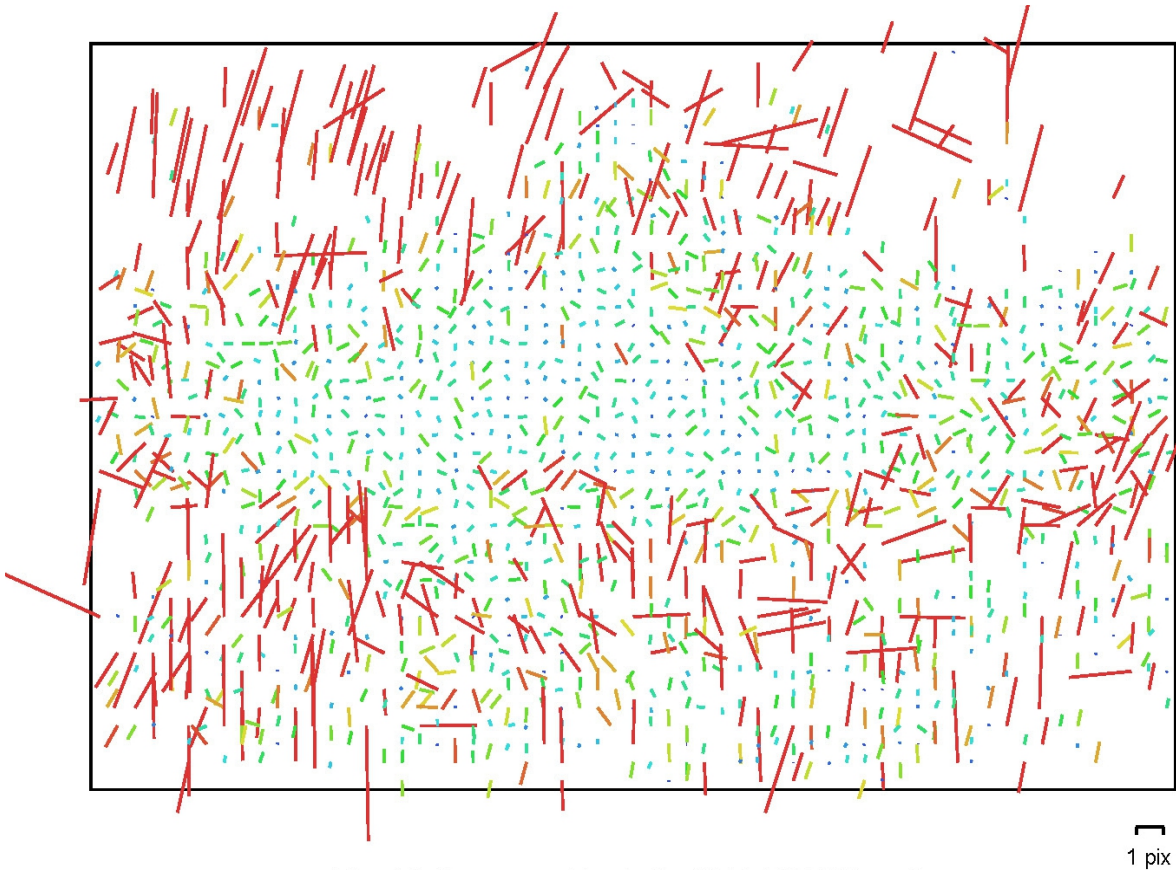


SLT-A35 (22 mm)

Type:	Frame	K1:	-0.0937259
Fx:	4320.94	K2:	0.0021404
Fy:	4320.94	K3:	0.0507487
Cx:	2434.38	K4:	0
Cy:	1631.62	P1:	0
Skew:	0	P2:	0

Photogrammetry in Mediterranean Archaeology

Roman Arm and Torso Joined

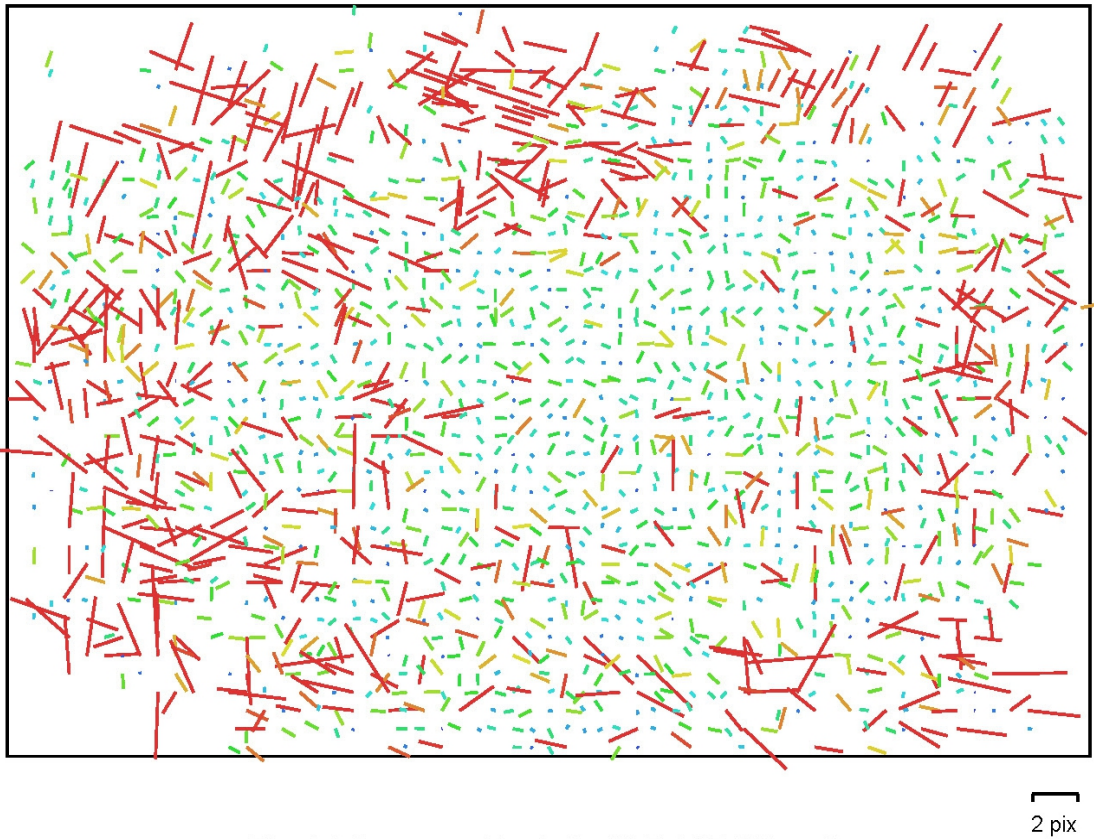


SLT-A35 (20 mm)

Type:	Frame	K1:	-0.0939442
Fx:	4162.77	K2:	0.0336999
Fy:	4162.77	K3:	-0.0219528
Cx:	2439.59	K4:	0
Cy:	1626.74	P1:	0
Skew:	0	P2:	0

Photogrammetry in Mediterranean Archaeology

Roman Arm and Torso Joined

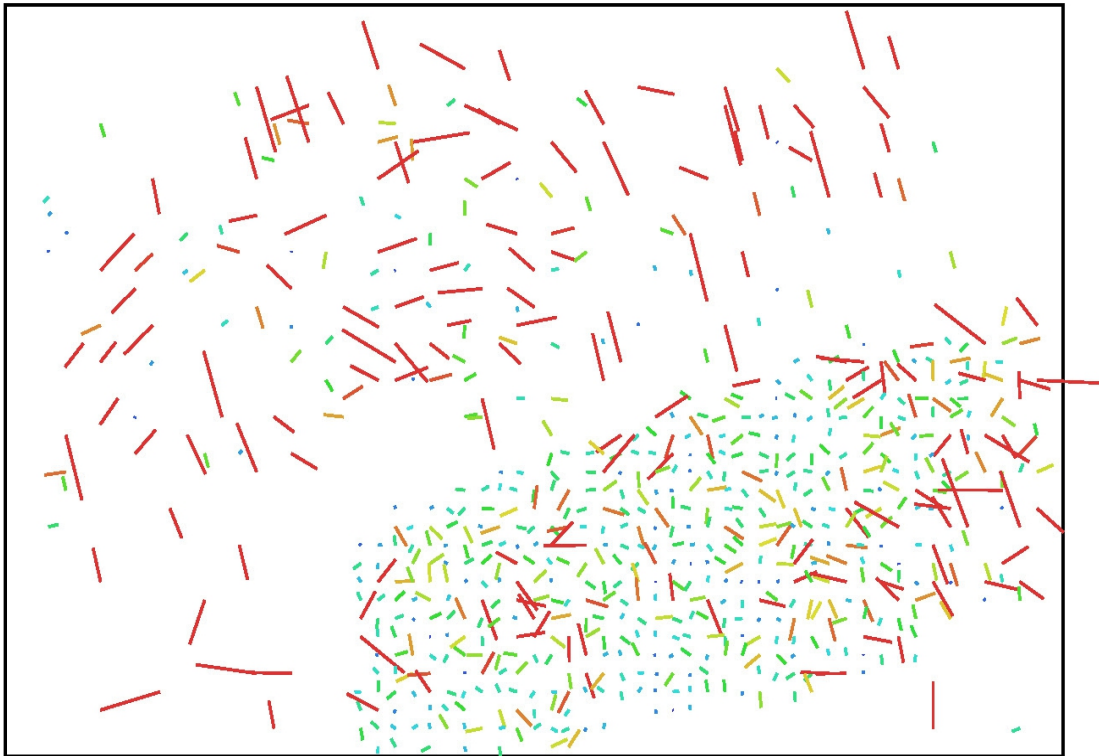


SLT-A35 (30 mm)

Type:	Frame	K1:	-0.0726618
Fx:	5998	K2:	0.176843
Fy:	5998	K3:	-0.664932
Cx:	2435.4	K4:	0
Cy:	1605.15	P1:	0
Skew:	0	P2:	0

Photogrammetry in Mediterranean Archaeology

Roman Arm and Torso Joined



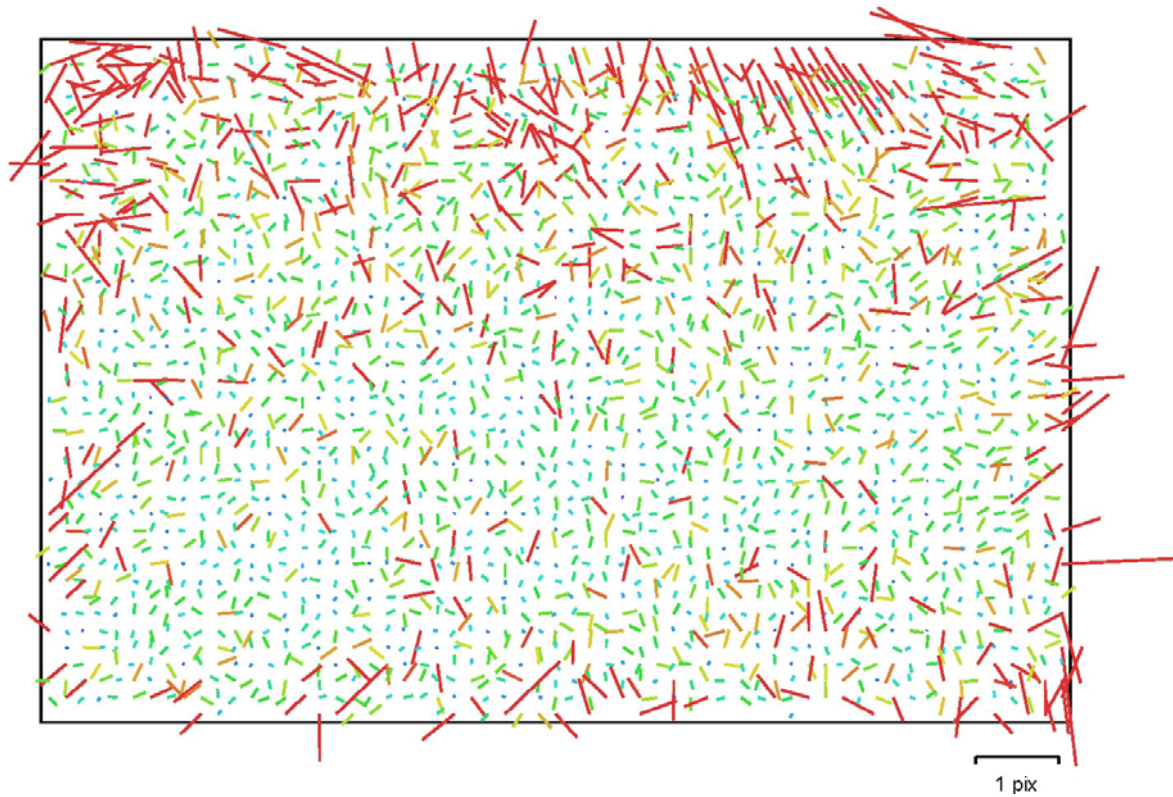
2 pix

SLT-A35 (28 mm)

Type:	Frame	K1:	-0.0293381
Fx:	5910.03	K2:	-0.286613
Fy:	5910.03	K3:	1.02048
Cx:	2418.34	K4:	0
Cy:	1600.63	P1:	0
Skew:	0	P2:	0

Agora Inscription

Photogrammetry in Mediterranean Archaeology

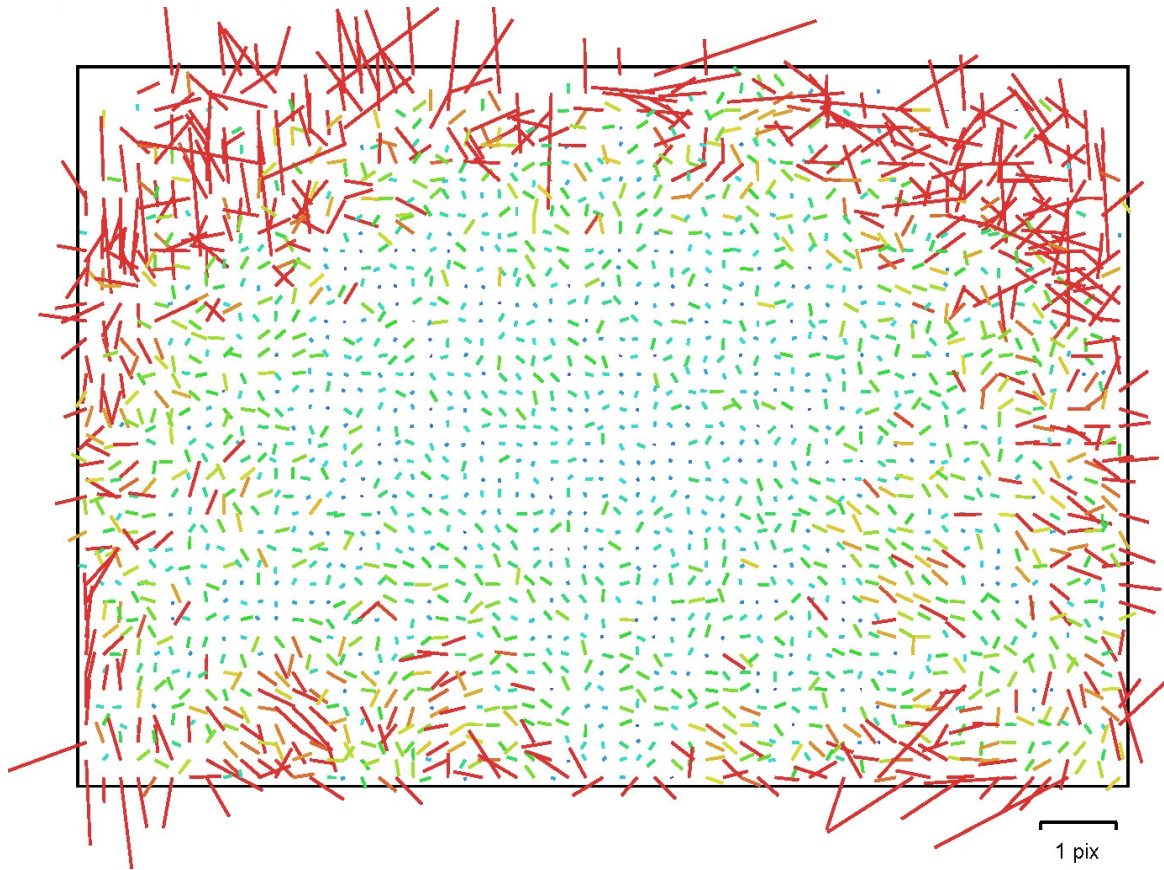


SLT-A35 (50 mm)

Type:	Frame	K1:	-0.0279948
Fx:	9326.17	K2:	0.258981
Fy:	9326.17	K3:	-1.84625
Cx:	2427.13	K4:	0
Cy:	1615.23	P1:	0
Skew:	0	P2:	0

Photogrammetry in Mediterranean Archaeology

Agora Inscription



SLT-A35 (18 mm)

Type:	Frame	K1:	-0.109066
Fx:	3663.59	K2:	0.0309549
Fy:	3663.59	K3:	-0.00411999
Cx:	2423.44	K4:	0
Cy:	1621.07	P1:	0
Skew:	0	P2:	0